João Pedro Mateus Gens dos Santos

Licenciatura em Ciências de Engenharia Biomédica

Brain circuits involved in self-paced motion: the influence of 0.1 Hz waves

Dissertação para obtenção do Grau de
Mestre em Engenharia Biomédica

Orientador: Alexandre Andrade,Doutor,
Instituto de Biofísica e Engenharia Biomédica,
Faculdade de Ciências da Universidade de Lisboa

Júri:

Presidente:	Doutora Carla Maria Quintão Pereira
Arguente:	Doutor Mário António de Basto Forjaz Secca
Vogal:	Doutor Alexandre da Rocha Freire de Andrade

FACULDADE DE CIÊNCIAS E TECNOLOGIA
UNIVERSIDADE NOVA DE LISBOA

Março, 2016

Brain circuits involved in self-paced motion: the influence of 0.1 Hz waves

Acknowledgements

First of all, I would like to express my sincere gratitude to my supervisor, Alexandre Andrade. This dissertation wouldn't have been possible without his introduction, guidance, useful comments, remarks and encouragement. I am very grateful for his example and testimony. He will be no doubt a reference in my life. Thank you very much!

My sincere thanks goes to the Technical University of Graz for kindly made available all the subjects datasets used on this work and, particularly, to Gert Pfurtscheller's group to discuss the results with me. A special thank to Joana Brito and João Rodrigues for introduce me to this project and clarify me all my doubts on the beginning of this dissertation. Your help was very important and is part of this dissertation.

I would like to thank all the professors at FCT-UNL who have gave me the scientific basis necessary to develop this project, in particular all the professors of Biomedical Engineering. I would also like to thank the Institute of Biophysics and Biomedical Engineering (IBEB), where this dissertation was conducted, for all the support provided during this time.

I wish to thank all my colleagues and friends of the FCT-UNL who have accompanied me during these last years. You are all different and special and I wish you all the best for the future. Thanks for all the help during these years. I would also like to thank my friends and colleagues I met during this project in IBEB, who have accompanied me and shared with me very valuable moments. You guys are amazing people! Thank you very much.

I would like to thank all the people of my hometown, that made me grow, and all the friends and colleagues that I have known. Thank you very much.

Gostava de agradecer a toda a minha família. Sem dúvida que nada era sem vocês. Obrigado Pai e Mãe por serem os meus pais, por serem a referência da minha vida. Obrigado Luis Miguel e Rui por serem os meus grandes irmãos. Obrigado Tia e Padrinho pelo vosso grande exemplo. E obrigado ao meu Padrinho e todos os meus Tios e Tias, Primos e Primas. Aos meus Avós que já partiram e à Avó. Por último gostava de agradecer a Deus por todo o seu Amor. Um grande obrigado a todos!

Abstract

The neural mechanisms behind human voluntary motion are not fully characterized yet, in spite of numerous research studies. Slow (0.1 Hz) brain oscillations are known to have a powerful modulatory effect on several cognitive and physiological phenomena, including free movement.

This study is based on fMRI data acquired from 25 young, healthy subjects. The tasks were: rest, self-paced motion, motion paced by a periodic 0.1 Hz stimulus. The temporal resolution was finer than standard fMRI protocols (TR=871 ms). After preprocessing, the signal from brain regions of interest was extracted, and functional connectivity was computed between brain regions using wavelet phase coherence. Complementarily, effective connectivity was measured using Granger causality. The final output was Phase-Locking (PL) and Granger Causality (GC) matrices reflecting inter-regional phase coherence and causal interactions, respectively, around 0.1 Hz.

Using the GraphVar toolbox, inter-task and inter-group comparisons were performed. In inter-task comparisons PL matrices showed encouraging results unlike GC matrices. Pairs of regions for which PL differs significantly between rest and self-paced movement were identified. These include mainly the Postcentral gyrus, Putamen, the Anterior Cingulum, the Precentral gyrus, the Calcarine, the Lingual and the Insula (all in the left hemisphere). Topological changes in the brain wiring were identified across the tasks by computing the node degree and global efficiency. Inter-group comparisons took into account the inter movement interval and the coupling between BOLD and heart rate beat-to-beat interval signals and showed changes in brain activity depending on the regularity of movement intervals and specific connectivity patterns for neural BOLD oscillations, respectively.

This methodological approach allowed to make a contribution towards the characterization of the functional connectivity of brain circuits related to voluntary motor behavior.

Keywords: Voluntary movement, Slow oscillations, BOLD fMRI, Wavelet Coherence, Granger Causality, Brain networks, Graph Theory, Mayer waves

RESUMO

Os mecanismos neuronais que estão por detrás das ações voluntárias humanas ainda não estão inteiramente caracterizados, apesar dos numerosos estudos realizados. As oscilações cerebrais lentas são conhecidas por terem um poderoso efeito modulatório em vários fenómenos cognitivos e fisiológicos, incluindo o movimento livre.

Este estudo é baseado em dados de fMRI adquiridos de 25 sujeitos jovens e saudáveis. As tarefas foram: repouso, movimento espontâneo e movimento regulado por um estimulo periódico de 0.1 Hz. A resolução temporal usada foi superior à da maioria dos protocolos de fMRI usados correntemente (TR = 871 ms). Depois do pré-processamento, o sinal das regiões cerebrais de interesse foi extraído e a conectividade funcional foi calculada entre regiões cerebrais usando a coerência de fase baseada em wavelets. Complementarmente, foi medida a conetividade efetiva usando a causalidade de Granger. O resultado final foram matrizes de coerência de fase e causalidade de Granger refletindo coerências de fase inter-regionais e interações causais, respetivamente, ao redor de frequências de 0.1 Hz.

Usando o software GraphVar, comparações inter-tarefa e inter-grupo foram realizadas. Para as comparações inter-tarefa, as matrizes de coerência de fase mostraram resultados encorajadores ao contrário das matrizes de causalidade de Granger. Pares de regiões para os quais a coerência de fase difere significativamente entre repouso e movimento espontâneo autónomo foram identificados. Incluídas estão principalmente regiões da circunvolução Pós-central, Putâmen, Cíngulo Anterior, circunvolução Pré-central, Calcarino, Lingual, e a Insula (todos no hemisfério esquerdo). Alterações topológicas nas redes de conectividade cerebrais foram identificadas ao longo das tarefas através do cálculo do grau do nó e eficiência global. Comparações inter-grupos tiveram em conta o intervalo entre movimentos e a relação entre o sinal BOLD e o intervalo entre picos R do sinal cardíaco registado em simultâneo e mostraram alterações na atividade cerebral dependendo da regularidade dos intervalos dos movimentos e padrões específicos de conetividade para as oscilações neuronais BOLD, respetivamente.

Esta abordagem metodológica deu um contributo para a caracterização da conetividade funcional dos circuitos cerebrais relacionados com o movimentos voluntário espontâneo.

Palavras-chave: Movimento voluntário, Oscilações lentas, BOLD fMRI, Coêrencia de fase,

Causalidade de Granger, Redes cerebrais, Teoria de Grafos, Ondas Mayer.

Contents

List of Figures

List of Tables

Acronyms

BOLD Bold Oxygen Level Dependent.

EEG Electroencephalography.

fMRI functional Magnetic Resonance Imaging.

GC Granger Causality.

M1 Primary Motor Cortex.

MEG Magnetoencephalography.

MRI Magnetic Resonance Imaging.

PET Positron Emission Tomography.

PL Phase Locking.

SMA Supplementary Motor Area.

WTC Wavelet Transform Coherence.

CHAPTER 1

INTRODUCTION

The impression that one can freely choose between different possible courses of action is fundamental to human life. This capacity has long been a topic of debate first for theologians and philosophers and nowadays also for psychologists and neuroscientists. The fundamental question is: are we completely defined by the deterministic nature of physical laws or do we have some independence in making choices and actions? A dualistic view is present in our normal language and suggests that the mental state "I" that is distinct from both brain and body, freely initiate the neural events in motor areas of the brain that lead to body movement. However, modern brain science has suggested that this subjective experience of freedom is no more than an illusion and that our actions are initiated by unconscious mental processes long before we become aware of our intention to act (Haggard, 2005).

Voluntary movements have been generally assumed to be a result from neural activity in premotor and motor cortical areas that precede the conscious decision to move. Studies in which subjects freely choose between moving the right of left hand showed activation of medial frontal cortex. In particular, regions such as supplementary motor area and anterior cingulate cortex are involved. Brass and Haggard (2010a) hypothesize the involvement of anterior insular cortex in evaluating the outcomes of intentional action decisions that are previously formed elsewhere (Brass and Haggard, 2010a).

An interesting propriety of the brain has been fundamental to unveil brain circuits behind voluntary motion. First detected in local field potential recordings (Aladjalova, 1957), the slow oscillations (0.1 Hz) have been observed also in eletroencephalography (Wolansky et al., 2006) and functional Magnetic Resonance Imaging (fMRI) (Koch et al., 2012) signals. It is believed that these slow oscillations may have a leading role in setting the cortical excitability (Steriade and Contreras, 1998) and are important for neocortical function regarding memory consolidation, performance, and sleep (Csercsa et al., 2010; Monto et al., 2008). In addition, slow fluctuations have also been observed in cardiovascular context,

for instances, the so called Mayer waves (Julien, 2006). This has lead researches to hypothesize that the intention to perform a motor act could be dependent on cardiovascular oscillations (Pfurtscheller et al., 2012b).

fMRI has played a prominent role in the quest to identify the brain regions involved in voluntary action. This technique has enabled researchers to visualize changes in brain activity noninvasively. Bold Oxygen Level Dependent (BOLD) technique has been the most employed fMRI method. It is based on changes in the ration of oxy-to deoxyhemoglobin which consequently causes changes in the magnetic resonance signal. This technique has given support to the comprehension of how different parts of the brain are functionally organized (Huettel et al., 2004).

Functional organization of the brain has been characterized by segregation of local areas and their global integration during perception and behaviour. These functional interactions occur with synchronized activity between multiple local and distant brain regions and can be mapped in different networks: anatomical network, functional network, effective network. These represent patterns of anatomical links, of statistical dependencies, or of causal interactions, respectively. Normally, networks are formalized as a mathematical object consisting of a set of nodes and a set of links between the nodes. These can be quantitatively described by a set of local and global measures that characterize structural and functional regularities (Sporns, 2013).

To estimate functional relationships between two brain regions, different measures of synchrony have been applied. Among them are the wavelet phase coherence and Granger Causality (GC). The former is a practical method for the direct quantification of frequency-specific synchronization (i.e phase locking) between two neuroeletric signals. The latter identifies direct functional ("causal") interactions between two neuroeletric signals (Lachaux et al., 1999; Seth et al., 2015).

1.1 Objectives

Understanding the human brain is one of the most greatest challenges facing the 21st century science. The reasons are mostly because we still know little about the brain's complexity and because there are still many brain disorders like Alzheimer's, Schizophrenia, Autism, Epilepsy or traumatic brain injury that are incurable. Recently, several brain research initiatives have arisen all over the world such as the U.S. BRAIN initiative, the Europe's Human Brain Project or the Japan's Brain/MINDS. These projects aims to map the brain in a unprecedented detail, in terms of activity and anatomy and to develop theoretical neuroscience to make sense of it.

This thesis is in line with this world trend and has as foremost purpose to map brain circuits related to voluntary motor behaviour. For that, a time-frequency framework based on Wavelet Transform Coherence (WTC) is used to measure functional connectivity between pairs of brain regions on a specific narrow frequency band. This methodology

provides a measure of Phase Locking (PL) which has been associated to neural communications. Moreover, it allows to assess the statistical significance of PL values by mean of a surrogate-based statistical test.

Additionally, a complementary method based on the work developed by Seth et al. (2015) is followed. This aims to measure effective connectivity among different brain regions to the same specific frequency band according to Granger causality formulation. This method is based on multiple equivalent representations of a VAR model by regression parameters, the auto-covariance sequence and the cross power spectral density.

At last, this project aims to apply a new tool for network analysis, the "GraphVar", which allows one to do group and inter group comparisons of subjects and construct, characterize, and to do statistics on network topological measures (Kruschwitz et al., 2015).

1.2 Dissertation overview

The remainder of this dissertation is organized as described in this section.

Chapter 2 reviews the background literature related to the work developed in this dissertation. In particular, it provides lights on voluntary actions, their brain circuits and ongoing oscillation underpinning these actions, overviews the functional magnetic resonance imaging technique, and comes within the concept of brain connectivity, introducing brain networks, their types and topological measures, as well as a detailed explanation of some measures of signal synchrony relevant to this project.

Chapter 3 details the relevant materials for this study and explains the methodology followed in this project.

Chapter 4 summarizes the key results that show brain networks involved in self-paced motion.

Chapter 5 provides the overall conclusions and suggestions for future work.

CHAPTER 2

BACKGROUND

2.1 Voluntary movements

It is difficult to explain what makes a particular action voluntary. One of the most common ways to conceptualize voluntary action in cognitive neuroscience has been to contrast it with stimulus-driven actions (Goldberg, 1985). This distinction is based on the notion that action strongly guided by the environment are experienced as less volitional. For instances, the reflexes are immediate motor responses determined by stimulus which do not leave much space for volition. Considering this perspective, a voluntary action is defined as internally guided behaviour wherein the occurrence, timing and form are not directly determined. This conception of intentional action is quite controversial because the internally guided behaviour is difficult to define operationally since internal causes of behaviour are not experimentally tractable (Nachevemail and Husain, 2010; Schüür and Haggard, 2011). However a large number of studies have considered this conception and progress has been achieved.

The common experimental measurement procedure in which a known input or stimulus is delivered to a system and the system's response is measures can not be applied to voluntary action since it is stimulus-independent. To measure volition most experimental studies have given a stimulus or instruction that only partly determines what a participant should do, in one of three ways: the participant performs a fixed action but chooses when to do so (Libet et al., 1983);the participant performs an action at a specific time but chooses which of a number of actions to perform; or the participant chooses whether or not to perform an action (Brass and Haggard, 2010b). This methodology can be criticized because there is no reason or value that motivates the participant to choose one action over another, which fails to capture the context of natural human volition and because instructing a person to be voluntary is quite paradoxical. However it does capture the cognitive information generated by the participant needed to perform an action, which is

a key feature of voluntary action (Haggard, 2008).

To better understand voluntary action it is worth comparing them with reflex actions. Voluntary action involves the cerebral cortex, whereas some reflexes are purely spinal. Volition has a late maturation in individual development, whereas reflexes can be presented at or before birth. Finally, voluntary action involves the subjective experiences of "intention" and "agency" which are absent in reflexes. "Intention" is related to planning to do or being about to do something and the experience of "agency" is the later feeling that one's action caused a external event (Haggard, 2005).

2.1.1 Brain circuits

Several distinct cortical motor circuits that contribute to voluntary action have been identified in the human brain (Fig.2.1). These circuits converge on the Primary Motor Cortex (M1) which executes motor commands by transmitting them to the spinal cord and muscles (Haggard, 2008). The first circuit (FIG. 2.1a) starts with the input from the basal ganglia to the Supplementary Motor Area (SMA) which is thought to play the major part in the initiation of action. This linkage is based on studies of patients with Parkinson's disease which show less frequent and slower actions than healthy controls (Jahanshahi et al., 1995) and recordings from scalp electrodes that detected a signal of a forthcoming voluntary response, 2 seconds before the movement onset (Loukasa and Browna, 2004). Then, the input reaches the preSMA which forms part of a wider frontal cognitive-motor network that includes the premotor, the cingulate and the frontopolar cortices (Dum and Strick, 2005). Several neuroimaging studies have shown the strong activation of preSMA for self-paced actions (Deiber et al., 1999; Jenkins et al., 2000). Moreover, the role of the preSMA is confirmed by recordings from scalp electrodes, which show a prolonged and increasing negativity, the so called "readiness potential", that begins 1s or more before the onset of voluntary movement and which its early part has been localized in the preSMA (Shibasaki and Hallett, 2006). Finally, and as a result of the onset of the readiness potential (FIG. 2.1b), neural activity spreads from the preSMA back to SMA and M1, thus causing movement. The second circuit (FIG. 2.1a), starts in the early sensory cortices that relays the information to intermediate -level representations in the parietal lobe and thence to the lateral part of the premotor cortex, which projects in turn to M1 (Rizzolatti and Gd Luppino, 1998). This circuit plays a part in immediate sensory guidance of actions, however it also contributes to some aspects of voluntary behaviour. Thus, when a immediate action is required, the parietal- premotor circuit might arbitrate between action alternatives whereas, in the absence of immediate instruction, the basal ganglia-preSMA circuit might be more involved in initiation actions (Haggard, 2008).

2.1.2 Slow oscillations

Rhythmic oscillations in activity appear to be one of the hallmarks of brain physiology and are central to the way the brain process information. They range from very slow

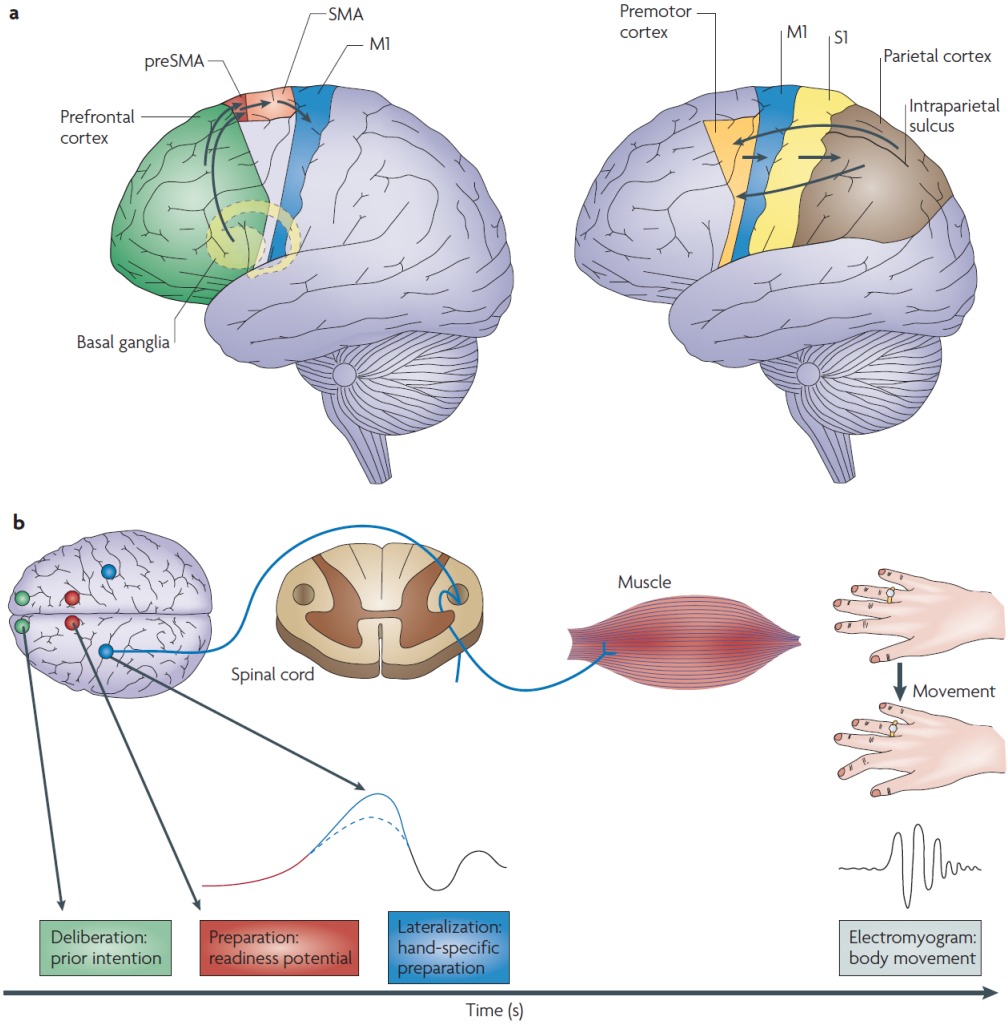

Figure 2.1: Brain circuits for voluntary action. a | Left-hand panel: The primary motor cortex (M1) receives a key input from the SMA and the preSMA, which in turn receives inputs from the basal ganglia and the prefrontal cortex. Right-hand panel: information from early sensory cortices (S1) is relayed to intermediate-level representations in the parietal cortex, and from there to the lateral part of the premotor cortex, which projects in turn to M1. b | Brain activity preceding a voluntary action of the right hand. The frontopolar cortex (shown in green) forms and deliberates long-range plans and intentions. The pre-SMA (shown in red) begins the preparation of the action with other premotor areas generating the readiness potentials (red trace) that can be recorded from the scalp. Immediately before the action takes place, M1 (shown in blue) becomes active. In later stages of preparation the contralateral hemisphere is more active than the ipsilateral hemisphere; this is reflected in a lateralized difference between the readiness potentials that are recorded over the two hemispheres of the brain (solid and dotted blue traces). Finally, neural signals leave M1 for the spinal cord and the contralateral hand muscles. The contraction of the muscles is measured as an electrical signal, the electromyogram. Adapted from (Haggard, 2008)

oscillations with periods of minutes to very fast oscillations with frequencies reaching 600 Hz. Slower oscillations, or fluctuations have been detected in the brain when this is at rest and include the frequencies between 0.01 and 0.5 Hz. (Someren et al., 2011). In this dissertation the term slow oscillation is attributed to oscillations in the band frequency of 0.01-0.1Hz.

The slow oscillations were first detected in local field potentials recordings from the rabbit neocortex (Aladjalova, 1957) but have since been observed in several other mammals (Filippov and Frolov, 2004; Filippov et al., 2007; Leopold et al., 2003) and are readily detectable in full band Electroencephalography (EEG) recordings from humans (Vanhatalo et al., 2004). They have been detected during sleep by several EEG methods (Achermann and Borbély, 1997; Nir et al., 2008) but their role in physiology of sleep is still poorly understood. It is believed that this very slow oscillations are well suited to coordinate activity across large corticocortical networks (Buzsaki, 2006) and that they could, in this way organize sleep-dependent neuroplastic processes such as the consolidation of episodic memory. In addition, these fluctuations have been shown influence the precipitation of certain types of epileptic seizures (Vanhatalo et al., 2004).

Fluctuations in brain activity below 0.1 Hz have also been observed in the BOLD fMRI signal (Biswal et al., 1995). These oscillations have evidenced correlated regions in the motor cortex and in other neuroanatomical systems including visual (Cordes et al., 2000; Lowe et al., 1998), auditory (Cordes et al., 2000), memory (Vincent et al., 2006), language (Hampson et al., 2002) and the most prominent, the default – mode network (Fransson, 2005).

In addition, slow arterial blood pressure, heart rate, oxygen availability of cortical tissue, cerebral blood-flow velocity, oxyhemoglobin changes and cerebrospinal fluid have shown oscillations around 0.1 Hz (Taga et al., 2000; Toronov et al., 2007; Tzeng et al., 2010; Vanhatalo et al., 2004; Zhang et al., 1998; Zheng et al., 2010). In particular, arterial blood pressure oscillations, the so called Mayer waves have evidenced a significant correlation with oscillations of sympathetic nerve activity. Studies have shown that these waves are not simply a surrogate of sympathetic nerve activity but they undoubtedly reflect the sympathetic response to perturbations in the overall baroreceptor –vascular system (Julien, 2006). However, the origin of these waves is still unknown.

The intriguing possibility that the slow oscillations may influence brain responses and other brain activities seems increasingly likely. It has been hypothesized that these oscillations reflect the excitability dynamics of cortical networks (Pfurtscheller et al., 2011). In particular, it has been investigated if these oscillations can be related to the intention to perform a motor act (Pfurtscheller et al., 2012a; Pfurtscheller et al., 2012b; Pfurtscheller et al., 2014a; Pfurtscheller et al., 2011).

2.2 Magnetic Resonance Imaging

Magnetic Resonance Imaging (MRI) is a non-invasive diagnosis technique used to image the anatomy and the physiological processes of the body. To do so, MRI focuses on the

atomic nuclei magnetic proprieties, in particular, those of the hydrogen atoms.

Hydrogen atoms are constituted by a single proton and are used in MRI due both to their magnetic proprieties and abundance in the human body. They can be seen as positively charged spheres that are spinning around their axis giving rise to a magnetic moment along the direction of the axis of the spins. This magnetic field is the source of the signal that is to be measured. In the absence of an external magnetic field the nuclei are randomly oriented and therefore do not give rise to a magnetic moment. In contrast, when placed into a strong magnetic field the nuclei stay align with the field creating a magnetization in the direction of the field. While aligned the nuclei precess about the field with an angular frequency determined by the Larmor frequency, but at a random phase with respect to one another.

In order to measure the magnetization of the nuclei one must perturb the equilibrium and "excite" the nuclei with a radiofrequency pulse. Radiofrequency causes the nuclei to absorb energy at a particular band frequency aligning their phases and tipping them over the transversal plane. With this pulse the longitudinal magnetization decreases and a new magnetization is established. After the radiofrequency pulse is removed, the system return to equilibrium disappearing the transversal magnetization (transversal relaxation) and growing back the longitudinal magnetization(longitudinal relaxation). The energy released is the signal that can be measure with a receiver coil.

The longitudinal relaxation is seen as an exponential recovery in magnetization described by time constant T_1 and transversal relaxation is seen as an exponential decay in magnetization described by a time constant T_2 caused by loss of phase coherence of the nuclei. These both times change from tissue to tissue providing the creation of MR images with a complete distinction between different tissue types. The term T_2^* is similar to T_2 but also consider the local inhomogeneities in the magnetic field created by changes in blood flow and oxygenation. In this case the nuclei de-phase quicker than they normally would. The T_2^* time underlies the fMRI technique as it detect neurovascular changes which follow psychological and behavioural functions.

2.2.1 functional Magnetic Resonance Imaging

functional Magnetic Resonance Imaging (fMRI) is a neuroimaging technique used to measure the hemodynamic response of the brain in relation to the neural activities. Basically, it measures changes in blood oxygenation and blood flow related to neuronal activity, providing the means to study human brain function in vivo, either in response to certain task or when at rest.

The mostly used method for performing fMRI uses the Blood Oxygenation Level Dependent (BOLD) contrast. Other methods are available, but less widely used such as Arterial Spin Labelling in its multiple variants. BOLD contrast mechanism relies upon the oxygenation level of blood. Red blood cells within the blood contain haemoglobin, which under normal circumstances is diamagnetic. However deoxygenated haemoglobin

is paramagnetic and hence forms local microscopic magnetic field gradients increasing proton dephasing. Neural activity is supported by a haemodynamic response in the local vasculature. This response leads to an increase in cerebral blood flow to the active region. This served to satisfy an increase in the rate of oxygen and glucose metabolism by increasing the delivery of these substrates. In practice the haemodynamic response oversupplies the active region with oxygenated blood, increasing blood oxygenation down-stream of the arteriole in the capillaries and veins. This reduces the concentration of paramagnetic deoxyhaemoglobin and hence reduces susceptibility induced dephasing. In turn this increases the relaxation time T_2^*. Thus, T_2^* weighted images are what enables fMRI to measures changes of oxygenation in the blood: a lower signal implies a higher concentration of deoxygenated haemoglobin than oxygenated haemoglobin while a higher signal implies a higher concentration of oxygenated haemoglobin than deoxygenated haemoglobin. Because neural activity elicits a substantial supply of oxygenated blood, a increase in signal in the correspondent voxel is expected, and this signal is the BOLD time-series (Filippi, 2009).

fMRI benefits of high spatial resolution compared with many other functional imaging modalities, such as Positron Emission Tomography (PET), Magnetoencephalography (MEG) and EEG. For humans studies it is on the order of 27-36mm^3. It has limiting factors such as the signal strength and the point-spread function of BOLD imaging, which typically extends beyond the actual neural activation sites into draining veins. Regarding data analysis, some choices limit the spatial resolution. For instances, spatially smoothing fMRI data prior to analysis leads to a decrease in the effective resolution of the data. Another issue is alignment of the individual brains through a registration or wrapping process which introduces substantial blurring and noise in a group average and limits the spacial resolution. However, advances in data aquisition and preprocessing can improve space resolution. For example, the use of multiple coils with different spacial sensitivities (parallel imaging) or the introduction of enhanced spatial inter-subject normalization techniques to avoid the most dramatic effects of blurring the data, respectively (deCharms, 2008), can be applied.

Regarding temporal limitations, fMRI temporal resolution ranges from 0.5 - 4.0 (TR) seconds in most of the research studies. These values are clearly incompatible with the underlying neuronal activity, which is on the order of tens of milliseconds. However, the statistical analysis of the fMRI data is primarily focused on oxygenation patterns taking place 5 - 8 seconds after activation. Thus, values in the range of 2 seconds have been considered adequate. Nevertheless, the currently used resolutions are not modelling physiological artefacts present in the fMRI signal. For instances, heart-rate and respiration give rise to periodic fluctuations that are difficult to model because the Nyquist criteria is violated. These fluctuations tend to be distributed throughout the time course because of the aliasing, giving rise to temporal autocorrelations in the signal. Also, they make up a large portion of the noise component which is a serious drawback. Recently, researchers have been involved in increasing the temporal resolution of fMRI studies, making TRs on

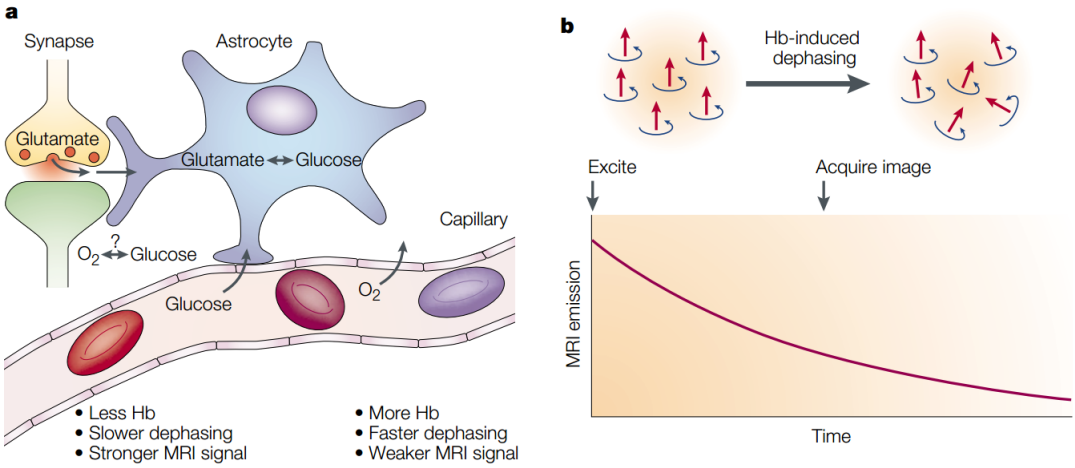

Figure 2.2: Upon activation, oxygen is extracted by the cells, thereby increasing the level of deoxyhaemoglobin in the blood. This is compensated for by an increase in blood flow in the vicinity of the active cells, leading to a increase in oxyhaemoglobin. An increase in the concentration of deoxyhaemoglobin would cause a decrease in image intensity, and a decrease in deoxyhaemoglobin would cause an increase in image intensity. Adapted from Heeger and Ress (2002)

the order of hundreds milliseconds. Recent technological developments designated by "simultaneous multi-slice" MRI, have sped up the temporal resolution by approximately an order of magnitude (from 2s to 0.2 s) and appear to offer the possibility to be faster (Faro and Mohamed, 2006).

2.3 Brain connectivity

In the history of neuroscience two extreme perspectives have alternated in an attempt to explain normal and impaired cognitive function of the brain: the perspective of functional localization and the perspective of functional segregation. One of the pionieers of functional segregation was the physician Franz Joseph Gall who promoted the idea that the brain forms the material basis for all mental function and that the brain is composed of numerous and independent cerebral "organs of mind", each devoted to a specific and innately specified mental faculty. This view was rapidly contested by opponents like the physiologist Jean Pierre Flourens who stated that the brain was a undifferentiated general-purpose organ where all sensations, perceptions, and volition resided concurrently. However, clinical studies of the effects of lesion in the human brain held by the physician and anthropologist Paul Broca, strongly supported the view that the integrity of specific mental functions depended on the integrity of specific brain regions. Furthermore, the anatomical studies of Korbinian Brodmann provided histological evidences for structural differentiation of the brain that lent further support to the perspective of functional localization. More recently, however, brain lesion studies (Absher and Benson., 1993) led to the

refutation of functional localization as a complete explanation of cortical organization in favor of functional specialization and integration as a more plausible theory. Nowadays, the understanding of the brain functioning follows these two principles of functional organization with connectivity as a mediator.

The functional organization of the brain has been characterized by principles of segregation of specialized neurons and brain areas, often organized into distinct neuronal populations, and integration between independent neuronal populations (Tononi et al., 1994). Lachaux et al. (1999) hypothesised the possibility that such integration could be mediated by neuronal groups, oscillating on specific narrow frequency bands, entering into a specific phase-locking over a limit period of time. Some years before, Roelfsema et al. (1997) reported evidence for long-range synchronizations between widely separated brain regions which was in accordance the notion that phase synchronization should subserve overall integration of all dimension cognitive acts, including associative memory, emotional tone and motor planning. Fries (2005) hypothesised that neural communication is mechanistically subserved by neural coherence, in other words the communication is due to a pattern of phase-locking among oscillations in the communicating neural groups. This was called "communication-through-coherence" (CTC) hypothesis and it is based on the fact that activated neuronal groups have the intrinsic property to oscillate and that those oscillations constitute rhythmic modulations in neuronal excitability that affects both the likelihood of spike output and the sensitivity to synaptic input. Thus, only coherence oscillating (or phase-locked) neuronal groups can communicate effectively, because their communication windows for input and for output are open at the same times (Fries, 2005).

2.3.1 Brain networks

A network (or graph) is a mathematical model of a real-world complex system and is defined by a collection of nodes (or vertices) and links (or connections) between pairs of nodes (Rubinov and Sporns, 2010). Nodes in large-scale brain networks usually represent brain regions, while links represent anatomical, functional or effective connections. Normally, the networks are represented by their connectivity (adjacency) matrices where rows and columns denotes the nodes and matrix entries denotes links. Figure (2.3) shows illustrative anatomical, functional and effective connectivity networks.

Anatomical connectivity networks: describe the fiber tracks linking spatially distant brain regions. The whole set of fiber tracks in the brain is called white matter linking cortical and subcortical regions. On short time scales (sec,min), anatomical connections are quite persistent and stable while for long time courses substantial plasticity may be observed. Currently only invasive tracking studies are capable of demonstrate direct axonal connections. Diffusion weighted imaging techniques, such as diffusion tensor imaging, have an insufficient spatial resolution, but are useful as whole brain in vivo markers of temporal changes in fiber tracks.

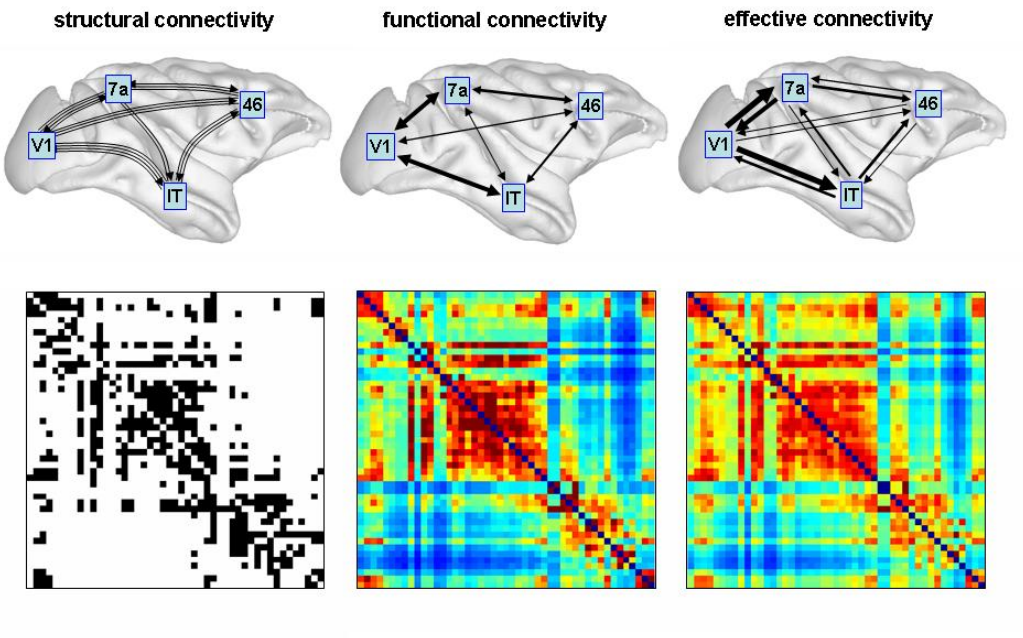

Figure 2.3: Examples of different types of brain connectivity networks and respective adjacency matrices. Adapted from http://www.scholarpedia.org/article/Brain_connectivity.

Functional connectivity networks: are expressed as statistical dependences between patterns of gray matter activity and thus does not necessarily reflect direct neural interactions along synaptic paths. Statistical dependences may be estimated by measuring cross-correlation, spectral coherence or mutual information from time series observation. Time series data may be derived with a variety of techniques, including EEG, MEG and fMRI. Functional connectivity is highly time-dependent exhibiting non-stationary fluctuations even with techniques that operate with a slow sampling rate such as fMRI.

Effective connectivity networks: describe the influence one neuronal system exerts upon another and provides directed networks that represent causal interactions between activated brain areas. It is not "model free" and requires the specification of a causal model including structural parameters. Experimentally, effective connectivity can be inferred through perturbations, or through the observation of the temporal ordering of neural events.

The generation of these networks involve the combination of brain mapping methods, anatomical parcellation schemes and measures of connectivity. The nodes normally can be defined based on regions from an atlas, such as the automated anatomical labelling atlas (Tzourio-Mazoyer et al., 2002) or voxel-based networks (Heuvel et al., 2008) where

small blocks of tissue represent each node. These parcellation schemes should completely cover the surface of the cortex, or of the entire brain, and individual nodes should not spatially overlap. Furthermore, as parcellation schemes may differ in their proprieties it should be used the same parcellation schemes in the network construction so that these could be compared.

Links can also be differentiated on the basis of their weight and directionality (Fig.2.4). Binary links denote the presence or absence of connections and weighted links contain information about connection strength. Weights in anatomical networks may represent the size, density, or coherence of anatomical tracts, while weights in functional and effective networks may represent respective magnitudes of correlation or causal interactions. Binary networks are in most cases simpler to characterize comparing to the weighted although weighted characterization usually focuses on different aspects of networks organization and may be useful in filtering the non-significant links. The weak and non-significant links tend to obscure the topology of strong and significant connections and when applying an absolute or weighted threshold are normally discarded. Usually, thresholds values are arbitrary determined and the networks should be characterized across a broad range of thresholds. Another characteristic of the link is that they can have directionality. Thus, effective connections can be represented with direct links (Sporns, 2011).

2.3.2 Topological measures of brain networks

Brain networks can be quantitatively described by a wide variety of measures. These variously detect aspects of functional integration and segregation, quantify importance of individual brain regions and characterize patterns of local anatomical circuitry. Network measures can be represented as measures of individual networks elements (nodes and links) which typically quantify connectivity profiles associated with these elements and hence reflect the way in which they are embedded in the network, or a measure of all individual elements providing a more global description of the network (i.e normally characterized by its mean). In addition, network measures also have binary and weighted, direct and undirected variants (Sporns, 2011).

- **Node Degree:** measures the number of links connected to the node. Connection weights are ignored in calculations;
- **Strength:** is the sum of weights of links connected to the node;
- **Clustering coefficient:** defined locally as the fraction of triangles around and individual node. It is equivalent to the fraction of that node's neighbours that are also each other's neighbours;
- **Modularity:** Statistical measurement that determines the number of non-overlapping modules
- **Characteristic path length:** is the average shortest path length in the network.

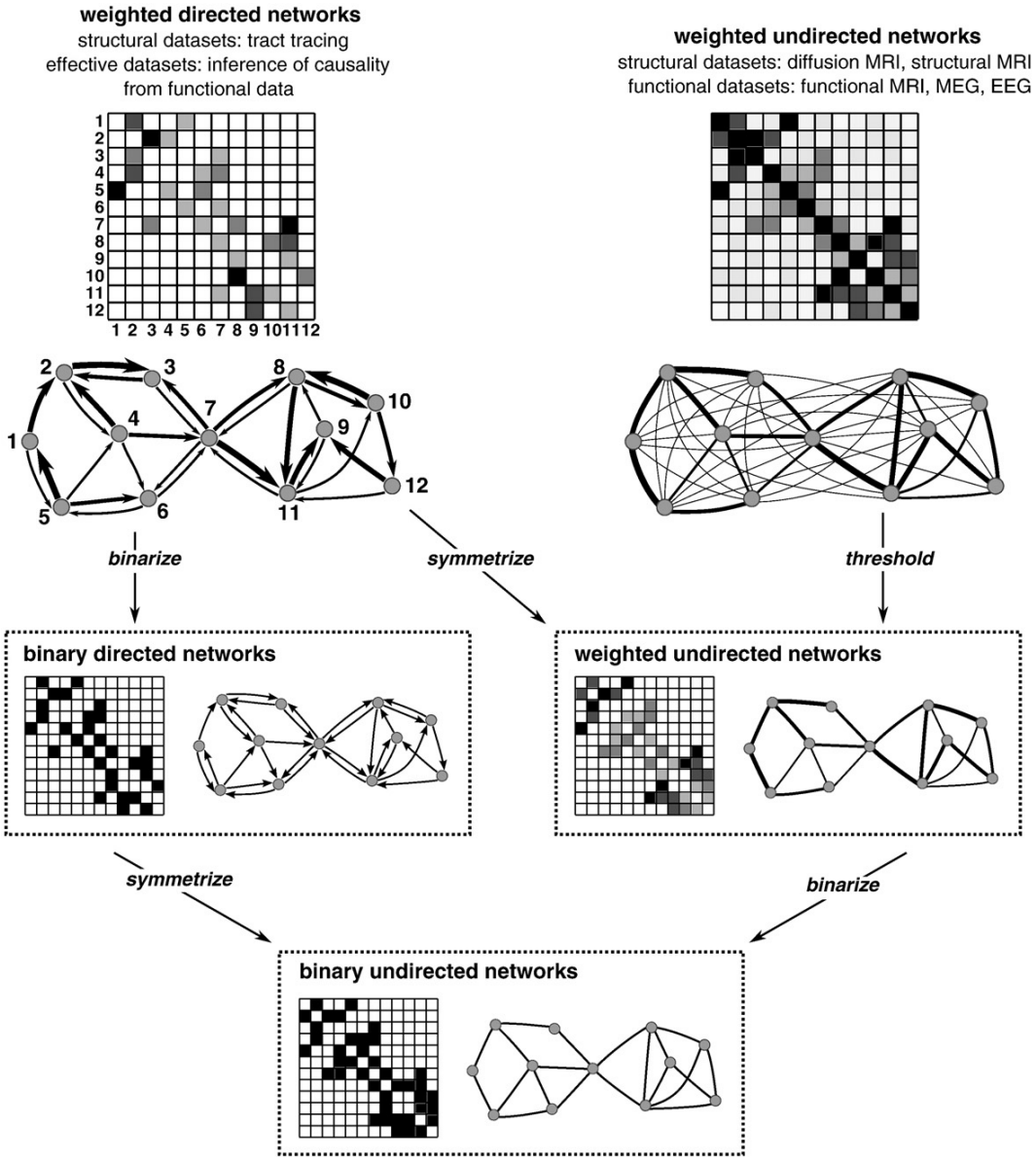

Figure 2.4: Illustration of brain networks from anatomical and functional datasets. Networks are commonly represented by their connectivity matrices, with rows and columns representing nodes and matrix entries representing links. To simplify analysis, networks are often reduced to a sparse binary undirected form, through thresholding, binarizing, and symmetrizing. Adapted from (Rubinov and Sporns, 2010)

- **Global efficiency:** is the average inverse shortest path length in the network, and is inversely related to the characteristic path length.
- **Betweenness centrality:** Node betweenness centrality is the fraction of all shortest paths in the network that contain given node. Nodes with high values of betweenness centrality participate in a large number of shortest paths;
- **Functional motifs:** are subsets of connection patterns embedded within structural motifs.
- **Radius:** is the minimum eccentricity and the diameter is the maximum eccentricity.
- **Paths:** are sequences of linked nodes that never visit a single node more than once.
- **Assortativity:** is a correlation coefficient between the degrees of all nodes on two opposite ends of the link. A positive assortativity coefficient indicates that nodes tend to link to other nodes with the same or similar degree.

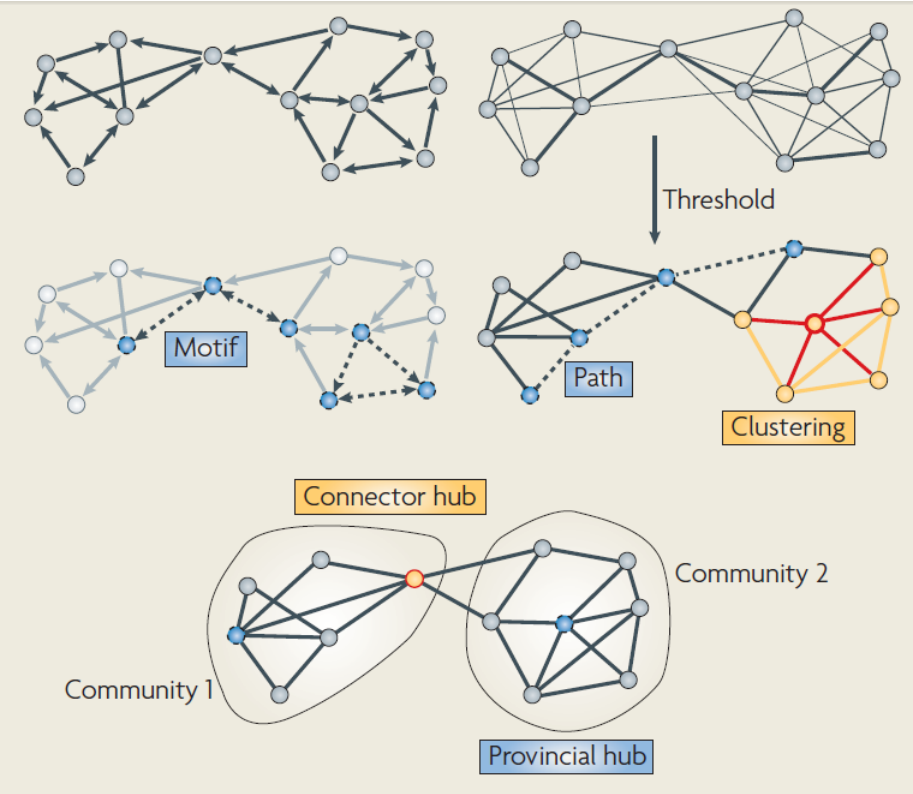

Figure 2.5: The figure shows a schematic diagram of a brain network drawn as a direct(left) and an undirected (right) graph as well as different structures such as nodes, links, a hub, motif, the representation of clustering, communities and Paths. Adapted from (Bullmore and Sporns, 2009)

2.3.3 Measures of neuronal signal synchrony

Most cognitive processes are based on the synchronized interactions of a large number of neurons within and across different specialized brain regions. To quantify that synchrony different measures have emerged in the last decades. A measure of signal synchrony is a value of synchrony between different two or more continuous time series of brain activity. Independent time series yield low values of synchrony while strong correlated time series yield high values. These measures can be separated into two groups, those with a linear behaviour such as the cross correlation or the cross-coherence and those with a non-linear behaviour such as mutual information, transfer entropy, Granger causality and phase synchronization.

2.3.3.1 Cross-correlation

Cross-correlation is one of the most traditional methods in functional connectivity. It provides a measure of similarity between two normalized series, $X(t)$ and $Y(t)$,with zero mean, unit variance and considering N pairs of observations, as a function of the lag (τ) of one relative to the other,

$$C_{xy}(\tau) = \frac{1}{N-\tau} \sum_{k=1}^{N-\tau} X(k+\tau)Y(k) \tag{2.1}$$

where $C_{xy}(\tau)$ is the correlation coefficient. It ranges from -1 to 1 , a complete inverse correlation to a complete direct correlation respectively, where 0 suggest no interdependence between variables (Pereda et al., 2005). When the time series are highly direct correlated that means that the two regions are on average active at the same time. In contrast, a high inverse correlation implies that one region is more active and the other is less active (Biswal et al., 1995). When τ is zero the cross-correlation is Person's product moment correlation coefficient (Pereda et al., 2005).

2.3.3.2 Cross-coherence

The coherence function (Wiener, 1930) corresponds to the calculation of the previous measure but as a function of frequency. It is defined as:

$$\varrho(f) = \frac{|S_{xy}(f)|}{[S_{xx}(f).S_{yy}(f)]^{1/2}} \tag{2.2}$$

where $S_{xy}(f)$ is the cross-spectral density between the two variables $X(t)$ and $Y(t)$ derived from the Fourier transform of the cross-correlation function (cross correlation number) (Lachaux et al., 2002).

The coherence estimation, based on Fourier analysis, has been repeatedly used in neuroscience, with the assumption that neural signals are stationary (Thatcher, 1995; Tremblay et al., 1994). However, non-stationarity is the rule rather than the exception in neural processing (Graya et al., 1992; Stiber and Sato., 1997). Thus, when dealing with

non-stationary signals, it is recommended that, instead of Fourier analysis, time-frequency analysis be used (i.e wavelet coherence analysis), where the spectrum is estimated as a function of time (Auger et al., 1997).

Wavelet Coherence Analysis

Wavelets are functions with zero mean which are localized in both frequency and time and are used in signals decomposition. The Morlet wavelet is one of the most used since it is simple and well suited for spectral estimations. It is defined for frequency f and time τ as:

$$\psi_{\tau,f}(u) = \sqrt{f}.exp(i2\pi f(u-\tau)).exp(-\frac{(u-\tau)^2}{\sigma^2}) \tag{2.3}$$

where $\psi_{\tau,f}(u)$ is simply the product of a sinusoidal wave at frequency f, with Gaussian function centred at time τ with a standard deviation σ proportional to the inverse of f, such that the number of cycles of the wavelet is the same for all frequencies.

A important feature of wavelet analysis is that the size of the window adapts to the frequency of the signal. For low frequencies, the wavelet analysis uses a long time window and for high frequencies it uses a narrow time window improving the temporal resolution (δ) of the coherence estimate. Thus,it becomes possible to follow the variations of coherence in time.

The wavelet transform of a signal $x(u)$ is a function of time (τ) and frequency (f) given by the convolution of x with the Morlet wavelet where * denotes the complex conjugate:

$$W_x(\tau,f) = \int_+^- x(u).\psi^*_{\tau,f}(u)du \tag{2.4}$$

From the wavelet transforms of two signals $X(t)$ and $Y(t)$, we can define the wavelet cross-spectrum between X and Y around time t and frequency f by:

$$SW_{xy}(t,f) = \int_{t-\frac{\delta}{2}}^{t+\frac{\delta}{2}} W_x(\tau,f).W^*_y(\tau,f)d\tau \tag{2.5}$$

where δ is a scalar that can depend on frequency (Lachaux et al., 2002).

Finally, similar to the Fourier-based coherence $\varrho(f)$ introduced above, the wavelet coherence $WCo(t,f)$ is defined at time t and frequency f by

$$WCo(t,f) = \frac{|SW_{xy}(t,f)|}{[SW_{xx}(t,f).SW_{yy}(t,f)]^{\frac{1}{2}}} \tag{2.6}$$

Several other tools have been developed for time-frequency analysis and can be applied efficiently to physiological signals, for instances the pseudo-smoothed Wigner-Ville (Lachaux et al., 1999) or the Choi-Williams transform (Bonato et al., 1996). However, the utility of wavelet analysis is that it provides not only the time-varying power-spectrum, but also the phase spectrum, which is needed to compute the coherence.

2.3.3.3 Phase Synchronization

Among different measures of phase synchronization, the phase locking is the most common used in neurophysiology. This measure consists in the persistence of a near constant phase difference between two time series, $X(t)$ and $Y(t)$ over a time period. To compute phase synchronization different methods can be used such as the Hilbert transform or the wavelet coherence.

Wavelet Phase Coherence

Wavelet phase coherence is a further elaboration of coherence that allows one to focus only on the phase relationships between two signals. This measure is used to detect phase locking between two signals and can be estimated efficiently with wavelet analysis. It expresses the extent to which phase difference changes within the time window, regardless of its value. Considering $X_f^{'}$ and $Y_f^{'}$ the correlation between $X(t)$ and $Y(t)$ at frequency f (coherence) and that instantaneous phase difference between $X_f^{'}$ and $Y_f^{'}$ at time τ is given by the angle of $W_{y'f}(\tau).W_{x'f}^{*}(\tau)$, phase coherence is defined as:

$$PLV(f,t) = |\frac{1}{\delta}\int_{t-\frac{\delta}{2}}^{t+\frac{\delta}{2}} \frac{W_{y'f}(\tau)}{|W_{y'f}(\tau)|}.\frac{W_{x'f}^{*}(\tau)}{|W_{x'f}(\tau)|}d\tau| \tag{2.7}$$

where the resulting phase locking indexes vary from 0 to 1 and are averaged values for each $[t-\frac{\delta}{2}; t+\frac{\delta}{2}]$ time window (Lachaux et al., 1999).

2.3.3.4 Granger Causality

Granger causality is a statistical concept based on the simple idea that causes both precede and help predict their effects. It was traced conceptually to Wiener (Wiener, 1956) and formulated by Granger (Granger, 1969) in the context of linear vector autoregressive (VAR) modelling of stochastic processes. Simply, it states that considering two jointly stationary stochastic time-series variables $X(t)$, $Y(t)$, if the prediction of certain time-series variable $X(t)$ can be improved by incorporating the knowledge of the past of a second time-series variable $Y(t)$, then $Y(t)$ is said to G-causes $X(t)$. The computational strategy for implementing G-causality analysis rest on estimating and comparing two VAR models, a restricted VAR model (2.8) that only looks at the past of $X(t)$ and a unrestricted MVAR model (2.10) that also includes the past of $Y(t)$:

$$X(t) = \sum_{j=1}^{p} A_{11,j}X_{t-j} + \epsilon_{1t}, var(\epsilon_1 t) = \Sigma_1. \tag{2.8}$$

$$Y(t) = \sum_{j=1}^{p} A_{12,j}Y_{t-j} + \eta_{1t}, var(\eta_1 t) = \Gamma_1. \tag{2.9}$$

$$X_t = \sum_{j=1}^{p} A_{11,j}X_{t-j} + \sum_{j=1}^{p} A_{12,j}Y_{t-j} + \epsilon_{2t}, var(\epsilon_{2t}) = \Sigma_2 \tag{2.10}$$

In the equations above p represents the maximum number of lagged observations included in the model (model order), the $A_{11,j}$ and $A_{12,j}$ contains the coefficients of the model, and Σ_2 is the residual covariance matrix (prediction errors) for each time series. In the equations (2.8) and (2.10) the value of Σ_1 measures the accuracy of the autoregressive prediction of $X(t)$ based on its previous values. Σ_2 represents the accuracy of predicting the present value of $X(t)$ based on the previous values of both $X(t)$ and $Y(t)$. If Σ_2 is smaller than Σ_1 in a suitable statistical sense, $Y(t)$ have a causal influence on $X(t)$ which can be quantified by

$$F_{Y\to X} = ln\frac{\Sigma_1}{\Sigma_2} \tag{2.11}$$

The value of $F_{Y\to X} = 0$ when there is no causal influence from Y to X and $F_{Y\to X} > 0$ when there is. The same happens when one defines causal influence from X to Y.

This standard approach has been predominantly followed in the context of neuroimaging applications, however nonlinear extensions of Granger causality have been developed such as Freiwald's approach (Freiwald et al., 1999) wherein the globally nonlinear data is divided into locally linear neighbourhoods, and Ancona's approach (Ancona et al., 2004) where it is used a radial basis function method to perform a global nonlinear regression.

With more then two time series, the above bivariate approach may lead to ambiguous results in terms of differentiating direct from mediated causal influences. In these cases Granger causality is easy to generalize to the multivariate case (pairwise-conditional GC) in which the G-causality of $Y(t)$ on $X(t)$ is tested in the context of multiple additional variables $Z(t)$, etc (Geweke, 1984).

$$X(t) = \sum_{j=1}^{p} a_{3j}X_{t-j} + \sum_{j=1}^{p} b_{3j}Z_{t-j} + \epsilon_{3t}, var(\epsilon_{3t}) = \Sigma_3 \tag{2.12}$$

$$X_t = \sum_{j=1}^{p} a_{4j}X_{t-j} + \sum_{j=1}^{p} b_{4j}Y_{t-j} + \sum_{j=1}^{p} c_{4j}Z_{t-j} + \epsilon_{4t}, var(\epsilon_{4t}) = \Sigma_4 \tag{2.13}$$

In this case $Y(t)$ G-causes $X(t)$ if knowing $Y(t)$ reduces the variance in $X(t)$'s prediction error when all other variables $Z(t)...Z(n)$ are also included in the regression model. The Granger causality from $Y(t)$ to $X(t)$ conditional on $Z(t)$ is defined as

$$F_{Y\to X|Z} = ln\frac{\Sigma_3}{\Sigma_4} \tag{2.14}$$

If $F_{Y\to X|Z} > 0$ then the inclusion of $Y(t)$ results in improved prediction of $X(t)$, indicating that $Y \to X$ has a direct component. In contrast, if $F_{Y\to X|Z} = 0$, the influence $Y \to X$ is said to be entirely mediated by $Z(t)$.

An important spectral decomposition of GC was proposed by Geweke in 1984 (GGC) (Geweke, 1984). This decomposition is additive meaning that the sum of all the frequency components from zero to the Nyquist frequency result in the Granger causality.

After Fourier transforming the bivariate autoregressive representation (2.10) a spectral density matrix is obtained.

$$S(f) = H(f)\Sigma H^*(f), \tag{2.15}$$

where * denotes the complex conjugate and matrix transpose, Σ is the covariance matrix of the model error terms and $H(f)$ is the transfer function matrix. Then the GGC influence of time-series $X(t)$ and $Y(t)$ can be computed as a function of frequency f:

$$f_{Y\to X}(f) = ln\frac{S_{11}(f)}{S_{11}(f) - (\Sigma_{22} - \frac{\Sigma_{12}^2}{\Sigma_{11}})|H_{12}(f)|^2} \tag{2.16}$$

The intrinsic spectral power of the time-series $X(t)$ in the denominator is obtained by subtracting the causal part from the total spectral power. If there are more than two time-series in the dataset, for instances the subset $Z(t)$ from (2.12) and (2.13), the formula (1.13) is not valid because the denominator does not exclusively reflect the intrinsic power any longer. Therefore, in order to implement the pairwise-conditional analysis, Geweke (Geweke, 1984) proposed a different method assuming the equivalence: $f_{Y\to X|Z}(f) = f_{Y\psi\to\Theta}(f)$

$$\left.\begin{aligned}\begin{pmatrix} X(f) \\ Z(f) \end{pmatrix} &= \begin{pmatrix} G_{11}(f) & G_{13}(f) \\ G_{31}(f) & G_{33}(f) \end{pmatrix} \begin{pmatrix} \Theta(f) \\ \Psi(f) \end{pmatrix} \\ \begin{pmatrix} X(f) \\ Y(f) \\ Z(f) \end{pmatrix} &= \begin{pmatrix} H_{11}(f) & H_{12}(f) & H_{13}(f) \\ H_{21}(f) & H_{22}(f) & H_{23}(f) \\ H_{31}(f) & H_{32}(f) & H_{33}(f) \end{pmatrix} \begin{pmatrix} E_1(f) \\ E_2(f) \\ E_3(f) \end{pmatrix}\end{aligned}\right\} \begin{pmatrix} \Theta(f) \\ Y(f) \\ \Psi(f) \end{pmatrix} = \\ = \begin{pmatrix} Q_{11}(f) & Q_{12}(f) & Q_{13}(f) \\ Q_{21}(f) & Q_{22}(f) & Q_{23}(f) \\ Q_{31}(f) & Q_{32}(f) & Q_{33}(f) \end{pmatrix} \begin{pmatrix} E_\Theta(f) \\ E_Y(f) \\ E_\Psi(f) \end{pmatrix} \tag{2.17}$$

The spectrum of Θ can be computed by:

$$S_\Theta(f) = Q_{11}(f)\Sigma_{11}Q_{11}^*(f) + Q_{12}(f)\Sigma_{22}Q_{12}^*(f) + Q_{13}(f)\Sigma_{33}Q_{13}^*(f) \tag{2.18}$$

where $*$ denotes complex conjugate and Σ is the covariance matrix of the rightmost model error term in (2.17). GGC can be computed as the ratio of total power to intrinsic power:

$$f_{Y\to X|Z}(f) = f_{Y\Psi\to\Theta}(f) = ln\frac{S_{|\Theta}(f)|}{|Q_{11}(f)\Sigma_{11}Q_{11}^*(f)|} \tag{2.19}$$

CHAPTER 3

MATERIALS AND METHODS

In this Chapter an explanation of how this study was conducted is presented. Firstly, the chapter starts by describing the participants involved as well as the image acquisition and data pre-processing methods followed in this study. Secondly, a detailed explanation of the main methodology implemented based on Wavelet Transform Coherence and the complementary methodology implemented to extract causal interactions between time series is given. Finally, it is introduced a recent software, the "GraphVar", and performed graph theoretical analysis from the connectivity matrices.

3.1 Participants, Image acquisition and data pre-processing

A total of 25 participants (12 female) between 19-34 years (mean+-SD: 24 years+- 3.2) took part in the study. All were naive to the purpose of the study, had no former MRI experience, had normal or corrected-to-normal vision and were without any record of neurological or psychiatric disorders as assessed via self-report. All subjects gave informed written consent to the study protocol which had been approved by the local Ethics Committee at the University of Graz. The experimental task consisted of 2 resting sessions of 5 minutes each and 2 movement sessions of 10 minutes each (SELF and VIS) in between. In the first movement task (SELF), the subjects were instructed to press a button voluntarily (at free will) with their right hand; no further instruction was given. In the second movement task (VIS), the subjects were instructed to press the button whenever a visual cue was presented. The cue stimulus was presented in regular intervals of 10 s. Subjects were requested to keep their eyes open, stay awake, and avoid movements during rest. Each subject was scanned twice in two consecutive days. These acquisitions are henceforth called "a" and "b" sessions.

Functional images were acquired on a 3.0-T scanner (Magnetom Skyra, Siemens). A multiband echo planar Imaging (EPI) sequence with a multiband factor of 6 was applied

with the following features: voxel size of $2x2x2mm^3$, TR/TE = 871/34 ms, flip angle=52°, matrix $90x104$, 66 contiguous axial slices, FOV = $180x208mm^2$. 400 volumes and 650 volumes were acquired for rest and motion sessions, respectively. Pre-processing was done using the DPARSF toolbox (Chao-Gan and Yu-Feng, 2010) and included the removal of the first 10 volumes (to ensure signal stability), slice-timing correction, motion correction, normalization to MNI space by using the T1 images, resampling to $2mm$ isotropic voxels, spatial smoothing with a $4mm$ FWHM Gaussian kernel and linear detrending. Slice time correction followed an approach specific for multiband sequences (Woletz et al., 2014). Lastly, the BOLD time courses of all 116 regions from the AAL atlas (Tzourio-Mazoyer et al., 2002) were extracted using the same DPARSF toolbox.

3.2 Methodology 1

In the current study a time-frequency analysis based on Wavelet Transform Coherence (WTC) is applied. WTC is an approach for analyzing the coherence and phase lag between two time-series that contain nonstationary power, as a function of both time and frequency (Torrence and Compo, 1998). Generally, it has been used in the analysis of dense temporal sampling signals (e.g EEG and MEG), however its ability to achieve temporal and spectral specificity in the case of slower signals such as fMRI time-series has been demonstrated in several studies (Chang and Glover, 2010; Müller et al., 2004).

By computing WTC, one can extract time-frequency maps of phase coherence involving the instantaneous phase values associated with each time-series. These provide a measure of Phase Locking value (PLV) which reflects the stability of phase difference across an user defined time window of length delta. If the phase difference is perfectly stable and constant over the time window, PLV has the value 1 whereas PLV = 0 indicates maximal variability of phase difference.

This methodology was applied using the "Cross wavelet and wavelet coherence" toolbox implemented in Matlab (Grinsted et al., 2004). Figure 3.1 summarizes the two main sections of the method. Firstly, WTC between pairs of fMRI time-series associated with ROIs (Regions of Interest) defined previously from a user-chosen atlas is computed (1st Section). This provides phase difference profiles that are used to compute PLVs. Then a statistical test is applied in order to detect the significant periods of phase locking profiles (2nd section). This section is divided into three subsections (1, 2, and 3) where the first presents a surrogate approach to build a statistical distribution, the second calculates the PL indexes based on surrogates to define a threshold of significance and the latter identifies the significant PLVs.

3.2.1 Wavelet Coherence Analysis - Phase Locking

This method applies a continuous wavelet function based on the Morlet wavelet function, consisting of a plane wave modulated by a Gaussian, due to its simplicity and widespread

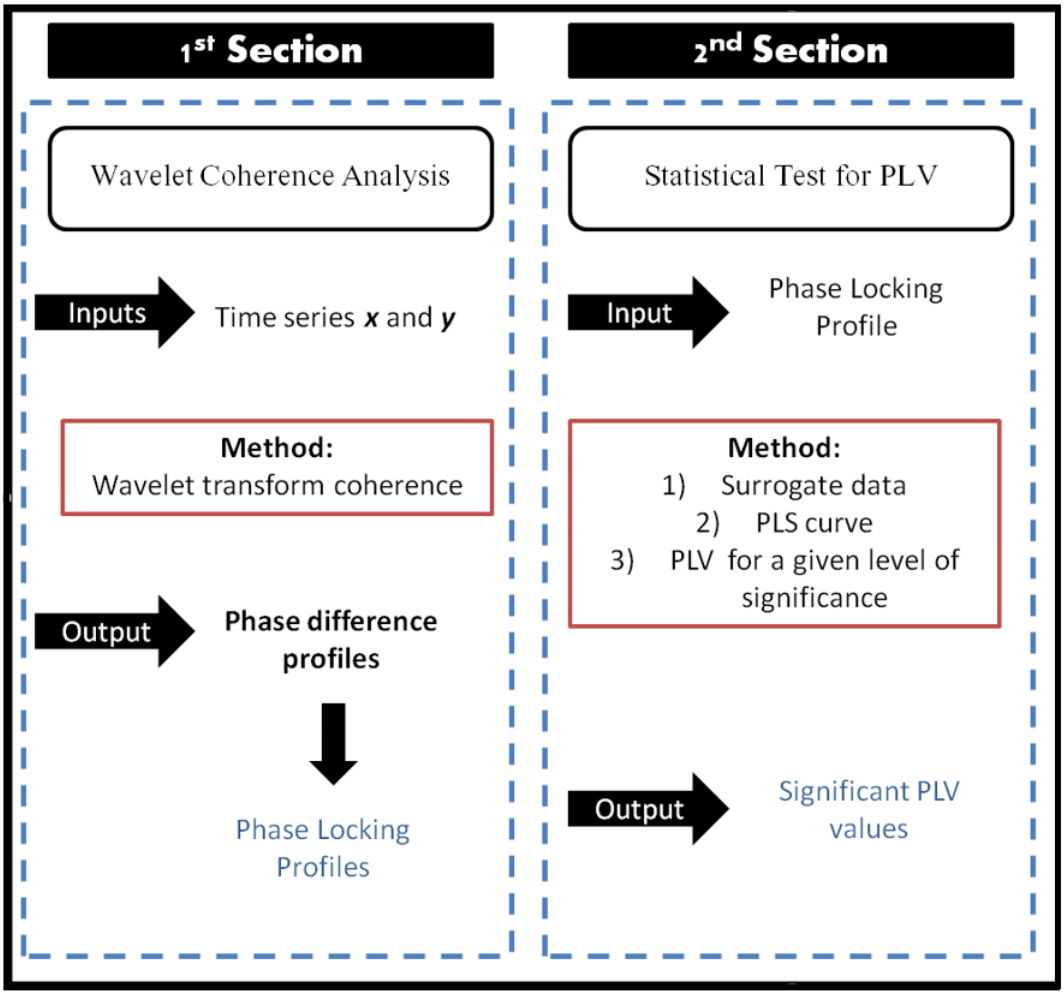

Figure 3.1: Analysis scheme for the two main sections of the methodology. The first section is based on Wavelet Coherence computation for time series x and y extracted from the ROIs of interest. The outputs from this step are the phase difference profiles from which the phase locking profiles are obtained. In the second section a statistical test is performed for phase-locking values (PLV) using the output from the first step as input to this section. A surrogate approach is applied followed by computation of the PLV values of surrogate pairs (Phase-Locking Statistics=PLS) and identification of PLV values (from the first section) above a user-defined significance level. Adapted from (Brito, 2014)

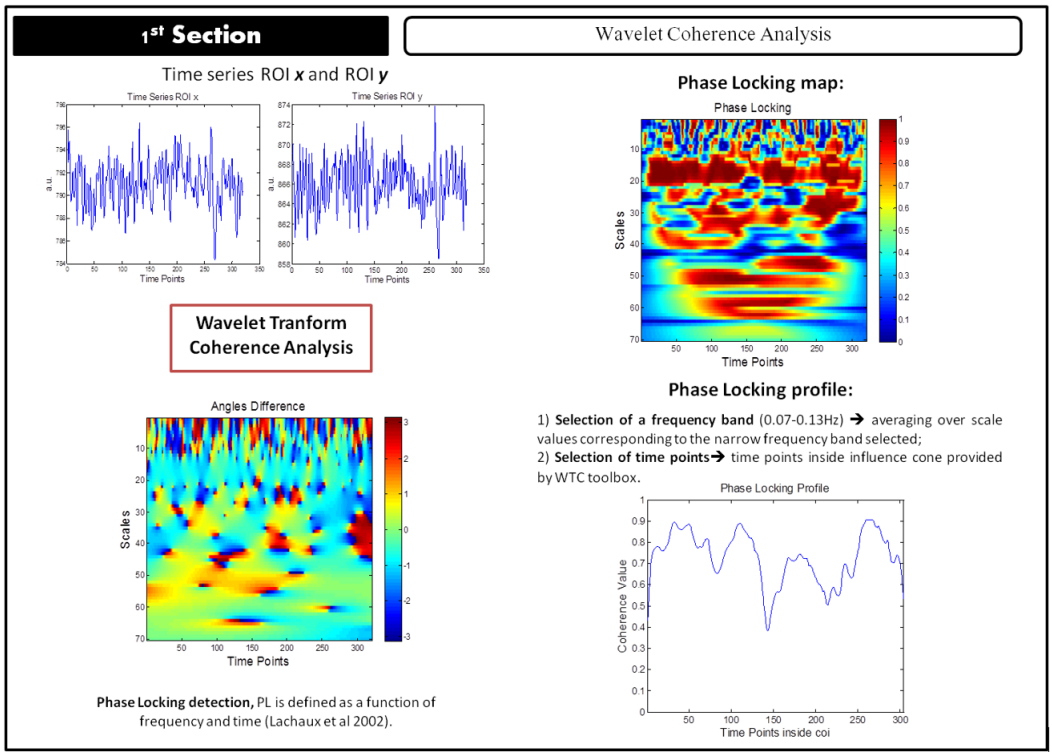

Figure 3.2: Analysis scheme for the first section. From WTC the Angle/Phase differences maps over all time points and scales (time-frequency analysis) are obtained, followed by computation of the phase-locking map. In order to obtain phase-locking profiles, a frequency band is selected (in this example: $0.07 - 0.13Hz$) and the values corresponding to the selected frequencies are averaged and plotted as a function of time. Points outside the cone of influence are excluded. Adapted from (Brito, 2014)

use in neuroscience studies (Chang and Glover, 2010; Lachaux et al., 1999; Lachaux et al., 2002).

After the extraction of BOLD time courses by pre-processing as explained in "Participants, Image acquisition and pre-processing" section, pairs of time-courses were used as inputs in the WTC function provided by the DPARSF toolbox (Figure 3.2). As output, time-frequency maps were obtained containing phase differences across the time. The process was performed for all 116 AAL brain regions. Through phase difference values, a phase locking measure was calculated by computing the phase coherence integration (Equation 2.7) across a defined time-window. Hence, time-frequency maps of phase locking are extracted for each pair of ROIs. In order to analyse slow oscillations (around 0.1 Hz), a frequency band was selected (0.07 - 0.13 Hz) and the PL values were averaged giving rise to PL time profiles that could be plotted for visualization purposes. At this point, it was necessary to exclude from the averaging all the time points outside the so called "cone of influence" (Torrence and Compo, 1998), since these points were affected by edge effects that make them unreliable.

3.2.2 Statistical Test - Length of significant Phase Locking segments

The second section of the method consists in to build a statistical test to differentiate significant phase-locking values against background fluctuations. Since there is no prior knowledge of PLV statistics and following previous work (Hurtado et al., 2004; Lachaux et al., 1999) a surrogate-based statistical test is applied in order to distinguish between significant PLV-values. This test consists on the generation of a large set of surrogate time-series that share some statistical features with the original data in order to achieve a distribution under the null hypothesis of independent pairs of oscillatory activity. Thus, only values that depart significantly from what would be expected for independent oscillators can be considered as revealing the presence of phase locking. This surrogate statistical test allows determining the PLV values corresponding to any user-chosen significant level, for each time bin. The user can restrict the analysis only to those segments of the time-series whose PLVs are above the significant threshold.

Firstly, the generation of surrogate data was performed by applying the Hilbert Transform to a given time-series in order to achieve the instantaneous phase and frequencies. Then, it was made a random permutation of the instantaneous frequency vector by N times to obtain N frequency vectors. These allowed to create N surrogates having the same power spectrum as the original time-series. The last step was the phase reconstruction. The statistical test was repeated for all ROIs of interest.

Once generated the surrogate data, the WTC approach was applied to all N surrogate pairs generated from the two initial ROIs of interest giving rise to N surrogate phase locking profiles. From these, the empirical distribution of the PLVs for each time point of each surrogate was obtained and a percentile curve with 95% cutoff value was created (95th percentile curve). Thus, only PL index values that were on the high end of the distribution (95th percentile) could be considered to indicate the presence of phase locking. This percentile curve was named Phase Locking Statistic curve and could be plotted alongside the PLV plot for any ROI pair thereby providing a visual overview of significant and non-significant PL periods (Figure 3.2). The reader is referred to Hurtado et al. (2004) for a more detailed treatment of WTC.

3.3 Methodology 2

Granger causality measures the directed influence between two neural time series. This concept was proposed by Wiener (Wiener, 1956) and relies on the notion that if prediction of certain time-series variable is improved by the knowledge of the past of a second time-series variable, then the second variable has a causal influence on the first. Granger operationalized this dependence on temporal precedence in the context of linear autoregressive modelling of stochastic processes (Granger, 1969).

In the current project Granger causality was applied using the MVGC Toolbox implemented in Matlab (Seth and Barnett, 2014). This toolbox allows calculating multivariate

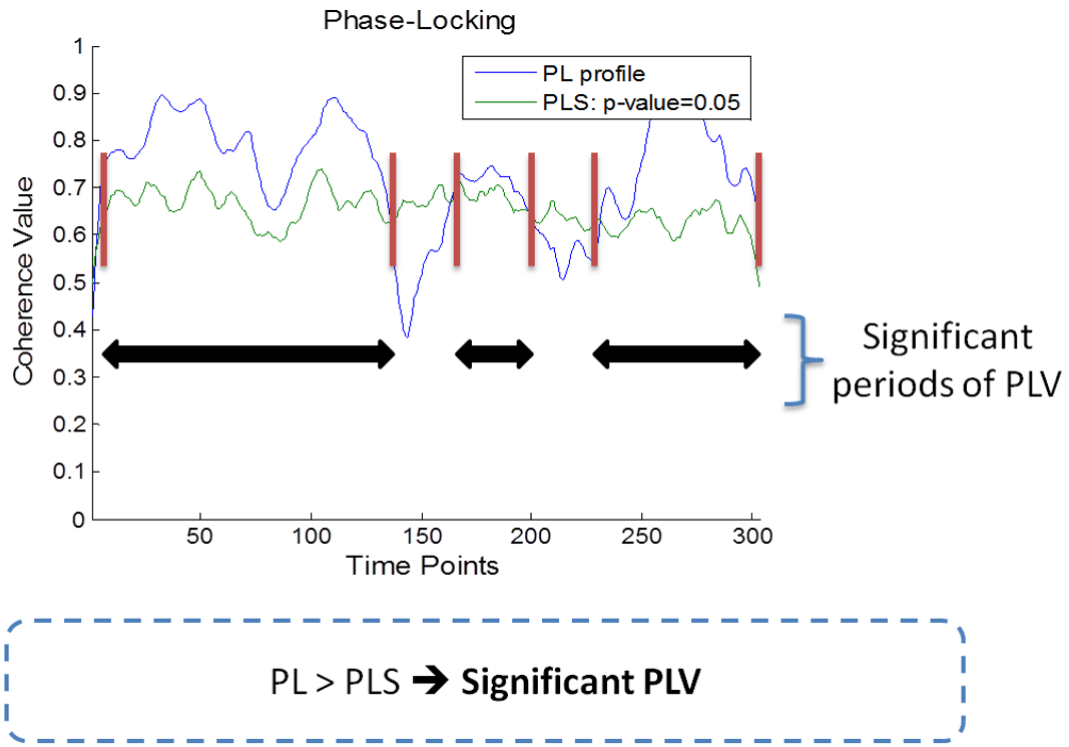

Figure 3.3: Phase-locking analysis. In blue: Phase-locking (PL) profile for a sample pair of ROI signals. In green: Phase-Locking Statistics (PLS) curve corresponding to p<0.05. Adapted from (Brito, 2014)

Granger causality(MVGC) from time series data, both unconditional and conditional, in the time and frequency domains. Figure 3.4 outlines the method followed here.

3.3.1 Granger Causality Analysis

The current method involves the computation of pairwise-conditional Granger Causality matrices to the same narrow band frequencies used in the methodology 1 ([0.07;0.13] Hz). The BOLD time-series were extracted by pre-processing the fMRI raw data as explained in "Participants, Image acquisition and data pre-processing" section.

The first stage of this methodology was to determine an appropriate model order (p) for the regression. This was done by applying the standard techniques, Akaike Information Criterion(AIC) and Bayesian Information Criterion (BIC). After that, a VAR model was fitted to the time series data just once and all the subsequent calculation were based on the estimated model parameters A_k, Σ. Then, the autocovariance sequence (Γ_k) was calculated. (Γ_k) measures how strongly a time series is related with itself p samples later or earlier. This matrix is computed because through it can be extracted the reduced regression VAR parameters needed to calculate G-causality. From the autocovariance sequence, Granger causality in the frequency domain was computed. In order to average (integrate) frequency-domain causality over specified frequency range, it was used the *smvgc_to_mvgc* function.

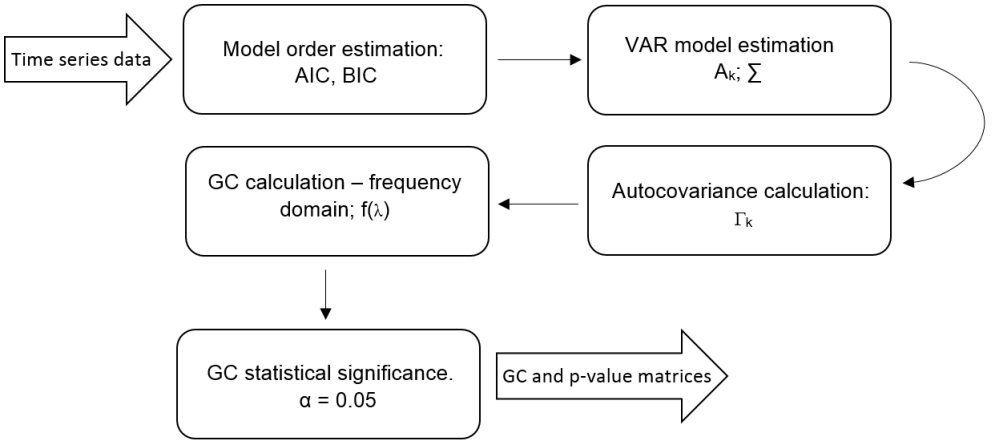

Figure 3.4: Schematic of the computational process followed with the MVGC Toolbox (Seth and Barnett, 2014)

This calculates the time-domain causality from spectral causality by integration over the frequency range [0.07, 0.13]. Finally, it was established the statistical significance of the estimated causality against the null hypothesis of zero causality based on theoretical asymptotic null distribution (Seth and Barnett, 2014).

3.4 GraphVar toolbox - comprehensive graph analysis

As introduced in the Chapter 2, brain connectivity can be described by brain networks which comprise regions of interest ("nodes") and interregional structural,functional or effective connections ("links"). Graph theory is a mathematical formulation normally used to study networks, in particular brain networks. It provides a powerful new way of characterize brain's systems by quantifying global and local topological networks proprieties of complex brain connectivity or identify localized sub-networks associated with particular effects of interest across the brain. Recently, software packages such as Brain Connectivity Toolbox (BCT) (Rubinov and Sporns, 2010), Graph Analysis Toolbox (GAT) (Hosseini et al., 2012) or Network Based Statistics(NBS) Toolbox (Zalesky et al., 2010) have become popular by applying graph theory for characterization of brain networks.

In the current project the "GraphVar" software is used, an user-friendly graphical-user-interface(GUI)-based toolbox for comprehensive graph-theoretical analyses of functional brain connectivity. This includes pipeline network construction and characterization, statistical analysis on network topological measures, network based statistics and interactive exploration of results. GraphVar is based on features of multiple currently available toolboxes such as BCT, GAT and NBS and aims to be a more comfortable way to perform graph-theoretical analysis. It runs in MATLAB (MathWorks,Inc).

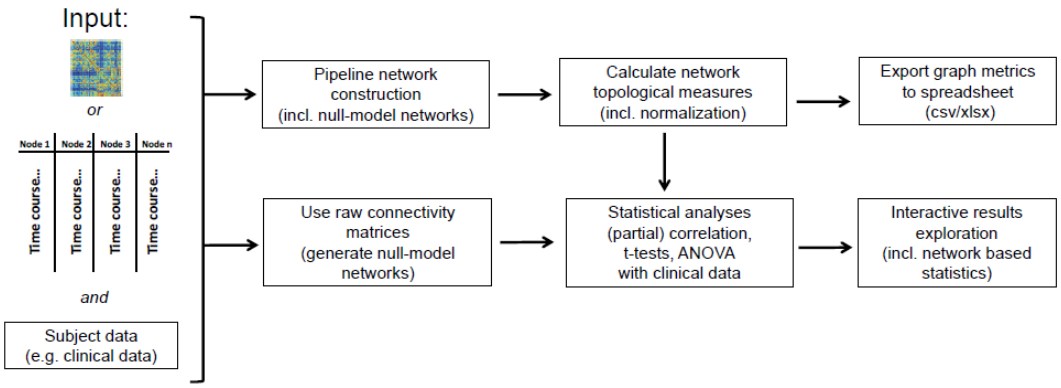

Figure 3.5: Schematic workflow of GraphVar. Adapted from (Kruschwitz et al., 2015)

3.4.1 GraphVar - overview

Since GraphVar is a very new tool and will be the basis for most of analysis performed in this thesis, it will be given a general explanation of its operation. The use of this tool involved talking with the lead author, Johann Kruschwitz from Charité - Universitätsmedizin Berlin, in order to fix some bugs as well as adapt the tool to undirected connectivity matrices when doing raw matrix analysis (it was just allowed to network construction and characterization analysis). Figure 3.5 depicts the schematic workflow of GraphVar.

GraphVar accepts any nxn matrix containing information about connectivity among network nodes in .mat format. It can also generate connectivity matrices based on Pearson correlation, partial correlation, spearman correlation, percentage bend correlation or mutual information from input time series. However this functionality is not applied in this project since the connectivity matrices were obtained using the above methodologies. Along with the connectivity matrices GraphVar requires a parcellation scheme for the brain (e.g AAL atlas) thereby defining the nodes of the network in spread sheet format (.csv or excel). There is no limit to a specific number of nodes and the user can define the brain parcellation scheme according to his or her requirements. Moreover, GraphVar provides statistical analysis functions on network pipeline and raw connectivity matrices such as correlations or group comparisons. Thus, one may enter demographic, clinic, or other subject specific data (.csv or excel) for statistical analysis.

GraphVar offers two different analysis possibilities: a pipeline construction of graph networks in order to calculate network topological measures and a direct use of raw connectivity matrices (Figure 3.6).

3.4.1.1 Raw connectivity matrix

When using connectivity matrices in GraphVar, one can simply choose to do statistics with the raw matrices and analyse the results. Figure 3.6 shows the raw matrix panel which is activated when selecting the option "Raw matrix". "Connectivity Thr" allows to restrict analysis on links that are significant in the first place. "r to z" should be used when

working with correlations (r) matrices and transforms the correlation values in z values using Fisher's r to z transformation as the r distribution is not a Gaussian distribution. "Generate random networks" allows one determine whether a Graph-Component with a certain size as a result of the correlational analysis is non-random. GraphVar offers two options to create subject specific random networks, the "*random_shuffle*" and the "*Null_model_und_sign*". The former randomly shuffle the values comprising the subject's association matrix keeping the degree of positive and negative weights for the random networks the same as in the original network. The later reassigns edge weights while preserving the weight, degree and strength distribution of each graph. For connectivity matrices ranging positive and negative weights, GraphVar allows to choose between all the weights, absolute weights, or negative weights to zero.

3.4.1.2 Network construction and calculation

Another way to analyse connectivity matrices in GraphVar is through the pipeline construction and calculation of graph networks (Figures 3.6).

In Network construction panel association matrix from each subject is transformed into subject specific networks by applying relative, absolute or significant thresholding. Significant-based thresholding is based on non-parametric p-values that are derived during the creation of random time series. Relative thresholding refers to thresholding of the association matrix in a proportional way (i.e., 0.1 indicates that 10% of the strongest connections will be maintained as links). Absolute thresholding thresholds the adjacency matrix in an absolute way, corresponding the selected value to the minimum to display a connection between two nodes (i.e 0.2 indicates that everything below this threshold will not be considered as a link in the adjacency matrix). GraphVar also allows choosing "no thresholding", which may be used to particular graph measures as modularity, global clustering, etc. Apart from these "more traditional" thresholding methods, GraphVar allows constructing binary graphs with predefined densities using sparse inverse covariance estimation "SICE"(Huang et al, 2010). Other functionalities present in Network construction panel are the possibility to transform all edge connection weights to positive values, absolute values or to set all negative weights to zero and the easily conduction of sub-network analysis by selecting the specific nodes without reloading any new data. Moreover, GraphVar allows creating binary and weighted null-model networks that can be used for normalization of the network topological measures and for non-parametric statistic.

In the Network calculations panels (Figure 3.6) one can access a set of topological measures included in the Brain Connectivity Toolbox (Rubinov and Sporns, 2010). Here the user can calculate, normalize and export binary or weighted, directed or undirected topological measures by selecting the respective function. Furthermore, GraphVar allows normalizing the topological measures by the according network measure computed from the subject specific null-model network (normalization by the mean of the null model

derived measure).

3.4.1.3 Statistical analysis

To perform statistical analysis with network topological measures or the raw connectivity matrices, GraphVar uses routines from MATLAB's statistical toolbox. It allows one to select between correlation analysis (pearson correlation), partial correlational analysis or group comparisons. The user can perform comparisons between two groups (i.e., two sample t-test) or test for differences between more than two groups (i.e., ANOVA). To evaluate the significance of network statistics, these should be compared with statistics calculated on null-hypothesis distributions. GraphVar allows performing also non-parametric statistics. For correlational analysis GraphVar offers two types of non-parametric testing: null-model testing on the network level, and null-model testing on metric level. For group comparison analysis, GraphVar features non-parametric permutation testing with a user defined amount of repetitions. In each repetition, the network measures between randomized groups are calculated resulting in a permutation distribution of difference under the null hypothesis. The actual between-group difference in network measures is then placed in the corresponding permutation distribution and a p-value is calculated based on its percentile position.

Parametric and non-parametric statistics

In parametric statistics the data are assumed to be normally distributed, and as such it is possible to draw the statistical curve exactly by simply knowing a set of parameters (mean, standard deviation, variance, etc). Parametric tests such as t-test, ANOVA are usually used to test differences between independent groups concerning the mean value of variable of interest. Pearson correlation is a parametric test used to express a relationship between two variables (Nichols and Holmes, 2001).

Non-parametric statistics enables to process data of "low quality" from small samples and on variables about which nothing is known concerning their distribution. They do not rely on the estimation of parameters (such as the mean or the standard deviation) describing the distribution of the variable of interest in the population. There is one non-parametric equivalent for each parametric general type of test. For instances, nonparametric alternatives for t-test is the Wilcoxon Rank sum test, for ANOVA test is the Kruskal-Wallis analysis of ranks and the Median test and for Pearson correlation coefficient are Spearman R, Kendall Tau, and coefficient Gamma. Each non-parametric procedure has its peculiar sensitivities and blind points so that it is advisable to run different nonparametric tests (Nichols and Holmes, 2001).

3.4.2 GraphVar - Methods

In this dissertation, GraphVar was used to perform group comparisons. All the 25 subjects were considered and each one had four connectivity matrices associated, concerning the

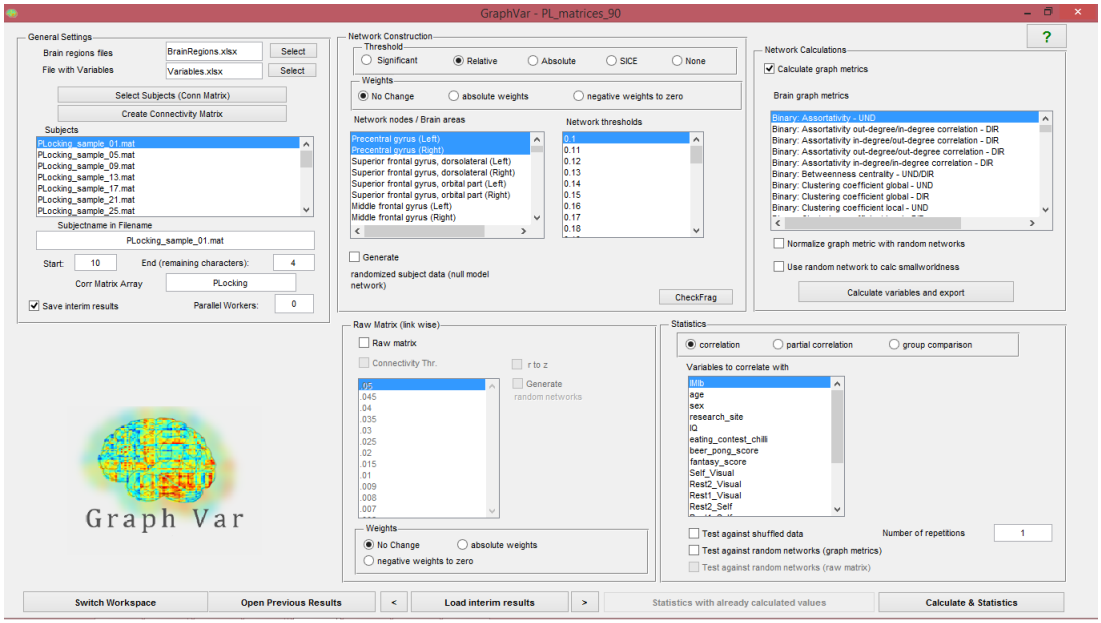

Figure 3.6: GraphVar setup interface. Adapted from (Kruschwitz et al., 2015)

four task sessions performed (REST1, REST2, SELF and VISUAL). Two spread sheets (excel) were created and inserted in GraphVar, one with the 116 brain regions from AAL atlas and the other one with labels associating each matrix to its paradigm and each subject to its group. A subset of relevant brain regions were selected from the 116 in order to allow a comprehensive graph analysis.

From the methodologies 1 and 2 explained before, three different types of data were generated: The mean Phase Locking matrices by averaging the PL profiles obtained in methodology 1, matrices containing percentage of bins that phase Locking values were significant, and Granger causality matrices (with the respective p-values). Then inter-task comparisons and inter-group comparisons were performed taking into account the four task sessions performed and the inter-movement interval, anxiety/STADI scales and the BOLD RR interval coupling, respectively. Figure 3.7 depicts the steps followed.

3.4.2.1 Networks Nodes / Brain areas

The methodologies implemented so far (1 and 2) have considered all the 116 brain regions since the propose was only to measure the connectivity between different pairs of ROIs. Once obtained the functional and effective matrices from these methodologies, one should restrict the Graph analysis to ROIs expected to be involved on paradigms under analyses (Rest, Self and Visual). Thus, a set of non relevant brain regions is excluded and the graph analysis becomes considerably easier.

From the literature, several brain circuits have been identified concerning voluntary motor behaviour. As introduced in chapter 2, regions such as primary motor cortex, pre-supplementary motor area (preSMA), premotor cortex, cingulate cortex, frontopolar cortex and supplementary motor area have been related to voluntary motor

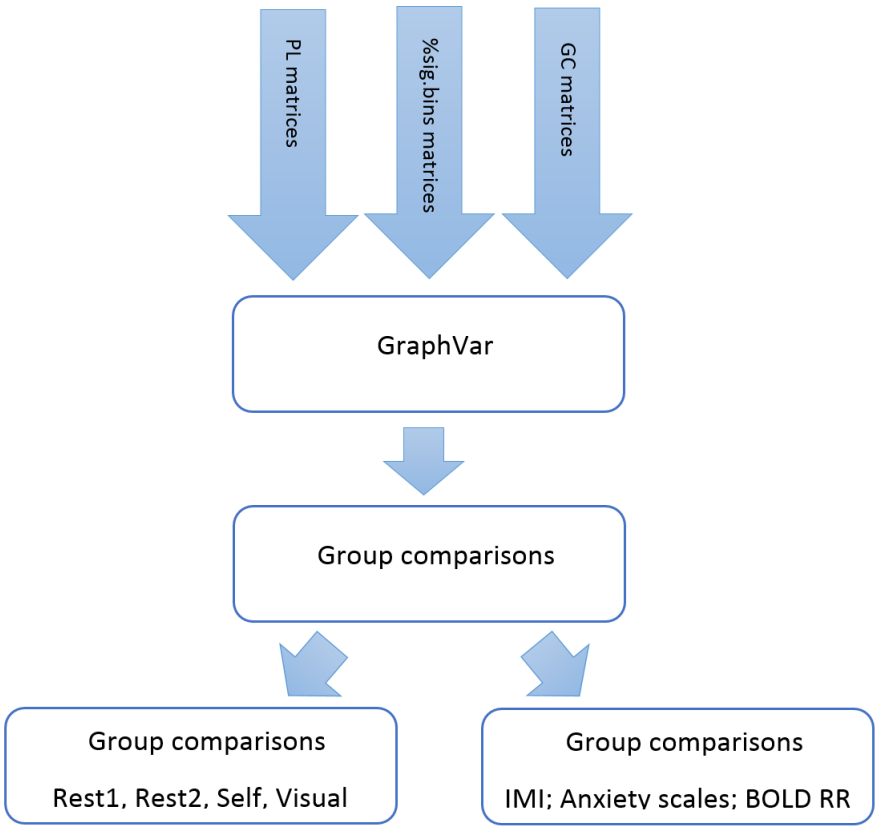

Figure 3.7: Schematic depicting the methods followed with GraphVar. Matrices containing PLVs, percentage of bins that PLVs were significant and Granger causality were used as inputs. Two different types of group comparisons were performed: inter-task and inter-group. Inter-task comparisons involved the task sessions performed by the participants (Rest1, Rest2, Self and Visual). Inter-group comparisons took into account the inter movement interval, the Anxiety scales and the BOLD RR interval.

actions(Haggard, 2008). Additionally, the inferior frontal gyrus, precentral sulcus, and the bilateral superior temporal gyri have shown engagement with temporal aspects of the voluntary movement (Bengtsson et al., 2004). The anterior insular cortex is believed to have an important role in intentional action decisions (Brass and Haggard, 2010a). Studies found Basal Ganglia activation when performing discrete finger movements with a complex rhythm and greater activations in the inferior frontal gyrus and inferior parietal regions associated with temporal processes. For instances, substantial portions of the putamen bilaterally and sections of the caudate as well as ventrolateral portions of the thalamus has shown activation for voluntary movement conditions (Bednark et al., 2015). Regions such as supramarginal gyrus and ipsilateral posterior parietotemporal regions have been suggested being recruited during movement selection (Ariani et al., 2015).

Regarding stimulus-driven motor actions, regions such as the cerebellum , thalamus ,dorsal premotor cortex are believed to play a prominent role (Gowena and Miallb, 2007). Some studies detected brain regions common to internal driven actions, such as parietal

cortex, dorsal premotor cortex and primary motor cortex contralateral to the acting hand (Ariani et al., 2015). Supplementary motor cortex and presupplementary motor cortex have also shown activation for motor externally stimulus-responses(Ariani et al., 2015).

Considering these regions listed, others related to visual stimulus such as the Calcarine (where the primary visual cortex is concentrated) and the Amygdala which gives information about emotional events, a set of regions were selected from the initial 116.

Firstly, it was selected 14 regions known to be involved in voluntary motor actions and external stimulus-driven actions in order to test GraphVar. These included the Precentral (Left), Precentral (Right), Supplementary Motor Area (Left), Insula (Left), Insula (Right), Anteriror Cingulate (Left), Calcarine (Left), Calcarine (Rigth), Cuneus (Left), Lingual (Left), Postcentral (Left), Postcentral (Right), Caudate (Left) and Putamen (Left). In a more advance stage of the current thesis, when the computing time constraints had been properly assessed, it was decided to expand the subset of regions included in the analysis. The table 3.1 summarizes the AAL brain regions used on the present work.

Table 3.1: Brain regions used in the current project. Blue regions concern the 1st subset being then extended to all the regions of the table in the 2nd subset.

Brain Regions	**AAL region number**
Precentral gyrus (Left)	1
Precentral gyrus (Right)	2
Supplementary motor area (Left)	19
Supplementary motor area (Right)	20
Insula (Left)	29
Insula (Right)	30
Anterior cingulate and paracingulate gyri (Left)	31
Anterior cingulate and paracingulate gyri (Right)	32
Median cingulate and paracingulate gyri (Left)	33
Median cingulate and paracingulate gyri (Right)	34
Posterior cingulate gyrus (Left)	35
Posterior cingulate gyrus (Right)	36
Amygdala (Left)	41
Amygdala (Right)	42
Calcarine fissure and surrounding cortex (Left)	43
Calcarine fissure and surrounding cortex (Right)	44
Cuneus (Left)	45
Lingual gyrus (Left)	47
Postcentral gyrus (Left)	57
Postcentral gyrus (Right)	58
Precuneus (Left)	67
Precuneus (Right)	68
Caudate nucleus (Left)	71
Lenticular nucleus, putamen (Left)	73

3.4.2.2 Inter-task comparison

In this subsection, an inter-task comparison is performed on three different types of matrices: mean phase locking matrices, the time length of significant phase locking matrices and, as a complementary analysis, Granger Causality matrices.

Mean Phase-Locking matrices

The first analysis involved the comparison between different tasks directly on the raw matrix. The mean PL matrices were inserted and one selected the "Raw matrix" check box and deselected the remaining check boxes of Network construction and calculation panels. This allows to do statistics directly from PL matrices inserted in the toolbox. In this analysis the significance of PL periods was not considered, therefore the "Connectivity Thr" was not selected. In addition, the "r to z" check box was not also selected because it is only applicable for correlation (r) matrices. To do group comparison it was chosen the option "group comparison" in the statistics panel and selected the variable which define the groups. In this case the "Paradigm" (Appendix B). Then, since there were not a big amount of data (only 25 subjects), it was selected "Test against random groups" and defined "1000" number of repetitions in order to perform a non-parametric statistic. Finally the analysis was launched by pressing the "Calculate & Statistics" button.

Time length of significant phase locking matrices

In order to know if the mean PL values used for group comparison in the previous steps were significant, it was necessary to create matrices representing the time length of significant phase locking. Thus, from each PLV plot with the correspondent PLS curve for any ROI pair, it was calculated the percentage of bins that PLV was significant. Then, it was performed group comparison where all the parameters used in the previous analysis (raw matrix analysis) were preserved.

Granger causality matrices

From the methodology 2 explained above, matrices containing causal information between different pair of ROI's were obtained. For each matrix there is a matrix with the respective p-values.

Different tasks were compared on the Raw matrix. Files relating to the 25 subjects were inserted and each one had two matrices: a GC matrix and a p-values matrix. The "Raw matrix" checkbox was activated, and the remaining were deselected (Network construction and Network calculations panels). Then, it was activated the "Connectivity Thr." When this is done, a window opens for the user choose between the two matrices inserted. It was selected the p-values matrix and defined the threshold to "0.05". The "r to z" check box was not selected. To do group comparison it was chosen the option "group comparison" in the statistics panel and selected the variable which define the groups ("Paradigm"). It was

performed non-parametric statistic (number of repetitions: 1000).

Mean Phase-Locking matrices - Network Calculations

In order to expand the analysis, the first group comparison (Mean Phase Locking matrices) was made but now using the Network Construct and Calculations panels. Here, the spatial pattern of inter-regional phase synchrony can be quantitatively analysed using graph theory measures. The "Threshold" was defined as "Relative" and the values, 0.1, 0.2, 0.3, 0.4 and 0.5 were chosen. Since group comparison was performed, it was not necessary to generate null model networks because the p-values are derived by permutation testing. In the Network Calculations panel, two binary network metrics were selected, one which characterize the network locally (the node degree) and another which provides a more global description of the network (the global efficiency). Then "Calculate & Statistics" was performed. As in the previous procedure, in the Statistics panel, the number of repetitions of the non-parametric test was "1000". This analysis was restricted to binary network topological measures.

3.4.2.3 Inter-group comparison

The second analysis involved inter-group comparisons taking into account three key variables: the inter-movement interval (IMI), the Anxiety/STADI scales and the BOLD RR Interval coupling (time lag between ECG's R peaks).

Inter-movement interval

The first comparison is based on the fact that among participants there exists different types of personality and different strategies to initiate movements at free will. This lead one to hypothesise if the participants were divided according their inter movement interval (IMI) histograms in two groups and their connectivity matrices were computed, different results will be expected.

This group comparison arise from the work of Pfurtscheller et al. (2014b) and aims to detect specific connectivity patterns that could support the entrainment between slow intrinsic oscillations and voluntary movements.

Only subjects with similar IMIs in both session (a and b), more than 1 movement(all except subjects 10 and 23), less than 1000 movement (subject 13 $>$ 1000 movements) and similar standard deviation (SD)(no difference$>$ 50%) in session a and b(large SD difference subjects 2 and 21) are used, and the rest is divided in group A ($SD < 8 : N = 12$) and group B ($SD > 8 : N = 8$). Thus, the group A contains subjects $1, 3, 4, 5, 6, 7, 8, 9, 12, 16, 19, 25$, and the group B, $11, 14, 15, 17, 18, 20, 22, 24$. The procedures followed on GraphVar were the same mentioned in Inter-task comparison section, with the exception that only mean PL matrices concerning the "SELF" state were inserted and the variable selected in the statistics panel was the "IMI". IMI data are not shown here because they stem from unpublished

analysis carried out by a collaborator of this project.

Anxiety/STADI scales

The second comparison was based on the similarity of Anxiety/STADI scales . There are subjects with similar Anxiety/STADI scales and subjects with different Anxiety/STADI scales during REST1, session "a" and REST2, session "b". They can be assigned to group A (nearly no change in anxiety):1, 2, 5, 7, 9, 10, 13, 14, 15, 16, 17, 25; and group B (substantial decline in anxiety in the course of the session): 3, 4, 6, 8, 11, 18, 19, 20, 21, 23, 24; respectively. Anxiety data are not shown here because they stem from unpublished analysis carried out by a collaborator of this project. The procedures followed with GraphVar were the same mentioned above, with the exception that only mean PL matrices relating to the "REST1 and REST2" states were inserted and the variable selected is the "Anxiety/STADI".

BOLD RR coupling

The last comparison followed the work of Pfurtscheller et al. (submitted) based on phase-coupling between spontaneous BOLD oscillations (0.1Hz) and heart rate beat-to-beat interval (RRI) oscillations. Briefly Pfurtscheller et al. (submitted) hypothesize that measuring phase-locking between BOLD signals and RRI signals at 0.1 Hz, neural and vascular BOLD signals could be differentiated and support for the existence of a "central pacemaker" that modulates heart rate could be achieved.

Thus, the subjects were divided between two groups: the positive time delay (pTD) that indicates a lead and a negative delay (nTD) that indicates a lag of RRI oscillations in comparison to BOLD oscillations. During the REST1 the subjects 7,9,10,17,18,20,22 showed pTD BOLD-RRI and the subjects 3,6,8,11,12,13,16,21,23 25 showed nTP BOLD- RRI. Delay data are not shown here because they stem from unpublished analysis carried out by a collaborator of this project. The procedures followed on GraphVar were the same.

CHAPTER 4

RESULTS AND DISCUSSION

The following results are based on dataset "a" and "b". They aim to show the potential of methodology 1 and to do preliminary inferences about brain networks involved in voluntary behaviour. Additionally, complementary methodology 2 is also tested. The present results are used to discuss the potential of the implemented analysis approaches as well as to evaluate the potential of GraphVar toolbox to be used by neuroscientists.

4.1 GraphVar - Exploration of Results

In order to analyse the results, GraphVar offers an interactive viewer that allows intuitive exploration of statistical results (Figure 4.1). The results viewer is basically divided into three parts: the results selection box, the results display and the general functions panel.

The results selection box contains four selection windows (Variable, GraphVar, Threshold and Brain Areas) that allows one to select the independent variables under analysis (i.e, Paradigm, Anxiety scale etc), the dependent variables (i.e., graph metrics), the thresholds (selected in Network Construction) and the brain areas (selected in Network Construction, network nodes/brain areas).

The results display is adaptive to what one select in the "The results selection box" and will change according to the dimensionality of the graph measure (for instances, node degree is two-dimensional, global efficiency is one-dimensional and raw connectivity matrix is three-dimensional). It provides "mouse-over info box" to indicate the network node/brain area(first line); the threshold (second line); the level/ degree of the computed variable (third line) and the p-value (fourth line). When performing group comparisons, GraphVar enables a new field to select to either to display the F-value or the respective group differences.

In the general functions panel, one can choose the level of significance to apply to the results by specifying a reference alpha level, hiding the non-significant values according

with the specified alpha level and applying several corrections methods to parametric and non-parametric results(Bonferroni and False discovery rate (FDR) correction). In addition, plotting of graph components and direct export into BrainNetViewer software (Xia et al., 2013) is also possible.

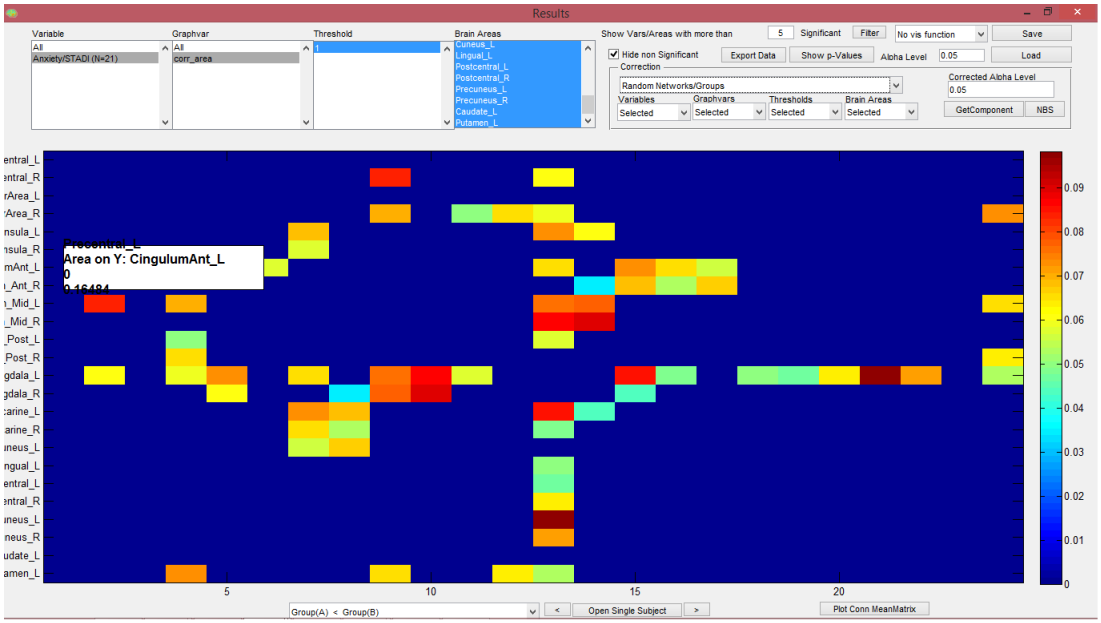

Figure 4.1: GraphVar interactive results viewer

4.2 Phase Locking and Granger Causality - Relationship

The current study involved the use of a first methodology which yielded a Phase Locking measure between pairs of brain regions. In addition, by using the method developed by Seth and Barnett (2014), Granger Causality matrices were extracted. Both the measures provide a value of connectivity between brain regions. Thus, when there is a connection it is believed that a relationship between them might be expected.

The following results show the scatter plots, for the two rest sessions and two movement sessions performed by the 25 participants. They show the relationship between the Phase Locking (PL) and Granger Causality (GC) measures of two brain regions that have been shown to be involved in movement planning, namely the supplementary motor area and the insular cortex (Pfurtscheller et al., 2014a).

Figure 4.2 depicts the scatter plots for PL and GC, where GC measure is from supplementary motor area to the Insula. This results show a similar pattern along the tasks with most of the points concentrated between GC [0,0.04], PL [0.4, 0.8]. For Rest1 and Rest2 the cluster of points is most evident than for task sessions.

Figure 4.3 depicts the scatter plots for PL and GC, where GC measure is from Insula to the supplementary motor area. This results show a similar pattern along the tasks with

most of the points concentrated between GC [0,0.04], PL [0.4, 0.8].

With this analysis a relationship between the two different measures of connectivity was expected. However, that was not verified and can not be concluded. Although both measures measure brain connectivity it could not be inferred that for a given pair of regions with a high phase locking value there was also a high Granger causality value and vice versa. Recent studies support these findings by showing confounding effects involving phase synchronization and Granger causality(Vakorin et al., 2013). Furthermore, across the subjects it could be verified that the values of PL and GC change for the same connection.

4.3 Inter-task and inter-group comparisons

By using the GraphVar, group comparisons were performed in order to test the methodologies used and detect activations in brain regions related to voluntary motion. In each comparison the resulting graphs show only the links wherein non-parametric p-values were significant according to the specified alpha level (alpha = 0.05). The line thickness is proportional to the strength of the connection. The results are shown in the form of inequality where paradigm/group X > paradigm/group Y means the measure of connectivity is higher in X than Y and vice versa.

4.3.1 Inter-task comparison

In this subsection the results of the inter-task comparisons performed from the mean PL matrices, time length of significant phase locking matrices, and Granger causality matrices of the 25 participants in the acquisitions "a" and "b" are depicted. Initially, 14 brain regions from the 116 of AAL altas were considered in order to test the methodologies implemented and the GraphVar. In a more advanced stage, this subset was extended for the 24, highlighted in the chapter 2, section "Networks and Brain Regions", for a more precise analysis.

4.3.1.1 Mean PL matrices - 14 Brain Regions

The first results are shown in the Figure 4.4. They relate to acquisition "b" and show the significant contrasts between different tasks. To evaluate the neural effects of internal timing selection (when to move), self paced-motion, stimulus driven motion and rest condition were contrasted.

For Rest1 > Rest2; Rest1 > Visual; Rest2 > Visual; Self > Visual; Self > Rest2; Self > Rest1 there were no significant results. The absence of significance in Rest1,2 > Visual suggest that networks activated during rest (i.e Default Mode Network) are kept during visual-stimulus driven tasks. Recent studies support this results showing that spontaneous activity continues during task performance showing a similar functional distribution to that observed at rest (Goparaju et al., 2014). The absence of significance for Self > Rest

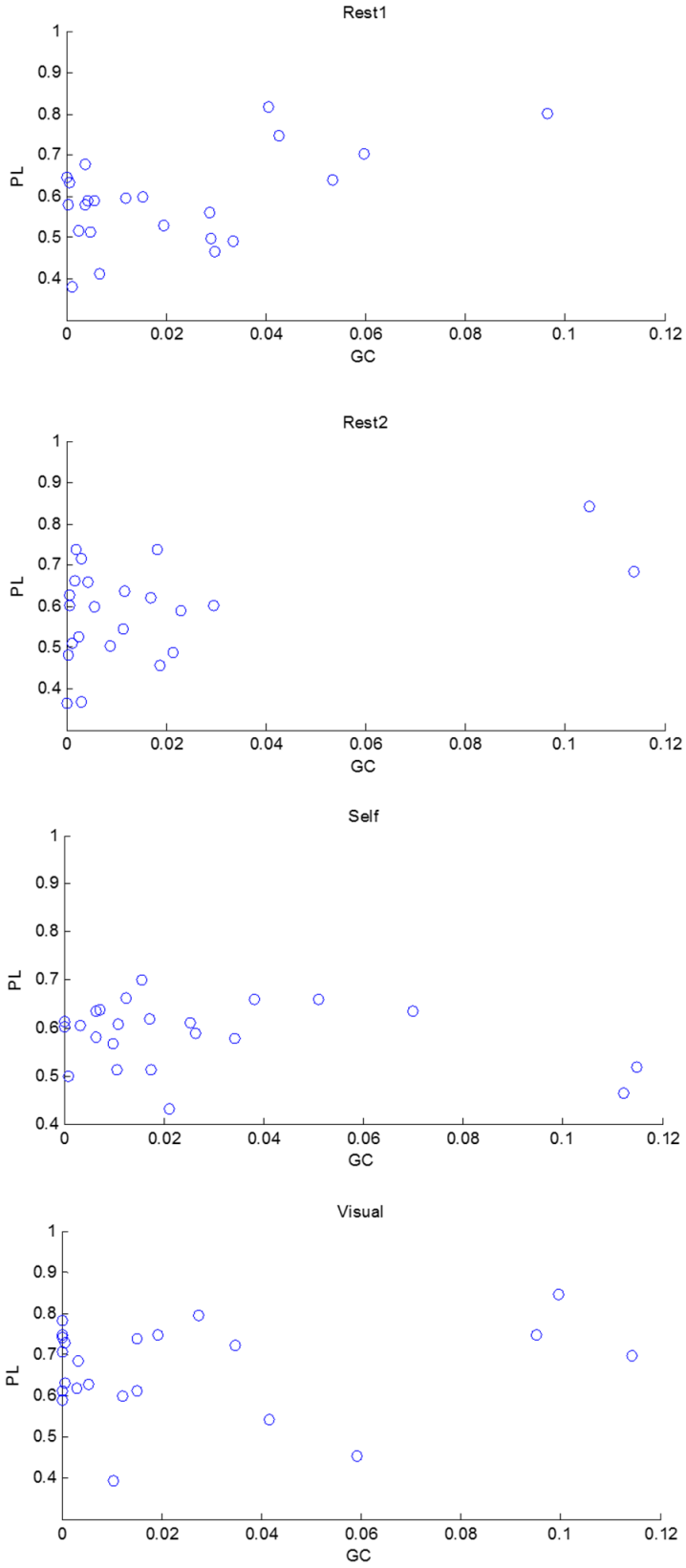

Figure 4.2: Scatter plots containing information about the PL and GC, where GC is from region Supplementary motor area to Insula. All the 25 participants were considered

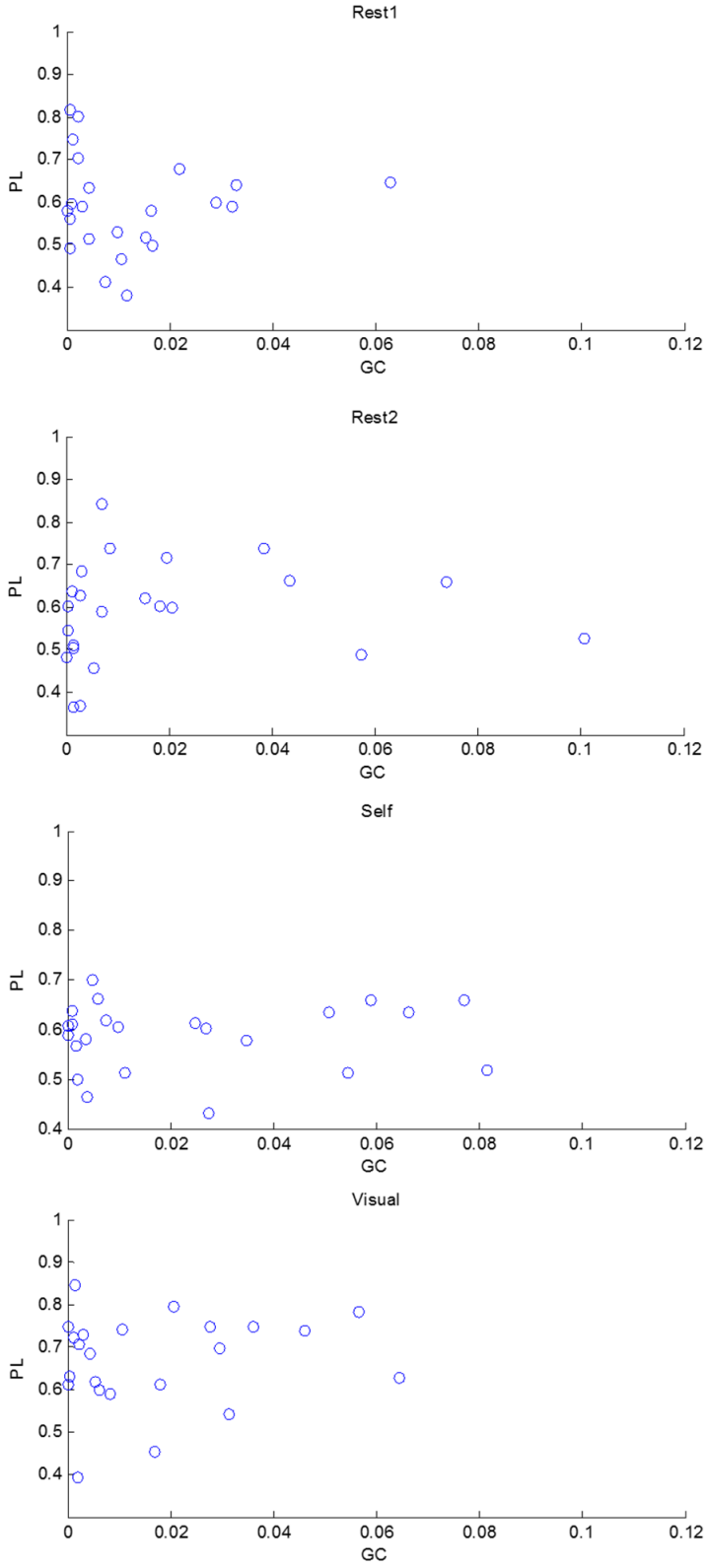

Figure 4.3: Scatter plots containing information about the PL and GC, where GC is from region Insula to Supplementary motor area. All the 25 participants were considered

1,2 suggest two possible explanations: that there were not different connections from those present in resting state which supports the explanation that networks of spontaneous activity remains constant between task and rest and that the observed changes in correlations are due to a simple superposition of spontaneous and task-evoked activity (Fox and Raichle, 2007), or that there is a loss of phase synchrony when performing a self-paced movement. Phase resetting has been proposed as a mechanism inherent to neural events such as evoked potentials or motor commands. It is conceivable that the "readiness potential", known to be a hallmark of motor preparation and associated to an effect of event-related desynchronization, would decrease phase-locking across the time series. Hence, this specific connectivity trait would be undetectable by this phase-locking approach (Deecke and Kornhuber, 2003; Pfurtscheller and Silva, 1999; Yeung et al., 2004).

Contrasting resting states with self-movement task, Rest1 > Self and Rest2 > Self (Figure 4.4 (a),(b)), significant connections are observed in the resting state suggesting the loss of connections during self-paced motion that were present at rest. Several regions known to be involved in internally guided behaviour are significant. These include the insular cortex, the anterior cingulate cortex, the Putamen (Basal Ganglia), the primary motor cortex (precentral gyrus) and the primary somatosensory cortex (Postcentral gyrus). These results strengthen the existence of intrinsic activity in the absence of any task or external stimulation. These results are consistent with a number of group resting-state studies that have reported the formation of functionally linked resting-state networks where the most known are the primary sensorimotor network, the primary visual and extra-striate visual network, a network consisting of bilateral temporal/insular and anterior cingulate cortex regions, left and right superior parietal and superior frontal regions and the so-called default mode network which includes the precuneus (Heuvel and Pol, 2010).

For those comparisons involving the visual-stimulus driven task, a large number of significant connections are observed where most of the defined brain regions are involved (Figure 4.4, (d)(e)(f)). One can notice a high number of links in motor cortex involving the supplementary motor area, Precentral and Poscentral, visual cortex involving the Calcarine, Cuneus and Lingual and in Basal Ganglia (Caudate) and Insula. These results are consistent with the work of Sun et al. (2015) which highlight the activations of premotor, primary somatosensory and primary motor area in preparation of cued finger movements. The involvement of supplementary motor area in externally triggered movement plans is in agreement with Ariani et al. (2015). In Figure 4.4 (f), the activation of anterior cingulate cortex confirms its role in motor control (Asemi et al., 2015). The insula is heavily involved bilaterally and is believed provide an interface between cognition and action (Chang et al., 2013). Although there are some significant connections involving regions in the right hemisphere, most of the significant brain regions and connections are located in the left hemisphere which was expected since right-hand motion was involved. Overall, the high number of connections involved was expected because we are analysing a frequency band that matches the frequency of the stimulus (0.1 Hz).

The second rest period shows a higher number of significant connections than the first

rest period (Figure 4.4, (a),(b),(c)). These results are intriguing and may suggest habituation or practice effects.

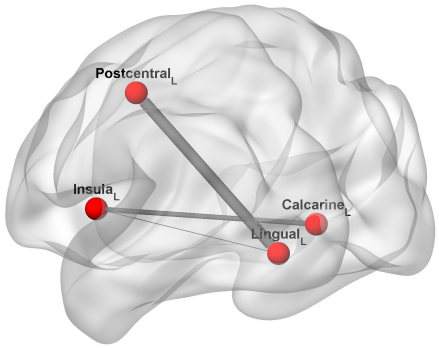

(a) Rest1 > Self

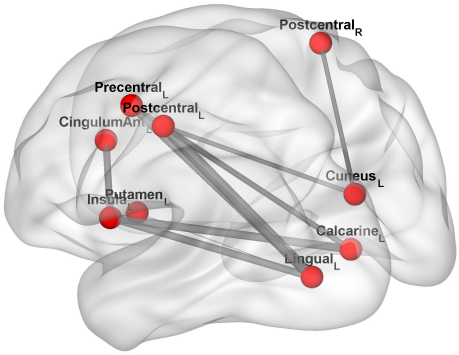

(b) Rest2 > Self

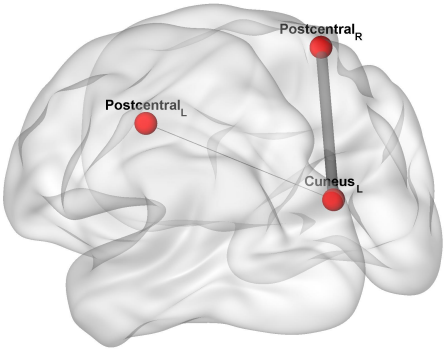

(c) Rest1 < Rest2

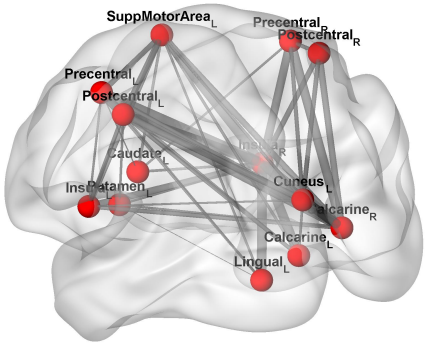

(d) Rest1 < Visual

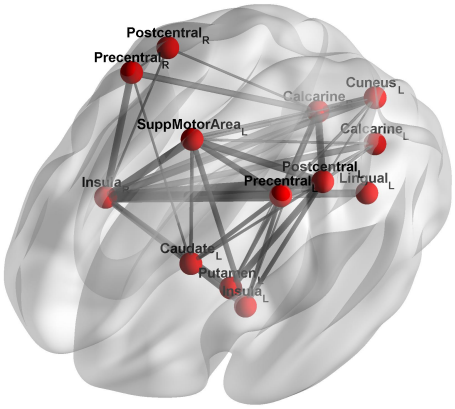

(e) Rest2 < Visual

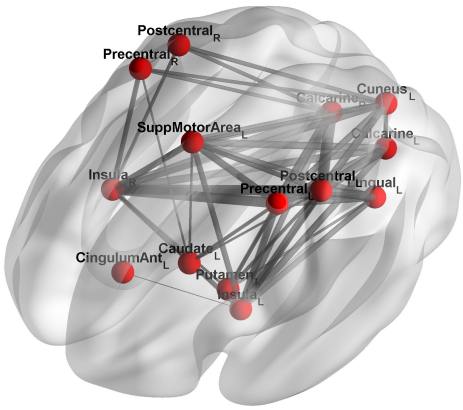

(f) Self < Visual

Figure 4.4: Inter-task comparison involving the four tasks performed by participants, two resting sessions and two movement sessions. Matrices containing information about Phase Locking were used.

4.3.1.2 Time length of significant phase locking matrices - 14 Brain Regions

After performing inter-task comparison with Phase Locking (PL) measure, considering the 14 regions, a new analysis was done, with matrices containing the percentage of bins for which PL values were significant. The aim was to know the extent to which a measure based on statistical significance would yield results similar to those obtained with the simple mean PL. These results concerning the data of acquisition "b".

As for the mean Phase Locking (PL) matrices, the comparisons Rest1 > Rest2; Rest1 > Visual; Rest2 > Visual; Self > Visual; Self > Rest2 did not show any significant connection.

Regarding Rest and Self contrasts (Figure 4.5, (a),(b)) one can notice that mostly the same connections detected with mean PL matrices were also obtained using the percentage of significant bins.

A higher number of connections is observed in the first rest period when compared with the second, as in mean PL matrices analysis (Figure 4.5, (a),(b),(c)).

For Visual stimulus task the activated network involves all the brain regions.

The fact that similar results were obtained for mean phase-locking value and time-length of significant phase-locking period is encouraging for future studies, because the former method does not require statistical validation (e.g surrogate-based) and is therefore computationally much faster. These results allow to consider expanding the subset of regions included in the analysis.

4.3.1.3 Granger Causality - 14 Brain Regions

The effective matrices containing causal information between pairs of brain regions were used here.

The results are displayed by color matrices where the color represents the strength of connection. The reason was because GraphVar option "Get components" which allows the graph construction is not still adapted to effective connectivity matrices.

Figure 4.6(a)(b) show group comparisons between Rest and Self-paced motion. Significant connections between several regions are detected, however they are mainly inter-hemispheric. There were directional causal influences between Insula (Left) -> Calcarine (Left), Postcentral(Right) -> Anterior Cingulum (Left), Caudate (Left) -> Calcarine (Right), Caudate (Left) -> Putamen (Left) in the contrast Rest1 > Self that were not verified in Rest2 > Self. In Rest2 > Self only one connection was significant between Caudate (Left) -> Calcarine (Right).

Similarities with the group comparison made from mean PL matrices were not detected. For the remaining contrasts not showed here, the same incongruence with the previous results was observed. The amount of unexpected inter-hemispheric connections suggests that then results should be appreciated with caution.

Within this thesis, a decision was made to focus on phase locking analysis and leave further Granger-based studies for future work. Clearly, the application of Granger Causality to fMRI data requires a deeper study concerning parameter choice.

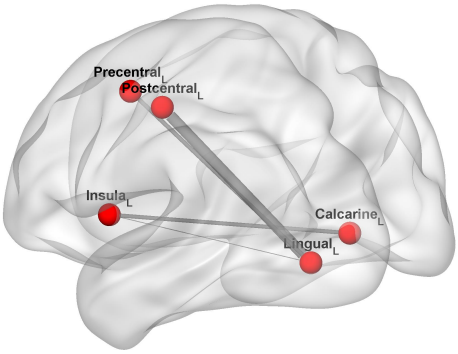

(a) Rest1 > Self

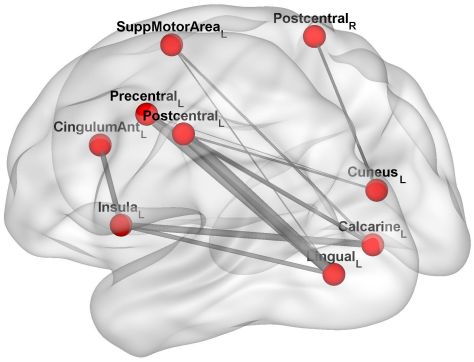

(b) Rest2 > Self

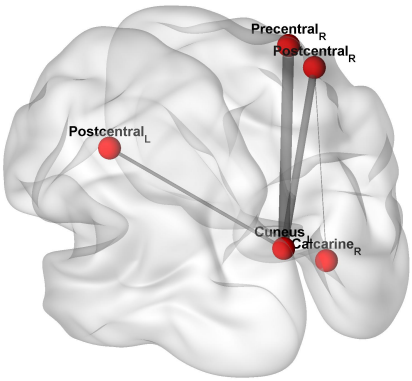

(c) Rest1 < Rest2

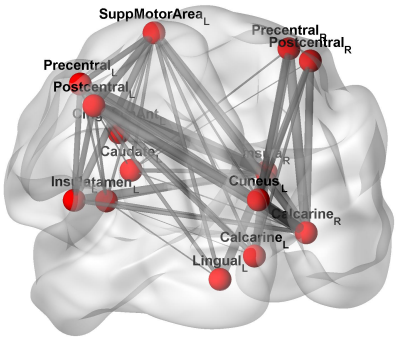

(d) Rest1 < Visual

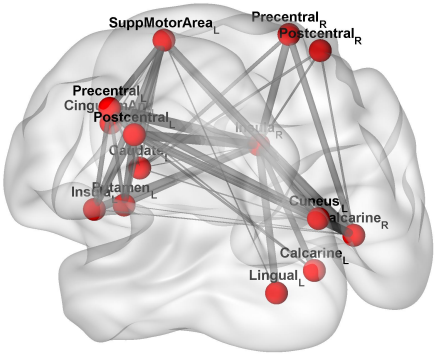

(e) Rest2 < Visual

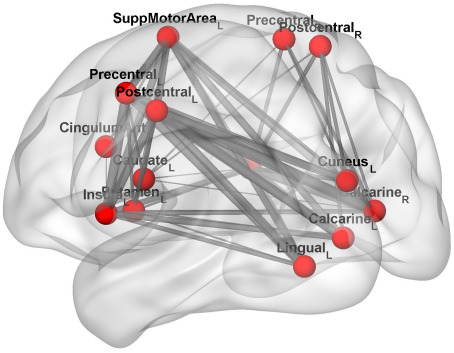

(f) Self < Visual

Figure 4.5: Inter-task comparison involving the four tasks performed by participants, two resting sessions and two movement sessions. Matrices containing information about time length of significant Phase Locking were used.

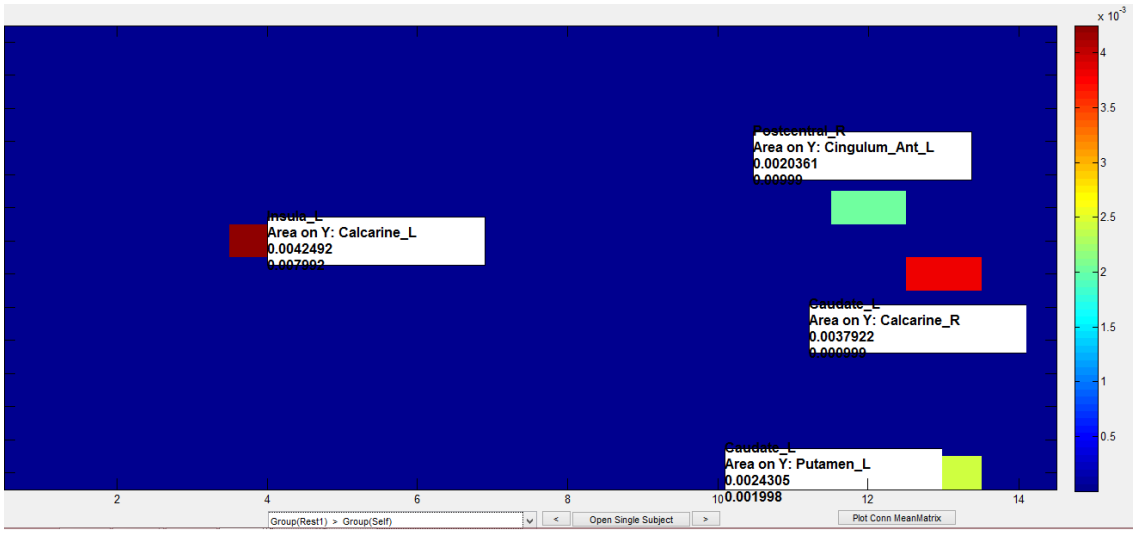

(a) Rest1 > Self

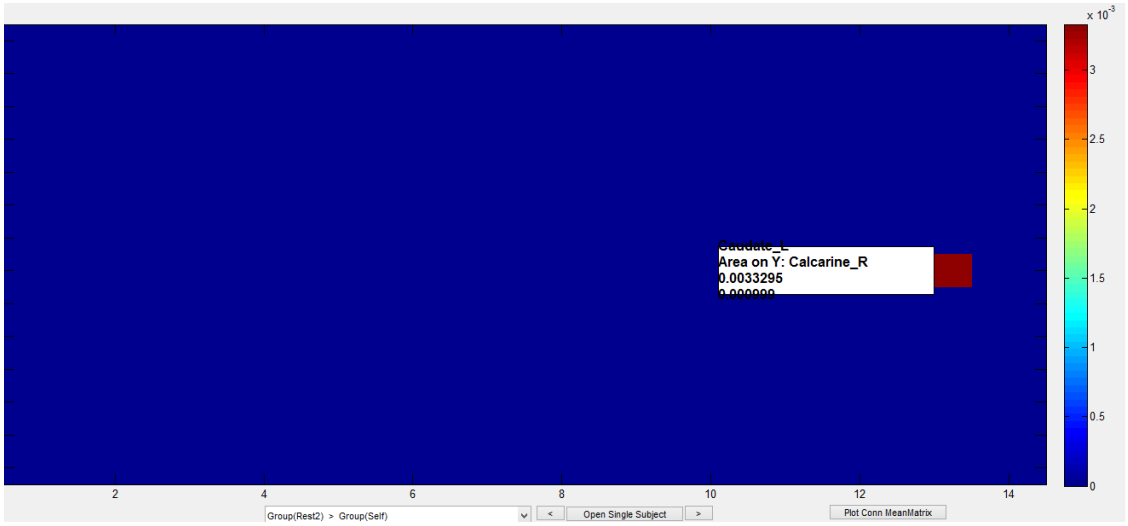

(b) Rest2 > Self

Figure 4.6: Inter-task comparison involving the four tasks performed by participants, two resting sessions and two movement sessions. Matrices measuring Granger Causality were used

4.3.1.4 Mean PL matrices - 24 Brain Regions

After the previous results (in particular those regarding Phase Locking measure and time length of significant Phase Locking), which showed ability to investigate brain connectivity, a new analysis was performed including more brain regions.

These results concerning the analysis of the 24 regions highlighted in table 3.1, Chapter 3.

Figure 4.7 (a),(b),(c),(d) shows the inter-regional connections for which the mean phase locking value was significantly different between Rest and Self. (a) and (b) concern the acquisition "a", (c) and (d) concerns the acquisition "b".

The Insula (Left) is strongly involved and functionally connected with Precentral, Supplementary motor area, Anterior cingulum, Precuneus, Calcarine and Lingual, all in the left hemisphere. These suggest that motor regions are functionally connected with insula previously of the initiation of movement. Craig (2009) has shown that the anterior insular cortex is implicated in a wide range of conditions and behaviours including decision making, which support these results. The co-activation of Insula and anterior cingulate cortex showed in the results (Figure 4.7 a ,b ,c ,d) support the studies that have detected this connection in many behaviours and also during cognition, pain and emotions (Yarkoni et al., 2011).

In the aquisition "a" a connection between insula and supplementary motor area is verified in Rest1 > Self which is in agreement with Pfurtscheller et al. (2014a) who showed that brain activity spread from the insula to higher order motor areas such as supplementary motor area. Hoffstaedter et al. (2013) support this view by identifying the when-network which consist of superior supplementary motor area together with insula. However this functional connection is not observed in the remaining contrast (Figure 4.7,(b)(c)(d)) suggesting that the effect is not very robust.

The involvement of cingulate cortex in premovement activity for voluntary actions has been shown and is significantly present in all the contrasts here(Nguyen et al., 2014). These results suggest that anterior cingulate cortex influences action initiation, apart from its role in action selection (Williams et al., 2004). The work of Srinivasan et al. (2013) supports this conclusion.

The precuneus is also constantly involved and is in agreement with Utevsky et al. (2014) who suggest that the precuneus is engaged under a variety of processing states.

Calcarine, Lingual and Cuneus are brain regions known to be involved in visual processing. Their involvement here support the work of Raemaekers et al. (2014) which investigate resting state connectivity in human primary visual cortical areas.

This approach based on Wavelet Transform Coherence allows to make a contribution towards the characterization of the functional connectivity of brain circuits related to voluntary behavior. Although these results are preliminary, they suggest the potential of this approach.

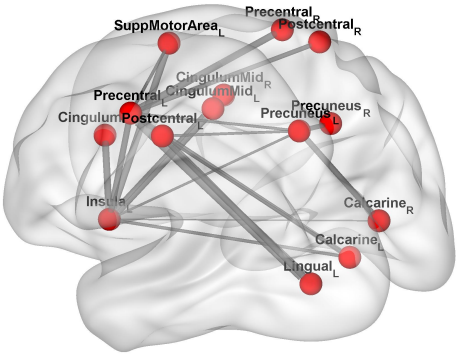

(a) Rest1 > Self

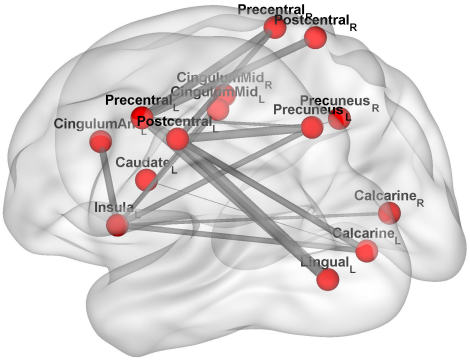

(b) Rest2 > Self

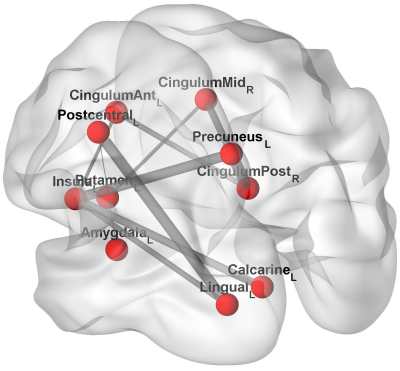

(c) Rest1 > Self

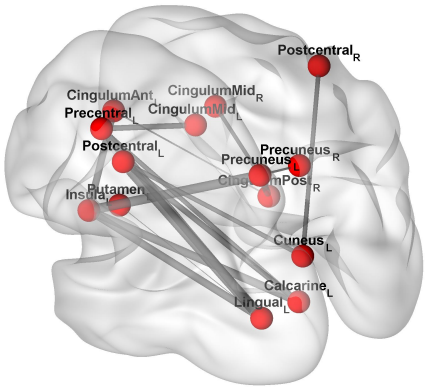

(d) Rest2 > Self

Figure 4.7: Inter-task comparison involving the four tasks performed by participants, two resting sessions and two movement sessions.(a),(b) and (c),(d) show Rest > Self contrast regarding the acquisition a and b, respectively. Matrices containing information about Phase Locking were used.

4.3.1.5 Mean PL matrices - Network Calculations

Up to now, all the analysis have been done directly in the "raw connectivity matrix" as explained in the Chapter 3, GraphVar-Methods. In order to characterize the networks activated when the participants perform the tasks on a global scale (90 brain regions) it was used the Network Construction and Calculation panels. Thus, raw matrices were thresholded, binarized and two networks measures were calculated, one of which measures the node degree and a second one which provides a more global description of the network, the global efficiency.

The results presented here show the comparison between the different task performed by the participants considering the measures of node degree and global efficiency across a set of thresholds (0.1,0.2,0.3,0.4,0.5). They are related to the data acquired in the acquisition "b" and show only regions where the p-values were significant. When paradigm A > paradigm B, the results display show the significant values that are higher in A than in B

and vice-versa.

Node Degree

Figures 4.8,4.9,4.10 and 4.11 shows all the contrasts between tasks related to node degree measure. For the comparisons Rest1 > Rest2, Rest1 > Self, Rest1 > Visual, Rest2 > Self and Rest2 > Visual mostly brain regions located in the left hemisphere have significant values of node degree. These include regions of the frontal, occipital and temporal lobes. On the other hand, for Rest2 > Rest1, Self > Rest1, Self > Rest2, Visual > Rest1, Visual > Rest2, most of the regions with high node degree are located in the right hemisphere. These results suggest that when performing a right hand self-paced movement there is a loss of phase synchronization in the left hemisphere among brain regions which were communicating during the resting state.

Rest1 > Self and Rest2 > Self show a high node degree to most of the thresholds in inferior frontal gyrus, middle frontal, rolandic operculum, middle and inferior occipital, heschl and inferior temporal. The significant node degree for all the thresholds of frontal inferior region is in agreement with previous studies that attribute to that region the responsibility for engaging in motor movements (Hoffstaedter et al., 2013) (Raea et al., 2014). A high degree suggest that the region is a key region in the network.

The number of brain regions where node degree was significant is higher in those contrasts involving Visual than Self. This results was expected because the previous results suggested that visual cue - task stimulates brain functioning in most of the brain regions.

For the particular case Visual > Self a high level of node degree is observed for all the thresholds, in the occipital region which was expected since the movement was driven by a visual external stimulus. When comparing Self > Visual, one can observe a strong involvement of the regions belonging to the Frontal lobe as well as anterior cingulate cortex, rectus, angular and temporal lobe.

Global Efficiency

Global efficiency is a network measure which allows characterizing the global integration proprieties of the network, in particular information exchange.

In Figure 4.13 red circles indicate the global efficiency values from which the p-values were significant. For Rest1 > Visual, Rest2 > Visual and Self > Visual, there are significant values and the highest value of global efficiency is for the threshold 0.2. On the other hand, the remaining contrast do not show any significant value. These results suggest that information transfer efficiency of the functional brain networks derived from fMRI data are different between rest and task. Functional brain networks change its network topology and information transfer efficiency depending on cognitive states as recently revealed by the study of Taya et al. (2014).

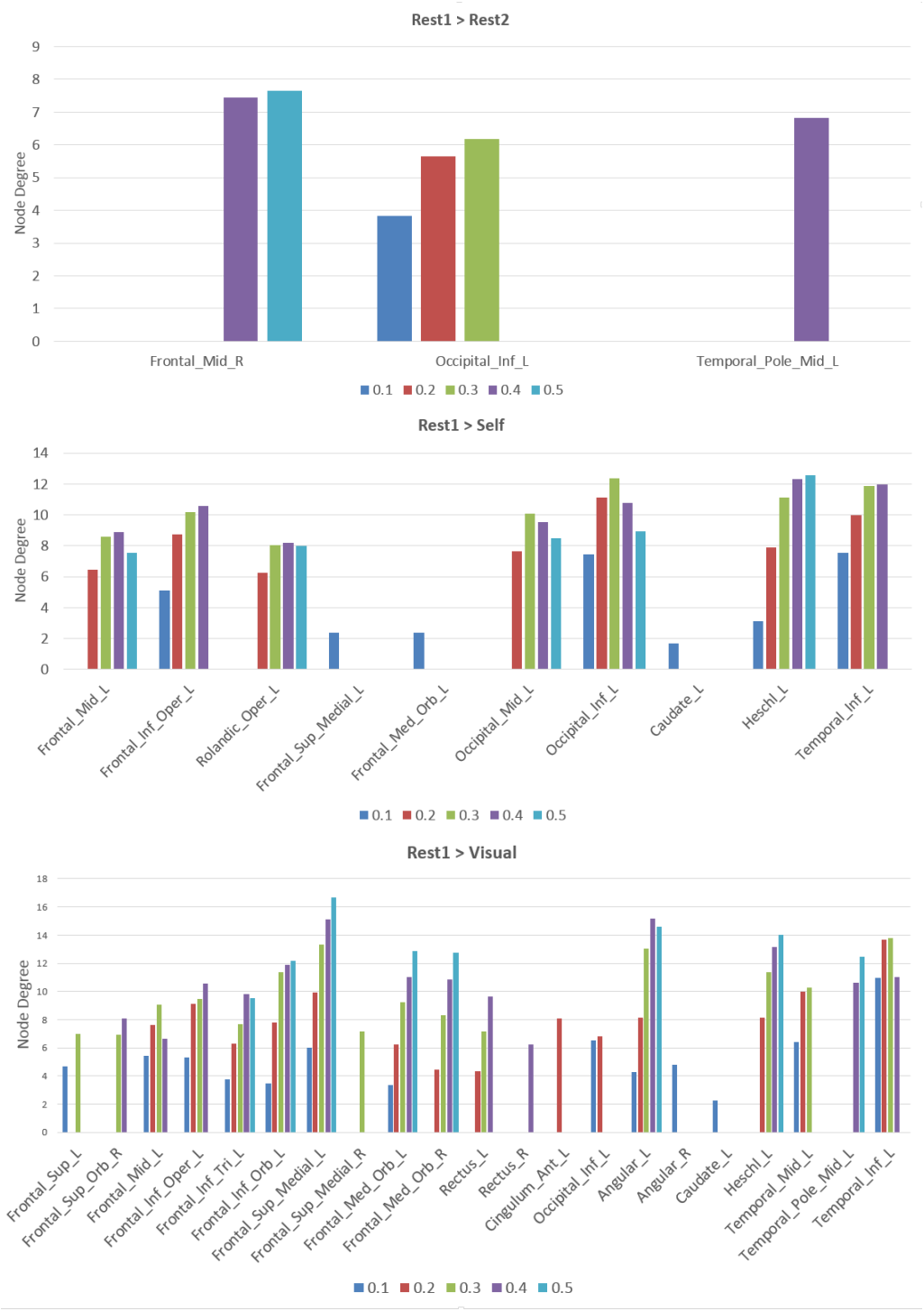

Figure 4.8: Inter-task comparisons considering the node degree measure. The contrasts Rest1 > Rest2, Rest1 > Self and Rest1 > Visual are shown. The values 0.1, 0.2, 0.3, 0.4 and 0.5 represent the relative thresholds applied to create the networks. Only the brain regions that p-values were significant are shown.

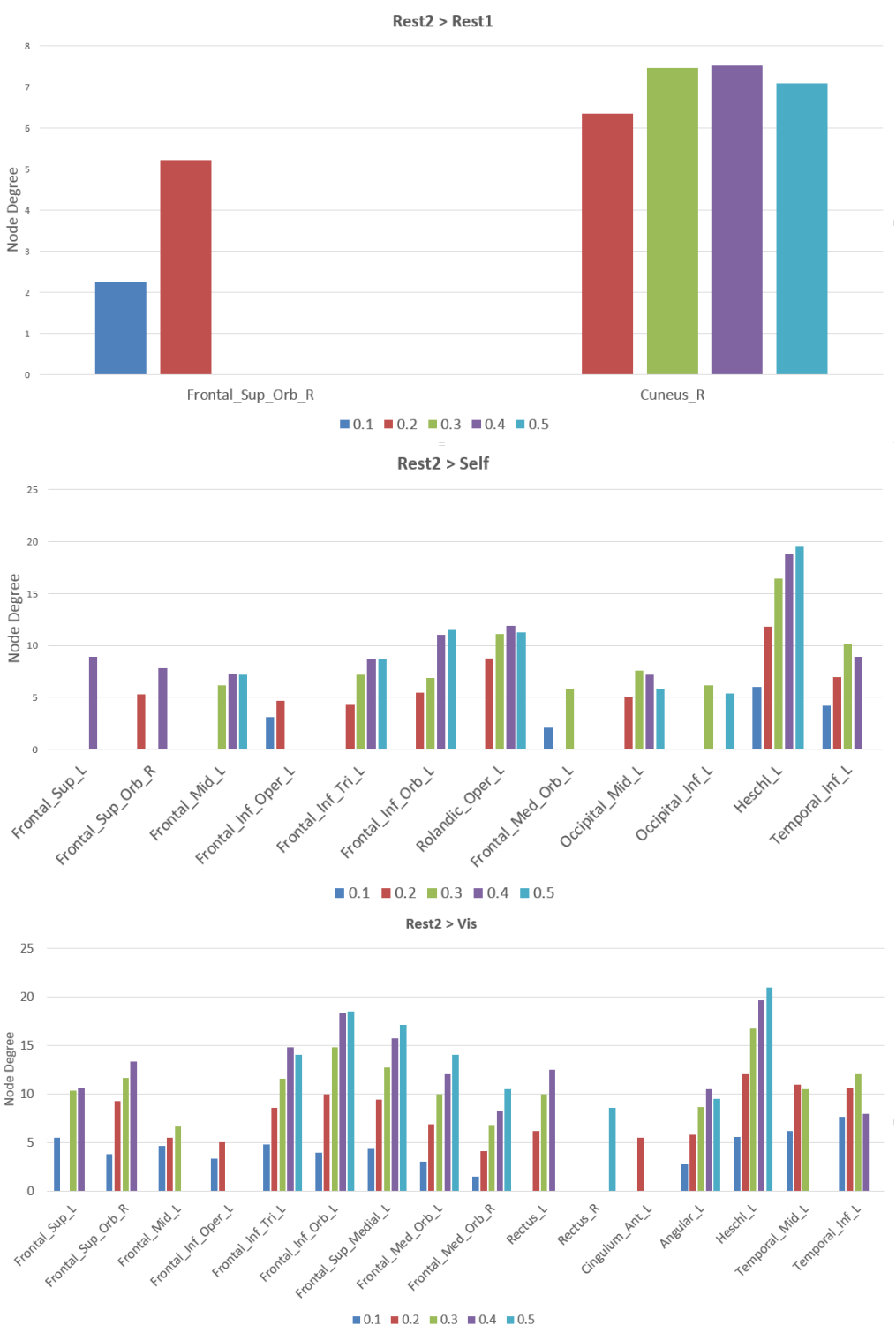

Figure 4.9: Inter-task comparisons considering the node degree measure. The contrasts Rest2 > Rest1, Rest2 > Self and Rest2 > Visual are shown. The values 0.1, 0.2, 0.3, 0.4 and 0.5 represent the relative thresholds applied to create the networks. Only the brain regions that p-values were significant are shown.

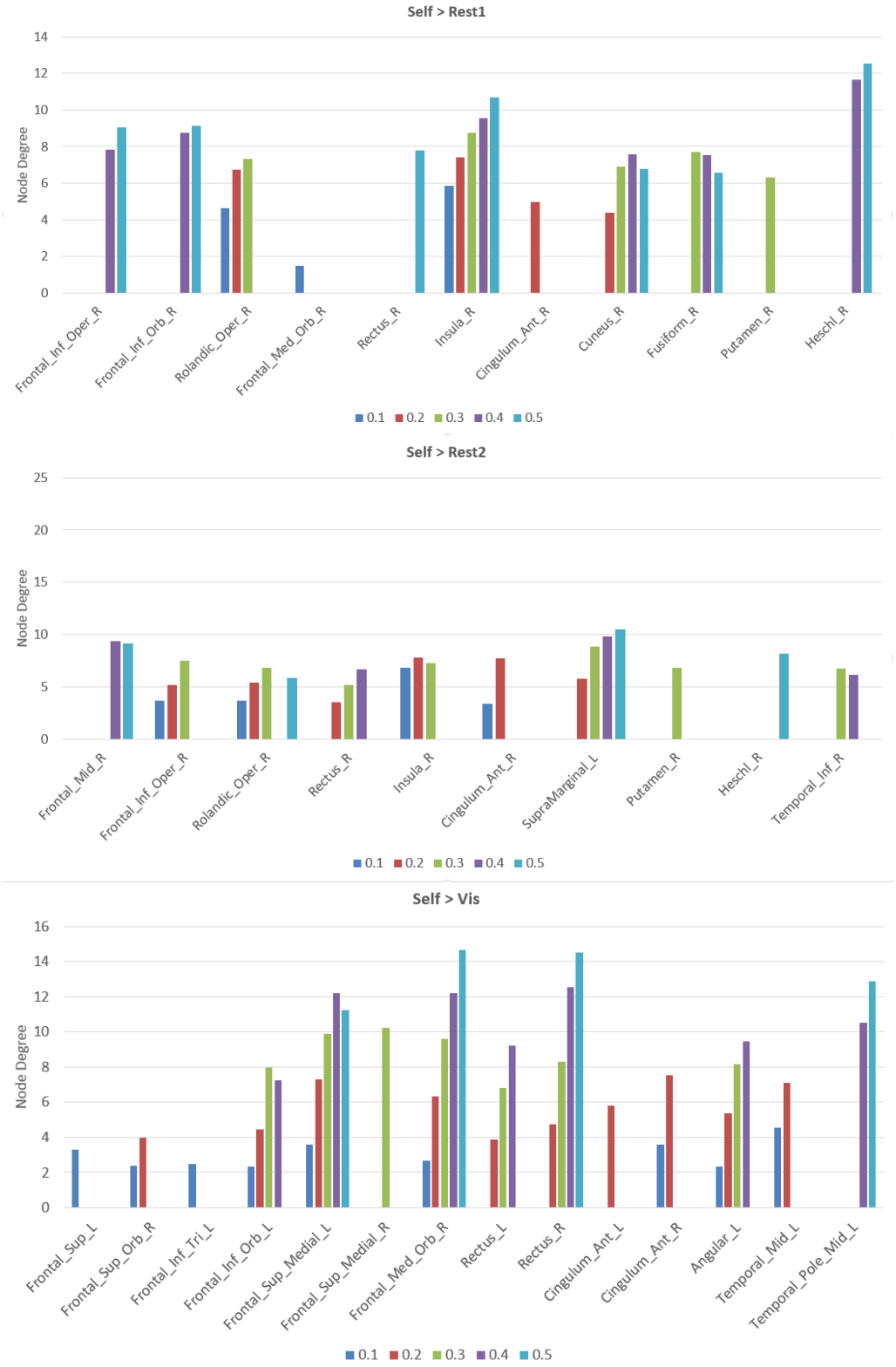

Figure 4.10: Inter-task comparisons considering the node degree measure. The contrasts Self > Rest1, Self > Rest2 and Self > Visual are shown. The values 0.1, 0.2, 0.3, 0.4 and 0.5 represent the relative thresholds applied to create the networks. Only the brain regions that p-values were significant are shown.

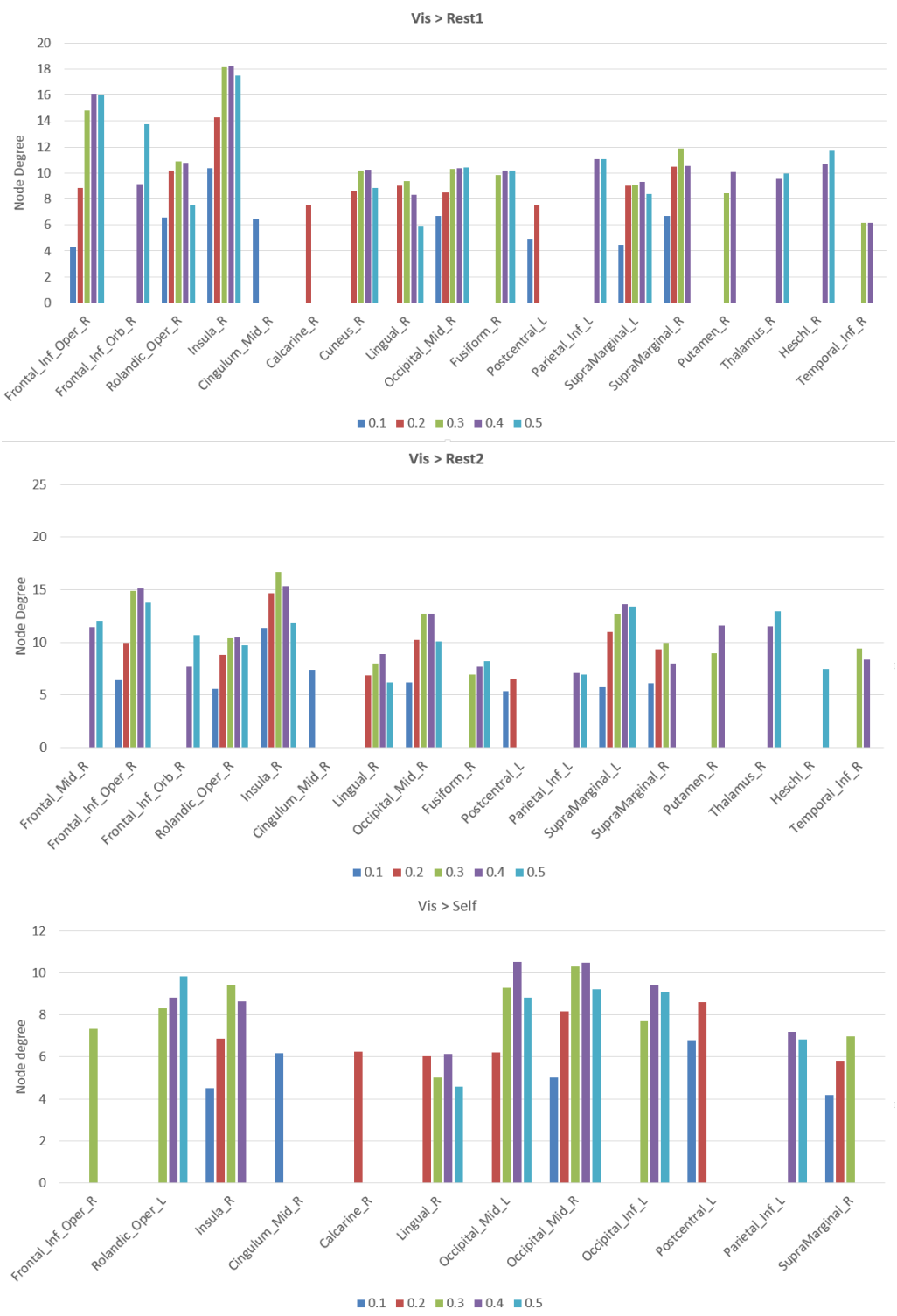

Figure 4.11: Inter-task comparisons considering the node degree measure. The contrasts Visual > Rest1, Visual > Rest2 and Visual > Self are shown. The values 0.1, 0.2, 0.3, 0.4 and 0.5 represent the relative thresholds applied to create the networks. Only the brain regions that p-values were significant are shown.

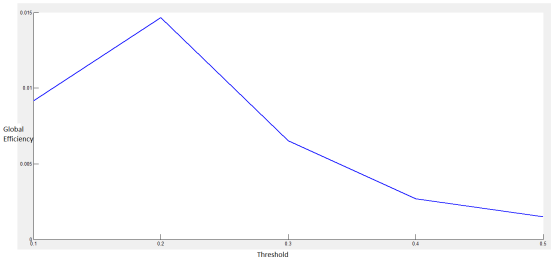

(a) Rest1 > Rest2

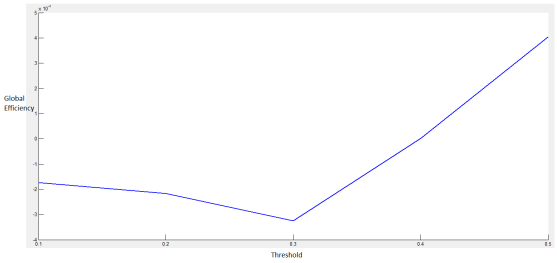

(b) Rest1 > Self

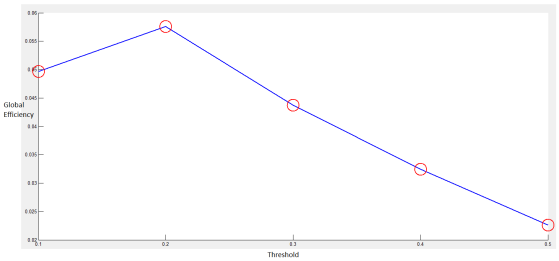

(c) Rest1 > Visual

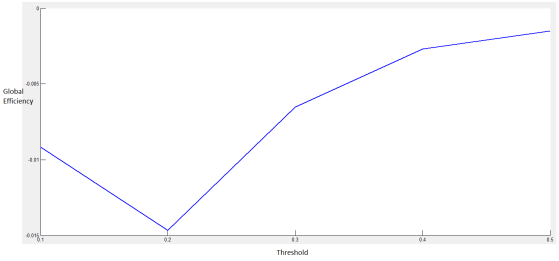

(d) Rest1 < Rest2

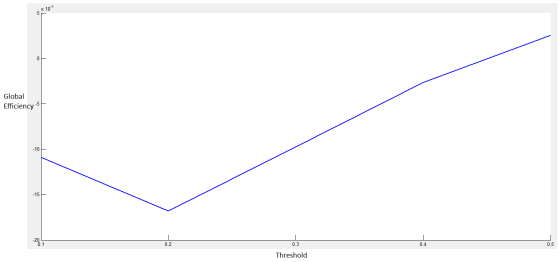

(e) Rest2 > Self

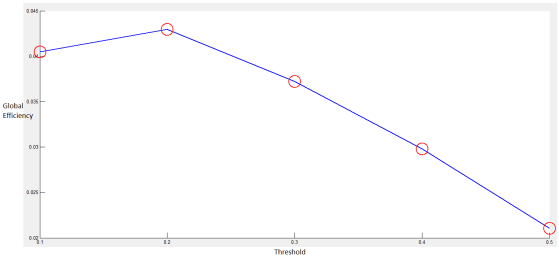

(f) Rest2 > Visual

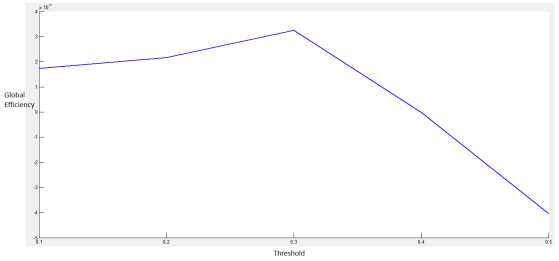

(g) Rest1 < Self

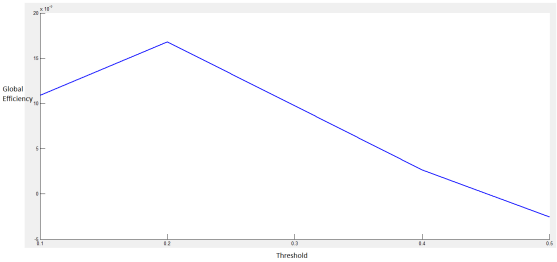

(h) Rest2 < Self

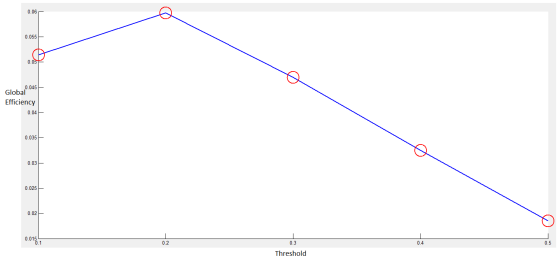

(i) Visual < Self

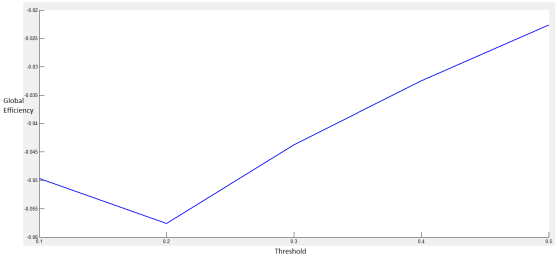

(j) Rest1 < Visual

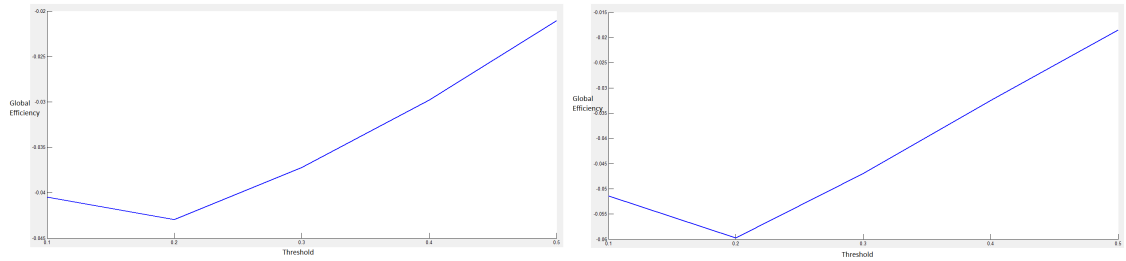

(a) Rest2 < Visual (b) Self < Visual

Figure 4.13: Inter-task comparisons considering the global efficiency measure. The values 0.1, 0.2, 0.3, 0.4 and 0.5 represent the relative thresholds applied to create the networks. Only the brain regions that p-values were significant are shown.

4.3.2 Inter-group comparison

The current project involved also the computation of group comparisons based on the inter-movement interval, the anxiety scales and the BOLD RR interval. The following analysis were performed taking into account the data of acquisition "a" and "b" related to the 25 participants. The mean PL matrices were used and only 24 brain regions were considered (Table 3.1).

4.3.2.1 Inter-movement interval

Following the work of Pfurtscheller et al. (2014b) this analysis aimed to understand the entrainment between slow oscillations and periodic motor responses. The entrainment in physiological systems can be manifest in cases where phase-synchronization between two signals takes place. To test whether voluntary movements has something in common with entrainment of slow oscillations to motor responses this group comparison was performed. A detailed explanation of the formation of groups is in section 3.4.2.3.

Figure 4.14 shows that for A < B the number of functional connections is higher than for A > B. That means the subjects who executed finger movements at relatively regular intervals showed less significant connection than those that showed random inter-movement intervals.

For A < B the functional connections are between Supplementary motor area, Precuneus, Caudate, Lingual and Calcarine. There are inter-hemispheric connections between regions associated to both motor and visual cortex. In the contrast A > B most of the regions are from the right hemisphere whereas in A < B the left hemisphere dominates.

When analysing the data of acquisition b (Figure 4.15) a higher number of connections is observed in the contrast A < B than for A > B. In the comparison A < B most of the regions are from the left hemisphere. These include the Anterior Cingulum, Postcentral, Precentral, Precuneus, Lingual and Calcarine regions. There is a high overlap between the regions involved in acquisition a and b In A > B, there is involvement of Insula, Postcentral and Supplementary motor area most of all in the left hemisphere.

The significant connection between SMA and Insula for A > B, acquisition b, is interesting because it provides support for the hypothesis that these regions are part of a modulatory circuit that influences the choice of when to make a movement and is dependent on 0.1 Hz oscillations. However, the fact that these regions do not show up in the a acquisition hints at low robustness of this effect or inadequate sample size.

The regions involved in the A < B comparison, in the other hand, were very reproducible between acquisition a and b. The more bilateral connectivity pattern in the case of more irregular inter-movement intervals, as well as the recruitment of many motion-related regions, is intriguing although no obvious explanations can be put forward to account for this.

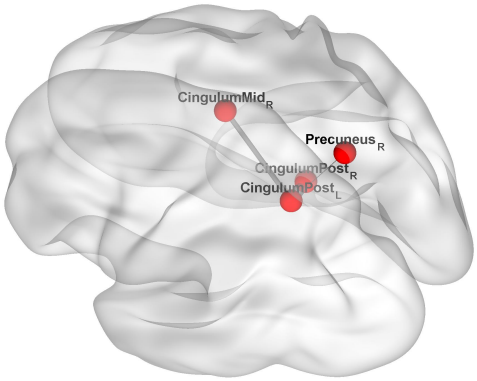

(a) A > B - 1st network

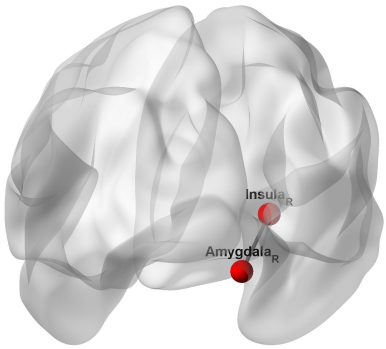

(b) A > B - 2nd network

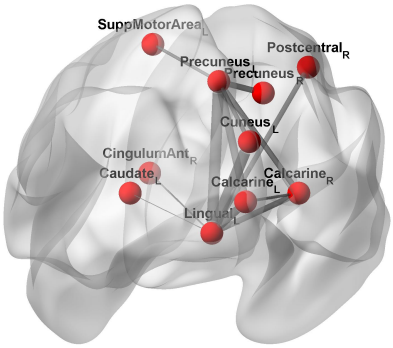

(c) A < B

Figure 4.14: Acquisition a; Inter-group comparison based on the inter movement interval of the participants when executing self paced motion.

4.3.2.2 Anxiety/STADI scales

This group comparison was based in the levels of Anxiety/STADI scales. The aim was to understand what happens in the brain when the anxiety changes across the time. The subjects of the group A showed stable levels of anxiety during the course of the study and subjects of the group B showed a drop in the level of anxiety.

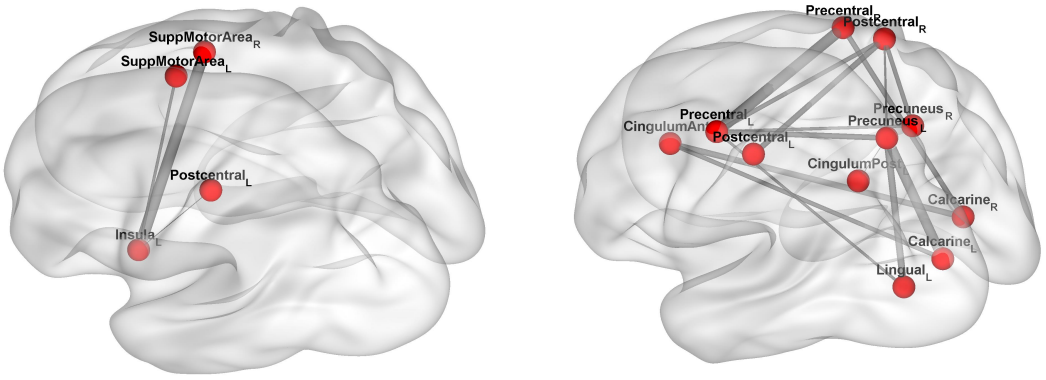

(a) A > B (b) A < B

Figure 4.15: Acquisition b; Inter-group comparison based on the inter movement interval of the participants when executing self paced motion.

In the acquisition "a" significant connections are observed when A > B and A < B. In the first resting (Rest1) state the subjects were naive to the experiment and the levels of anxiety were stable. Several regions known to be involved in voluntary motor actions were active in both the contrasts (Figure 4.16). The involvement of anterior cingulate which is functionally connected to supplementary motor area, precentral and postcentral suggest the activation of these regions during resting state. These results support the findings of Nguyen et al. (2014).

When contrasting the two groups regarding the second resting state (Rest2) a striking observation was noticed. At this point the level of anxiety was reported to drop for subjects gathered in group B. For A > B no significant connection was observed whereas for A < B one could visualize a web of connections involving regions of the left and right hemisphere. The appearance of the amygdala (left) linked to several regions, strengthen the relationship of these results with the levels of anxiety. Amygdala (Left) has been reported to be the heart of mental states and is associated to many psychological disorders such as social anxiety disorders and general anxiety (Duval et al., 2015; He et al., 2016; Vriend et al., 2015).

In the acquisition "b", the first resting state is in conformity with the previous results (Figure 4.18). Non significant results were obtained for A > B whereas A < B showed a high number of functional connections. As the level of anxiety was dropping throughout the study the brain circuits related to this phenomena remain active. The same is verified in the second resting state of the acquisition "b" (Figure 4.19). As anxiety drops the role of amygdala (left) is strengthened since the number of connections involving that region increase. Thus, these results suggest the involvement of amygdala in anxiety alterations.

4.3.2.3 BOLD-RR Interval

At last, group comparisons based on BOLD RRI coupling were performed between subjects with pTD brain-RRI (group A) and nTD brain-RRI (group B).The idea behind this was to

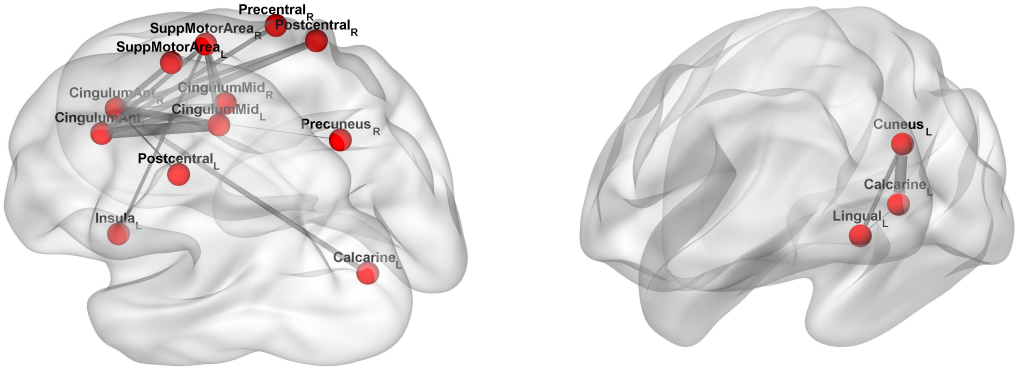

(a) A > B (b) A < B

Figure 4.16: Acquisition a; Inter-group comparison based on Anxiety scales of the participants in the first resting state.

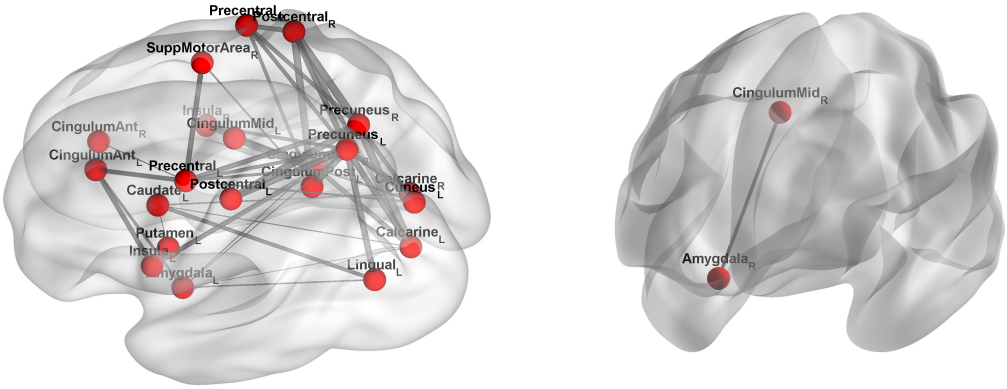

(a) A < B - network 1 (b) A < B - network 2

Figure 4.17: Acquisition a; Inter-group comparison based on Anxiety scales of the participants in the second resting state. Non-significant results to A > B

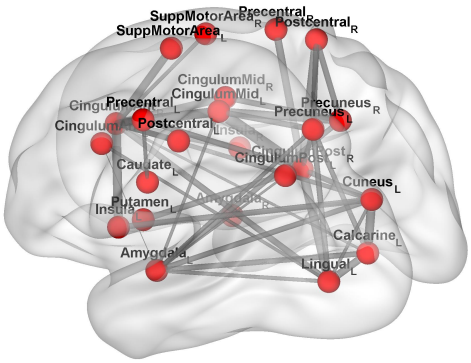

(a) A < B

Figure 4.18: Acquisition b; Inter-group comparison based on Anxiety scales of the participants in the first resting state. Non-significant results to A > B

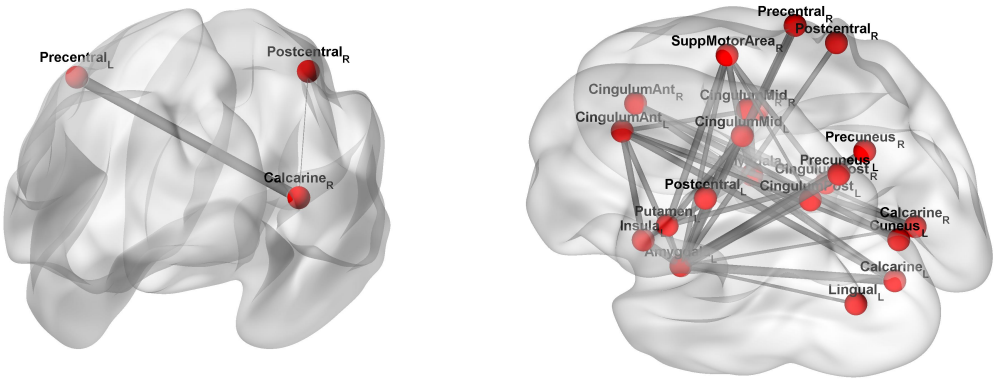

(a) A > B (b) A < B

Figure 4.19: Acquisition b; Inter-group comparison based on Anxiety scales of the participants in the second resting state.

search specific connectivity patterns for pTD (neural BOLD oscillations) and nTD (vascular BOLD oscillations). A detailed explanation of the formation of groups is in section 3.4.2.3.

The results showed specific connectivity patterns for neural BOLD oscillations in the acquisition a, for first and second resting states. In the first resting state (Figure 4.20) most brain regions are involved, especially the Anterior Cingulum, Supplementary Motor Area, Precentral and Postcentral. In the second resting state, most brain regions selected are significantly connected for subjects with pTD. The sheer number of connections that show up stronger in group A than B, as well as the involvement of the middle cingulum and motor-related regions (e.g bilateral SMA) support the findings of Pfurtscheller et al. (submitted) who showed that spontaneous BOLD oscillations could signal a "central pacemaker" not only for brain function, but also for the modulation of heart rate. Although the first resting state session in the b acquisition showed markedly different connectivity patterns, the extensive involvement of the middle cingulum in both A > B and B < A is noteworthy. This region is characterized by an excellent perfusion (nTD) and is a possible source for "central pacemaker" (pTD), hence its involvement in both A > B and B < A, connected to different regions, is understandable. Whilst a full description of the connectivity pattern differences that distinguish between oscillations of neural and vascular origin will require further investigations, this analysis allowed to establish a clear distinction between the two situations and to give creedence to the underlying hypothesis.

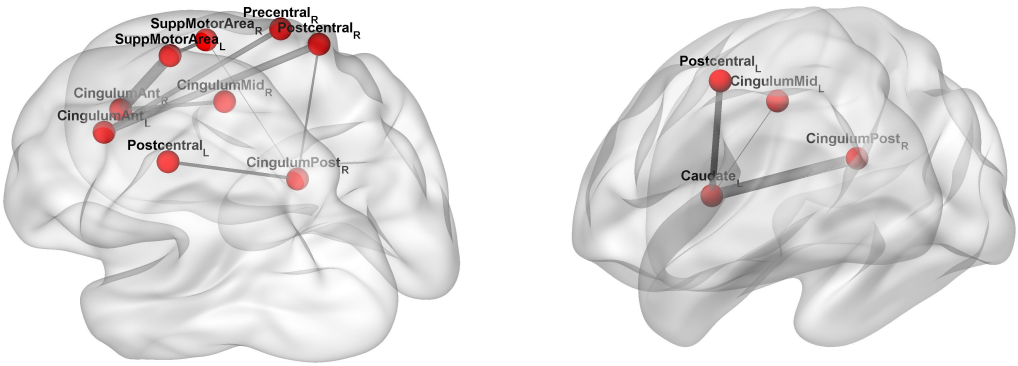

(a) A > B (b) A < B

Figure 4.20: Acquisition a; Inter-group comparison based on BOLD RR Interval of participants in the first resting state.

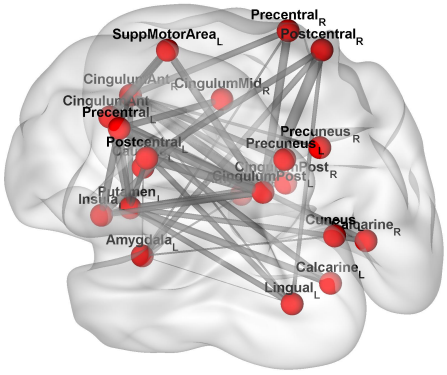

(a) A > B

Figure 4.21: Acquisition a; Inter-group comparison based on BOLD RR Interval of the participants in the second resting state.

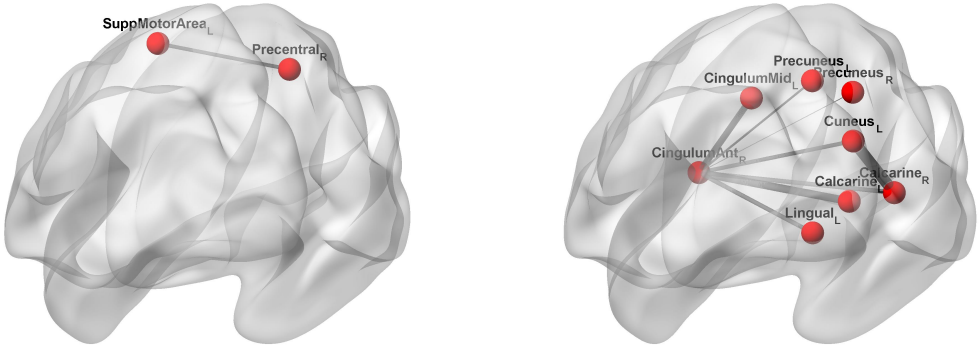

(a) A > B (b) A < B

Figure 4.22: Acquisition b; Inter-group comparison based on BOLD RR Interval of the participants in the first resting state.

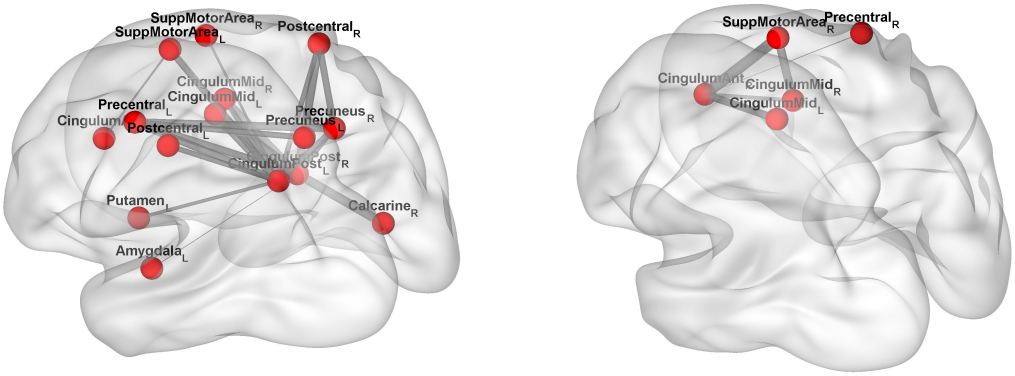

(a) A > B

(b) A < B

Figure 4.23: Acquisition b; Inter-group comparison based on BOLD RR Interval of the participants in the second resting state.

CHAPTER 5

CONCLUSIONS

The present study was carried out in the context of the current interest in describing the human connectome of the brain, particularly components related to voluntary motor behavior (Calhoun et al., 2014). With this goal in mind, an analysis protocol was carried out based on the computation of phase locking, a measure of signal synchrony which reflects the stability of phase differences between two signals across a defined time-window and, as a complementary procedure, Granger causality, a statistical measure of causality based on information theory. The former measure had been computed prior to the onset of this thesis by applying a time-frequency analysis based on Wavelet Transform Coherence which yielded phase locking profiles for the required pairs of regions of interest. The latter was computed within this thesis by calculating multivariate Granger causality from BOLD time-series yielding pairwise-conditional Granger causality matrices and their respective p-values. These analyses were restricted to a narrow frequency band (0.07-0.13) matching the infra-slow BOLD oscillation (0.1 Hz) since these are known to modulate the excitability in the human cortex. Finally, a graph theoretical analysis was performed by using the connectivity matrices obtained by the previous methods. Inter-task and inter-group comparisons were performed concerning the rest and task sessions of the experiment and three variables, the inter-movement interval, the anxiety scales and the BOLD RR coupling, respectively. Graph analysis was performed considering a subset of brain regions associated to motor and visual cortex, in particular, brain areas that have been associated to decision making. Additionally two network topological measures (node degree and global efficiency) were computed in order to characterize the different networks across the states.

In this study, we evaluated the extent to which the two connectivity measures, the Phase Locking and Granger causality were related. The results suggested high values of Phase Locking did not necessarily match high values of Granger causality. Clearly,

further studies are needed to address this question which has been mostly overlooked in the previous literature. Then, inter-task comparisons were performed in order to test the ability of methodologies used and study the brain regions involved in intentional actions. The inter-task comparisons were done firstly directly in the raw connectivity matrices and then considering network topological measures.

In raw connectivity analysis, the results were encouraging for phase locking matrices but ambiguous for Granger causality matrices. For phase locking matrices, we demonstrate that a set of brain regions related to voluntary motor function exhibit significant functional connectivity during the resting state supporting the existence of a large functional connectivity network related to motor function in the resting state. Comparing rest with visual-stimulus driven task, it was demonstrated that networks present in resting state endure during movements guided by visual stimulus and that the presence of a stimulus gives rise to a strong activation of the brain in most of the brain regions. Regarding rest and self-paced movement task we concluded that when performing a self-paced movement, brain networks present during resting state are attenuated. These involve regions known to be related to movement planning such as the insula, the anterior and middle cingulum, the basal ganglia, the primary motor cortex and the primary mostly in the left hemisphere. For Granger causality matrices, no conclusions were drawn because no interpretable patterns were detected. In particular, a high number of implausible inter-hemispheric connections were detected, which leads us to believe that further studies, and a more refined choice of analysis parameters, are needed.

In network analysis, two measures for global and local characterization of the networks were computed with phase locking matrices. Contrasting the rest and task sessions a high node degree for most thresholds was observed in regions of frontal lobe suggesting their important role in decision making. Computing the global efficiency we concluded that efficiency of the functional brain networks derived from fMRI data changes across the rest and task sessions.

Finally, inter-group comparisons considering the inter-movement interval, the anxiety/STADI scales and the BOLD-RRI coupling were performed. Regarding IMI, it was concluded that voluntary finger movements at irregular intervals activated the brain regions associated to voluntary movements more than for movements at regular intervals. For Anxiety/STADI scales, a clear web of brain communications for subjects whose level of anxiety was dropping was verified and amygdala was strongly involved. Thus, the involvement of amygdala in anxiety alterations was demonstrated. At last, the BOLD RRI coupling results provided partial support the central pacemaker theory.

Overall, the objectives of this dissertation were met. Several regions involved in motor decision making were identified and significant functional connections among them were detected. The time-frequency approach based on Wavelet Coherence showed ability to measure brain connectivity even for large datasets. The Granger studies were not so encouraging having been left for future work. GraphVar toolbox showed to be a powerful tool to perform graph theoretical analysis.

5.1 Future Work

As future work a more precise analysis on Granger causality method should be done. Obtaining a measure of effective connectivity allows us to understand the directionality of the brain connections and to extend our comprehension of brain circuits involved in voluntary motor actions. Thus, it is necessary to carefully evaluate all the parameters of the multivariate Granger causality toolbox in order to understand what could cause the results obtained. Additionally, deconvolution methods may be applied in order to remove the effect of differentially slow hemodynamic responses across the brain or across subjects, thus leading to more precise results.

Regarding GraphVar toolbox, the full adaptation to the directed Granger causality matrices should be done in order to extract the "glass brains" and analyse the graphs. Up to now, the toolbox allow to perform statistical analysis with Granger causality matrices in both raw connectivity and network construction sections but one can not visualize the graphs.

A deep study of the relationship between Phase Locking and Granger Causality also could be an asset to understand brain mechanisms. Whilst the current study suggested a moderate link between these two measures, further efforts are needed in order to clarify the overlap between the results of phase-based methods and causality-based methods.

Another issue that future studied may address is to what extent using a different atlas may be helpful in order to refine the spatial specificity of the analysis. For instance, conclusions drawn from the involvement of the insular cortex are conditioned by the fact that the whole insula is considered as a single ROI. However, the functional specialization of different subsections of the insula is well established, and therefore the use of a more spatially refined atlas might be able to yield more specific and accurate results.

Finally, the use of other association measures such as coherence magnitude and other topological measures (e.g. small-worldness, rich club coefficient) is a logical step towards a fuller characterization of the connectivity patterns involved in these tasks.

5.2 Contributions

The contributions of this dissertation are briefly summarized in this Section:

- Poster communication at the 1^{st} meeting of the PhD students, Mind-Brain College of the University of Lisbon, held in Lisbon on the 2^{nd} of December 2015. The present poster can be found in Appendix A
- Abstract approved to poster presentation in the 22^{nd} Annual Meeting of the Organization for Human Brain Mapping to be held in Geneva, Switzerland on June 26-30, 2016. The abstract submitted and approved can be found in Appendix B

BIBLIOGRAPHY

Absher, J. R. and D. F. Benson. (1993). "Disconnection syndromes: an overview of Geschwind's contributions." In: *Neurology* 43(5), pp. 862–867.

Achermann, P. and A. Borbély (1997). "Low-frequency (<1 Hz) oscillations in the human sleep electroencephalogram". In: *Neuroscience* 81, pp. 213–222. DOI: 10.1016/S0306-4522(97)00186-3.

Aladjalova, N. A. (1957). "Infra-Slow Rhythmic Oscillations of The Steady Potential of the Cerebral Cortex". In: *Nature* 179, pp. 957–959. DOI: 10.1038/179957a0.

Ancona, N., D. Marinazzo, and S. Stramaglia (2004). "Radial basis function approach to nonlinear Granger causality of time series". In: *Phys. Rev. E* 70.

Ariani, G., M. F. Wurm, and A. Lingnau (2015). "Decoding Internally and Externally Driven Movement Plans". In: *J Neurosci* 35, pp. 14160–71.

Asemi, A., K. Ramaseshan, A. Burgess, V. A. Diwadkar, and S. L. Bressler (2015). "Dorsal anterior cingulate cortex modulates supplementary motor area in coordinated unimanual motor behavior". In: *Frontiers in Human Neuroscience* 9.

Auger, F., P. Flandrin, P. Gonzalves, and O. Lemoine. (1997). "Time-frequency toolbox. For use with Matlab." In: *Tutorial*.

Bednark, J. G., M. E. J. Campbell, and R. Cunnington (2015). "Basal ganglia and cortical networks for sequential ordering and rhythm of complex movements." In: *Front Hum Neurosci.*. 9.

Bengtsson, S. L., H. H. Ehrsson, H. Forssberg, and F. Ullen (2004). "Dissociating brain regions controlling the temporal and ordinal structure of learned movement sequences." In: *Eur. J. Neurosci.* 19, pp. 2591–2602.

Biswal, B., F. Z. Yetkin, V. M. Haughton, and J. S. Hyde (1995). "Functional connectivity in the motor cortex of resting human brain using echo-planar MRI". In: *Magn Reson Med* 34(4), pp. 537–541.

Bonato, P., G. Gagliati, and M. Knaflitz (1996). "Analysis of myoelectric signals recorded during dynamic contractions." In: *IEEE Eng Med Biol Mag* 15, pp. 102–111.

Brass, M. and P. Haggard (2010a). "The hidden side of intentional action: the role of the anterior insular cortex". In: *Brain Structure and Function* 214, pp. 603–610. DOI: 10.1007/s00429-010-0269-6.

Brass, M. and P. Haggard (2010b). "To Do or Not to Do: The Neiral Signature of Self-Control". In: *The Journal of Neuroscience.* 27(34), pp. 9141–9145. DOI: 10.1523/JNEUROSCI.0924-07.2007.

Brito, J. P. F. de (2014). *Dynamic Functional Connectivity of BOLD fMRI signal during both rest and task execution states*. Master's Thesis.

Bullmore, E. and O. Sporns (2009). "Complex brain networks: graph theoretical analysis of structural and functional systems". In: *Nat Rev Neurosci* 10, pp. 189–198.

Buzsaki, G. (2006). *Rhythms of the Brain*. Oxford University Press: New York.

Calhoun, V. D., R. Miller, G. Pearlson, and T. Adalı (2014). "The Chronnectome: Time-Varying Connectivity Networks as the Next Frontier in fMRI Data Discovery". In: *Neuron* 84, pp. 262–274.

Chang, C. and G. H. Glover (2010). "Time-Frequency Dynamics of Resting-State Brain Connectivity Measured with fMRI." In: *NeuroImage* 50(1), pp. 81–98.

Chang, L. J., T. Yarkoni, M. W. Khaw, and A. G. Sanfey (2013). "Decoding the Role of the Insula in Human Cognition: Functional Parcellation and Large-Scale Reverse Inference". In: *Cereb Cortex* 23, pp. 739–749.

Chao-Gan, Y. and Z. Yu-Feng (2010). "DPARSF: a MATLAB toolbox for "pipeline" data analysis of resting-state fMRI." In: *Front Syst Neurosci* 4.

Cordes, D., V. M. Haughton, K. Arfanakis, G. J. Wendt, P. A. Turski, C. H. Moritz, M. A. Quigley, and M. E. Meyerand (2000). "Mapping Functionally Related Regions of Brain with Functional Connectivity MR Imaging". In: *American Journal of Neuroscience* 21, pp. 1636–1644.

Craig, A. D. (2009). "How do you feel — now? The anterior insula and human awareness". In: *Nat. Rev. Neurosci* 10, pp. 59–70.

Csercsa, R. et al. (2010). "Laminar analysis of slow wave activity in humans". In: *Brain* 133, pp. 2814–2829. DOI: 10.1093/brain/awq169.

deCharms, R. C. (2008). "Applications of real-time fMRI". In: *Nature Reviews Neuroscience* 9, pp. 720–729. DOI: 10.1038/nrn2414.

Deecke, L. and H. H. Kornhuber (2003). "Human Freedom, Reasoned Will, and the Brain: The Bereitschaftspotential Story". In: *M Jahanshahi, M Hallett (Eds.) The Bereitschaftspotential, movement-related cortical potentials.* Pp. 283–320.

Deiber, M.-P., M. Honda, V. Ibañez, N. Sadato, and M. Hallett (1999). "Mesial Motor Areas in Self-Initiated Versus Externally Triggered Movements Examined With fMRI: Effect of Movement Type and Rate". In: *Journal of Neurophysiology* 8(6), pp. 3065–3077.

Dum, R. P. and P. L. Strick (2005). "Frontal Lobe Inputs to the Digit Representations of the Motor Areas on the Lateral Surface of the Hemisphere". In: *The Journal of Neuroscience* 25(6), pp. 1375–1386. DOI: 10.1523/JNEUROSCI.3902-04.2005.

Duval, E. R., A. Javanbakht, and I. Liberzon (2015). "Neural circuits in anxiety and stress disorders: a focused review". In: *Ther Clin Risk Manag* 11, pp. 115–126.

Faro, S. H. and F. B. Mohamed (2006). *Functional MRI - Basic Principles and Clinical Applications*. McGraw-Hill. ISBN: 978-0-387-34665-6.

Filippi, M. (2009). *fMRI Techniques and Protocols, Neuromethods*. Vol. 41. DOI: 10.1007/978-1-60327-919-2_1.

Filippov, I. V. and V. A. Frolov (2004). "Very slow potentials in the lateral geniculate complex and primary visual cortex during different illumination changes in freely moving rats". In: *Neuroscience Letters* 373, pp. 51–56. DOI: 10.1016/j.neulet.2004.09.056.

Filippov, I. V., W. C. Williams, A. A. Krebs, and K. S. Pugachev (2007). "Sound-induced changes of infraslow brain potential fluctuations in the medial geniculate nucleus and primary auditory cortex in anaesthetized rats". In: *Brain Research* 1133, pp. 78–86.

Fox, M. D. and M. E. Raichle (2007). "Spontaneous fluctuations in brain activity observed with functional magnetic resonance imaging". In: *Nature Reviews Neuroscience* 8, pp. 700–711.

Fransson, P. (2005). "Spontaneous low-frequency BOLD signal fluctuations: An fMRI investigation of the resting-state default mode of brain function hypothesis". In: *Human Brain Mapping* 26, pp. 15–29.

Freiwald, W. A., P. Valdes, J. Bosch, R. Biscay, J. C. Jimenez, L. M. Rodriguez, V. Rodriguez, A. K. Kreiter, and W. Singer (1999). "Testing non-linearity and directedness of interactions between neural groups in the macaque inferotemporal cortex." In: *J Neurosci Methods* 94, pp. 105–19.

Fries, P. (2005). "A mechanism for cognitive dynamics: neuronal communication through neuronal coherence". In: *TRENDS in Cognitive Sciences* 9, pp. 474–480.

Geweke, J. (1984). "Measures of conditional linear dependence and feedback between time series." In: *J. Am. Stat. Assoc* 79, pp. 907–915.

Goldberg, G. (1985). "Supplementary motor area structure and function: Review and hypotheses". In: *Behavioral and Brain Sciences* 8, pp. 567–588. DOI: http://dx.doi.org/10.1017/S0140525X00045167.

Goparaju, B., K. D. Rana, F. J. Calabro, and L. M. Vaina (2014). "A computational study of whole-brain connectivity in resting state and task fMRI". In: *Medical Science Monitor* 20, pp. 1024–1042.

Gowena, E. and R. C. Miallb (2007). "Differentiation between external and internal cuing: An fMRI study comparing tracing with drawing". In: *Neuroimage* 36, pp. 396–410.

Granger, C. (1969). "Investigating causal relations by econometric models and crossspectral methods." In: *Econometrica* 37, pp. 424–438.

Graya, C. M., A. K. Engela, P. Königa, and W. Singera (1992). "Synchronization of oscillatory neuronal responses in cat striate cortex: Temporal properties." In: *Vis Neurosci* 8, pp. 337–347.

Grinsted, A., J. C. Moore, and S. Jevrejeva (2004). "Application of the cross wavelet transform and wavelet coherence to geophysical time series". In: *Nonlinear Processes in Geophysics* 11, pp. 561–566.

Haggard, P. (2005). "Conscious intention and motor cognition". In: *TRENDS in Cognitive Sciences* 9(6).

Haggard, P. (2008). "Human volition: towards a neuroscience of will". In: *Nature Reviews Neuroscience* 9, pp. 934–946. DOI: 10.1038/nrn2497.

Hampson, M., B. S. Peterson, P. Skudlarski, J. C. Gatenby, and J. C. Gore (2002). "Detection of functional connectivity using temporal correlations in MR images". In: *Human Brain Mapping* 15, pp. 247–262. DOI: 10.1002/hbm.10022.

He, Y., T. Xu, W. Zhang, and X.-N. Zuo (2016). "Lifespan Anxiety Is Reflected in Human Amygdala Cortical Connectivity". In: *Human Brain Mapping* 37, pp. 1178–1193.

Heeger, D. J. and D. Ress (2002). "What does fMRI tells us about neural activity?" In: *Nature Reviews Neuroscience* 3, pp. 142–151.

Heuvel, M. P. van den and H. E. H. Pol (2010). "Exploring the brain network: A review on resting-state fMRI functional connectivity". In: *European Neuropsychophamacology* 20, pp. 519–534.

Heuvel, M. P. van den, C. J. Stam, M. Boersma, and H. E. H. Pol (2008). "Small-world and scale-free organization of voxel-based resting-state functional connectivity in the human brain". In: *NeuroImage* 43, pp. 528–539.

Hoffstaedter, F., C. Grefkes, K. Zilles, and S. B. Eickhoff (2013). "The What and When of Self-Initiated Movements". In: *Cereb Cortex* 23, pp. 520–530.

Hosseini, S. M., F. Hoeft, and S. R. Kesler (2012). "GAT: A Graph-Theoretical Analysis Toolbox for Analyzing Between-Group Differences in Large-Scale Structural and Functional Brain Networks". In: *PLoS ONE* 7.

Huettel, S. A., A. W. Song, and G. McCarthy (2004). *Functional Magnetic Resonance Imaging, Second edition*. Sunderland, Massachusetts U.S.A. ISBN: 978-0878932863.

Hurtado, J. M., L. L. Rubchinsky, and K. A. Sigvardt (2004). "Statistical method for detection of phase-locking episodes in neural oscillations." In: *J Neurophysiol* 91, pp. 1883–98.

Jahanshahi, M., I. H. Jenkins, R. G. Brown, C. D. Marsden, R. E. Passingham, and D. J. Brooks (1995). "Self-initiated versus externally triggered movementsI. An investigation using measurement of regional cerebral blood flow with PET and movement-related potentials in normal and Parkinson's disease subjects". In: *Brain* 4, pp. 913–933. DOI: http://dx.doi.org/10.1093/brain/118.4.913.

Jenkins, I. H., M. Jahanshahi, M. Jueptner, and D. J. B. Richard E. Passingham (2000). "Self-initiated versus externally triggered movements. II. The effect of movement predictability on regional cerebral blood flow". In: *Brain* 6, pp. 1216–1228. DOI: http://dx.doi.org/10.1093/brain/123.6.1216.

Julien, C. (2006). "The enigma of Mayer waves: Facts and models". In: *Cardiovascular Research* 70, pp. 12–21. DOI: 10.1016/j.cardiores.2005.11.008.

Koch, G., M. Bozzali, S. Bonnì, V. Giacobbe, C. Caltagirone, and M. Cercignani (2012). "fMRI Resting Slow Fluctuations Correlate with the Activity of Fast Cortico-Cortical Physiological Connections". In: *PLoS ONE* 7(12). ISSN: e52660. DOI: 10.1371/journal.pone.0052660.

Kruschwitz, J., D. List, L. Waller, M. Rubinovc, and H. Walter (2015). "GraphVar: A user-friendly toolbox for comprehensive graph analyses of functional brain connectivity". In: *Journal of Neuroscience Methods* 245, pp. 107–115.

Lachaux, J.-P., E. Rodriguez, J. Martinerie, and F. J. Varela (1999). "Measuring Phase Synchrony in Brain Signals". In: *Human Brain Mapping* 8, pp. 194–208.

Lachaux, J.-P., A. Lutz, D. Rudrauf, D. Cosmelli, M. L. V. Quyen, J. Martinerie, and F. Varelar (2002). "Estimating the time-course of coherence between single-trial brain signals: an introduction to wavelet coherence". In: *Neurophysiol Clin* 32, pp. 157–174.

Leopold, D. A., Y. Murayama, and N. K. Logothetis (2003). "Very Slow Activity Fluctuations in Monkey Visual Cortex: Implications for Functional Brain Imaging". In: *Cerebral Cortex* 13(4), pp. 422–433. ISSN: 0362-1340. DOI: http://doi.acm.org/10.1145/1449955.1449783.

Libet, B., C. A. Gleason, E. W. Wright, and D. K. Pearl (1983). "Time of conscious intention to act in relation to onset of cerebral activity (readiness-potential). The unconscious initiation of a freely voluntary act". In: *Brain* 106, pp. 623–642. DOI: http://dx.doi.org/10.1093/brain/106.3.623.

Loukasa, C. and P. Browna (2004). "Online prediction of self-paced hand-movements from subthalamic activity using neural networks in Parkinson's disease". In: *Journal of Neuroscience Methods* 137, pp. 193–205. DOI: 10.1016/j.jneumeth.2004.02.017.

Lowe, M. J., B. J. Mock, and J. A. Sorenson (1998). "Functional Connectivity in Single and Multislice Echoplanar Imaging Using Resting-State Fluctuations". In: *Neuroimage* 7, pp. 119–132.

Müller, K., G. Lohmann, J. Neumann, M. Grigutsch, T. Mildner, and D. Y. von Cramon (2004). "Investigating the wavelet coherence phase of the BOLD signal." In: *J Magn Reson Imaging* 20(1), pp. 145–152.

Monto, S., S. Palva, J. Voipio, and J. M. Palva (2008). "Very Slow EEG Fluctuations Predict the Dynamics of Stimulus Detection and Oscillation Amplitudes in Humans". In: *The Journal of Neuroscience* 28(23), pp. 8268–8272. DOI: 10.1523/JNEUROSCI.1910-08.2008.

Nachevemail, P. and M. Husain (2010). "Action and the fallacy of the 'internal': Comment on Passingham et al". In: *Trends in Cognitive Sciences* 14(5), pp. 192–193. DOI: 10.1016/j.tics.2010.03.002.

Nguyen, V. T., M. Breakspear, and R. Cunnington (2014). "Reciprocal Interactions of the SMA and Cingulate Cortex Sustain Premovement Activity for Voluntary Actions". In: *Behavioral/Cognition* 34, pp. 16397–16407.

Nichols, T. E. and A. P. Holmes (2001). "Nonparametric Permutation Tests For Functional Neuroimaging: A Primer with Examples". In: *Human Brain Mapping* 15, pp. 1–25.

Nir, Y., R. Mukamel, I. Dinstein, E. Privman, M. Harel, L. Fisch, H. Gelbard-Sagiv, S. Kipervasser, F. Andelman, M. Y. Neufeld, U. Kramer, A. Arieli, I. Fried, and R. Malach (2008). "Interhemispheric correlations of slow spontaneous neuronal fluctuations revealed in human sensory cortex". In: *Nature Neurosciences* 11, pp. 1100–1108. DOI: 10.1038/nn.2177.

Pereda, E., R. Q. Quiroga, and J. Bhattacharya (2005). "Nonlinear multivariate analysis of neurophysiological signals". In: *Progress in Neurobilogy* 77, pp. 1–37.

Pfurtscheller, G., I. Daly, G. Bauernfeind, and G. R. Muller-Putz (2012a). "Coupling between intrinsic prefrontal HbO2 and central EEG beta power oscillations in the resting brain." In: *Plos one* 7, e43640. DOI: doi:10.1371/journal.pone.0043640.

Pfurtscheller, G., G. Bauernfeinda, C. Neuper, and F. H. L. da Silva (2012b). "Does conscious intention to perform a motor act depend on slow prefrontal (de)oxyhemoglobin oscillations in the resting brain?" In: *Neuroscience Letters* 508, pp. 89–94. DOI: 10.1016/j.neulet.2011.12.025.

Pfurtscheller, G., A. Andrade, K. Koschutnig, C. Brunner, and F. L. da Silva (2014a). "Initiation of voluntary movements at free will and ongoing 0.1-Hz BOLD oscillations in the insula—a pilot study". In: *Front Integr Neurosci* 8. DOI: doi:10.3389/fnint.2014.00093.

Pfurtscheller, G., A. Schwerdtfeger, A. Seither-Preisler, C. Brunner, C. S. Aigner, J. Brito, M. P. Carmo, and A. Andrade (submitted). "The enigma of Mayer waves: Evidence for "central pacemaker" in the Cingulum". In: *Cardiovascular Research*.

Pfurtscheller, G. and F. H. L. da Silva (1999). "Event-related EEG/MEG synchronization and desynchronization: basic principles". In: *Clinical Neurophysiology* 110, pp. 1842–1857.

Pfurtscheller, G., D. Klobassa, C. Altstätter, G. Bauernfeind, and C. Neuper (2011). "About the stability of phase shifts between slow oscillations around 0.1 Hz in cardiovascular and cerebral systems." In: *IEEE Trans Biomed Eng* 58(7), pp. 2064–2071.

Pfurtscheller, G., M. Walther, R. J. Barry, G. Bauernfeind, H. Witte, and G. R. Mueller-Putz (2014b). "Entrainment of spontaneous cerebral hemodynamic oscillations to behavioral responses". In: *Neuroscience Letters* 566, pp. 93–97.

Raea, C. L., L. E. Hughesa, C. Weavera, M. C. Andersona, and J. B. Rowea (2014). "Selection and stopping in voluntary action: A meta-analysis and combined fMRI study". In: *NeuroImage* 86, pp. 381–391.

Raemaekers, M., W. Schellekens, R. J. van Wezel, N. Petridou, G. Kristo, and N. F. Ramsey. (2014). "Patterns of resting state connectivity in human primary visual cortical areas: a 7T fMRI study". In: *Neuroimage* 84, pp. 911–921.

Rizzolatti, G. and M. M. Gd Luppino (1998). "The organization of the cortical motor system: new concepts". In: *Electroencephalography and clinical Neurophysiology* 106, pp. 283–296.

Roelfsema, P. R., A. K. Engel, P. König, and W. Singer (1997). "Visuomotor integration is associated with zero time-lag synchronization among cortical areas". In: *Nature* 385, pp. 157–61.

Rubinov, M. and O. Sporns (2010). "Complex network measures of brain connectivity: Uses and interpretations". In: *NeuroImage* 52, pp. 1059–1069.

Schüür, F. and P. Haggard (2011). "What are self-generated actions?" In: *Consciousness and Cognition* 20, pp. 1697–1704. DOI: 10.1016/j.concog.2011.09.006.

Seth, A. K. and L. Barnett (2014). In: *The Journal of Neuroscience Methods* 223, pp. 50–68.

Seth, A. K., A. B. Barrett, and L. Barnett (2015). "Granger Causality Analysis in Neuroscience and Neuroimaging". In: *The Journal of Neuroscience* 35(8), pp. 3293–3297. DOI: 10.1523/JNEUROSCI.4399-14.2015.

Shibasaki, H. and M. Hallett (2006). "What is the Bereitschaftspotential?" In: *Clinical Neurophysiology* 117, pp. 2341–2356. DOI: 10.1016/j.clinph.2006.04.025.

Someren, E. J. V., Y. D. V. D. Werf, P. R. Roelfsema, H. D. Mansvelder, and F. H. L. da Silva (2011). "Slow brain oscillations of sleep, resting state, and vigilance". In: *Prog Brain Res* 193, pp. 3–15.

Sporns, O. (2011). *Networks of the Brain*. First. Cambridge, London: The MIT Press.

Sporns, O. (2013). "Structure and function of complex brain networks". In: *Dialogues in Clinic Neuroscience* 15(3), pp. 247–262.

Srinivasan, L., W. F. Asaad, D. T. Ginat, J. T. Gale, D. D. Dougherty, Z. M. Williams, T. J. Sejnowski, and E. N. Eskandar (2013). "Action Initiation in the Human Dorsal Anterior Cingulate Cortex". In: *PLoS ONE* 8.

Steriade, M. and D. Contreras (1998). "Spike-wave complexes and fast components of cortically generated seizures. I. Role of neocortex and thalamus". In: *Journal of Neurophysiology* 80(3), pp. 1439–1455. ISSN: 0022-3077.

Stiber, B. Z. and S. Sato. (1997). "Visualization of EEG using time-frequency distributions." In: *Meth. Inf. Med* 36, pp. 298–301.

Sun, H., T. M. Blakely, F. Darvas, J. D. Wander, L. A. Johnson, D. K. Su, K. J. Miller, E. E. Fetz, and J. G. Ojemann (2015). "Sequential activation of premotor, primary somatosensory and primary motor areas in humans during cued finger movements". In: *Clinical Neurophysiology* 126, pp. 2150–2161.

Taga, G., Y. Konishi, A. Maki, T. Tachibana, M. Fujiwara, and H. Koizumi (2000). "Spontaneous oscillation of oxy- and deoxy- hemoglobin changes with a phase difference throughout the occipital cortex of newborn infants observed using non-invasive optical topography". In: *Neuroscience Letters.* 282(1-2), pp. 101–104.

Taya, F., Y. Sun, N. Thakor, and A. Bezerianos (2014). "Information Transfer Efficiency during Rest and Task A Functional Connectome Approach". In: *IEEE*.

Thatcher, R. W. (1995). "Tomographic electroencephalography/magnetoencephalography. Dynamics of human neural network switching." In: *J Neuroimaging* 5(1), pp. 35–45.

Tononi, G., O. Sporns, and G. M. Edelman (1994). "A measure for brain complexity: relating functional segregation and integration in the nervous system". In: *Proc. Nalt. Acad. Sci. USA* 91, pp. 5033–5037.

Toronov, V., M. A. Franceschini, M. Filiaci, S. Fantini, M. Wolf, A. Michalos, and E. Gratton (2007). "Near-infrared study of fluctuations in cerebral hemodynamics during rest and motor stimulation: Temporal analysis and spatial mapping". In: *Med. Phys* 27(4), pp. 801–815.

Torrence, C. and G. P. Compo (1998). "A Practical Guide to Wavelet Analysis". In: *Bulletin of the American Meteorological Society* 79(1), pp. 61–78.

Tremblay, M., D. Lacroix, Y. Chaput, V. Fraïle, R. Lamer, and J. M. Albert (1994). "Brain activation with a maze test: an EEG coherence analysis study in healthy subjects." In: *Neuroreport* 5, pp. 2449–2453.

Tzeng, Y., S. Lucas, G. Atkinson, C. Willie, and P. Ainslie (2010). "Fundamental relationships between arterial baroreflex sensitivity and dynamic cerebral autoregulation in humans". In: *J. Appl. Physiol* 108(5), pp. 1162–1168.

Tzourio-Mazoyer, N., B. Landeau, D. Papathanassiou, F. Crivello, O. Etard, N. Delcroix, B. Mazoyer, and M. Joliot (2002). "Automated anatomical labeling of activations in SPM using a macroscopic anatomical parcellation of the MNI MRI single-subject brain." In: *Neuroimage* 15, pp. 273–289.

Utevsky, A. V., D. V. Smith, and S. A. Huettel (2014). "Precuneus Is a Functional Core of the Default-Mode Network". In: *Behavioral/Cognition* 34, pp. 932–940.

Vakorin, V. A., B. Misic, O. Krakovska, G. Bezgin, and A. R. McIntosh (2013). "Confounding Effects of Phase Delays on Causality Estimation". In: *PLoS ONE* 8.

Vanhatalo, S., J. M. Palva, M. D. Holmes, J. W. Miller, J. Voipio, and K. Kaila (2004). "Infraslow oscillations modulate excitability and interictal epileptic activity in the human cortex during sleep". In: *PNAS* 101(14), pp. 5053–5057.

Vincent, J. L., A. Z. Snyder, M. D. Fox, B. J. Shannon, J. R. Andrews, M. E. Raichle, and R. L. Buckner (2006). "Coherent Spontaneous Activity Identifies a Hippocampal-Parietal Memory Network". In: *Journal of Neurophysiology* 96(6), pp. 3517–3531. DOI: 10.1152/jn.00048.2006.

Vriend, C., P. S. Boedhoe, S. Rutten, H. W. Berendse, Y. D. van der Werf, and O. A. van den Heuvel (2015). "A smaller amygdala is associated with anxiety in Parkinson's disease: a combined FreeSurfer—VBM study". In: *J Neurol Neurosurg Psychiatry*.

Wiener, N. (1930). "Generalized harmonic analysis". In: *Acta Mathematica* 55, pp. 117–258.

Wiener, N. (1956). *The theory of prediction.* Beckenbach, E. (Ed.), Modern Mathematics for Engineers. McGraw-Hill, New York.

Williams, Z. M., G. Bush, S. L. Rauch, G. R. Cosgrove, and E. N. Eskandar (2004). "Human anterior cingulate neurons and the integration of monetary reward with motor responses." In: *Nat Neurosci* 7, pp. 1370–1375.

Wolansky, T., E. A. Clement, S. R. Peters, M. A. Palczak, and C. T. Dickson (2006). "Hippocampal Slow Oscillation: A Novel EEG State and Its Coordination with Ongoing Neocortical Activity". In: *The Journal of Neuroscience* 26(23), pp. 6213–6229. DOI: 10.1523/JNEUROSCI.5594-05.2006.

Woletz, M., A. Hoffmann, S. Ganger, K. Paul, R. Seiger, D. M. Pfabigan, A. Hahn, R. Sladky, C. Lamm, R. Lanzenberger, and C. Windischberger (2014). "Slice-Timing Correction for Multi-Band Images in SPM". In: *20th Meeting of the Organization for Human Brain Mapping, HBM - Hamburg, 2014.*

Xia, M., J. Wang, and Y. He (2013). "BrainNet Viewer: A Network Visualization Tool for Human Brain Connectomics". In: *PLoS One* 8.

Yarkoni, T., R. A. Poldrack, T. E. Nichols, D. C. V. Essen, and T. D. Wagner (2011). "Large-scale automated synthesis of human functional neuroimaging data". In: *Nat. Methods* 8, pp. 665–670.

Yeung, N., R. Bogacz, C. B. Holroyd, and J. D. Cohen (2004). "Detection of synchronized oscillations in the electroencephalogram: An evaluation of methods". In: *Psychophysiology* 41, pp. 822–832.

Zalesky, A., A. Fornito, and E. T. Bullmore (2010). "Network-based statistic: Identifying differences in brain networks". In: *NeuroImage* 53, pp. 1197–1207.

Zhang, R., J. Zuckerman, C. Giller, and B. Levine (1998). "Transfer function analysis of dynamic cerebral autoregulation in humans". In: *Americal Journal Physiology* 274(1), pp. 233–241.

Zheng, F., A. Sassaroli, and S. P. Fantini (2010). "Phasor representation of oxy- and deoxyhemoglobin concentrations: What is the meaning of out-of-phase oscillations as measured by near-infrared spectroscopy". In: *J. Biomed. Opt.* 15(4), 040512–1–040512–3.

APPENDIX A

POSTER

This appendix contains the poster presented in the 1^{st} Meeting of PhD students, Mind-Brain College of the University of Lisbon held in Lisbon on the 2^{nd} December 2015. Here some initial results obtained in this dissertation were shown.

Brain circuits involved in self-paced motion: an fMRI study

João Gens[1,2], Joana Brito[2], Alexandre Andrade[2], Hugo Ferreira[2], Karl Koschutnig[3,4],David Fink[3,4], Gert Pfurtscheller[4,5]

jpm.santos@campus.fct.unl.pt

[1]Faculdade de Ciências e Tecnologia da Universidade Nova de Lisboa, Portugal; [2]Instituto de Biofísica e Engenharia Biomédica, Faculdade de Ciências da Universidade de Lisboa, Portugal; [3]Department of Psychology, University of Graz, Austria; [4]BioTechMed-Graz, Austria; [5]Institute for Knowledge Discovery (BCI-Lab), Graz University of Technology, Austria

Question

The goal of this project is to probe the role of slow (~0.1 Hz) oscillations in the initiation of self-paced movements, using a frequency-specific functional connectivity measure (Wavelet Coherence).

Background

- fMRI is a powerful technique but it is severely conditioned by slow temporal sampling and hemodynamic variability.
- Attempts to tap into the phase, time and spectral content of the BOLD signal (e.g. time-lag based or frequency specific connectivity, chronometry) have been numerous (e.g. [1][2]) but the above limitations harm the potential of these approaches.
- Very slow oscillations (~0.1 Hz and below) have been detected in the human brain using both EEG and fMRI. This frequency range is widely believed to be involved in functional connectivity. The significance and physiological basis of these oscillations is a very active topic in brain research.
- It has been suggested that slow rhythms influence phenomena such as epileptic activity and decision making, including the decision to initiate a self-paced movement [3] [4].
- Phase coherence, or phase locking, has been proposed several times as a mechanism for long-distance communication between neural populations [5].

Methods

- Data corresponding to 25 healthy subjects were acquired with an experimental design comprising two 10-minute task executions (**visual-paced** and **self-paced** finger movement sessions with the right hand) and two 5-minute **rest** sessions.
- In the self-paced task, the subject was told to press a button at will whenever he felt the urge. The frequency of the visual stimulus was 0.1 Hz. A 3T MRI scanner and a T2*-weighted gradient-echo multiband sequence with TR/TE=871/34 ms were used.
- Data pre-processing was accomplished using the DPARSF toolbox [6] and included removal of the first 10 time points, slice timing correction, motion correction, normalization to MNI space, spatial smoothing, linear detrending and removal of nuisance covariates.
- Lastly, the mean BOLD time courses of the 90 Automated Anatomical Labeling (AAL) [7] Regions-of-Interest (ROIs) were extracted.

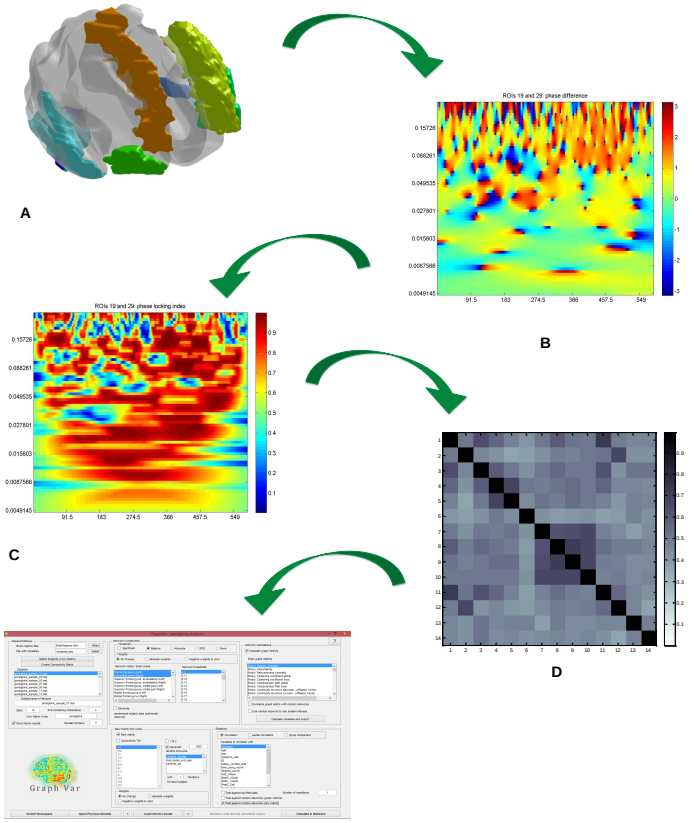

A) Extraction of **ROI time-series** (DPARSF).
B) **Phase component of the Wavelet Coherence** (time-frequency map showing phase differences between ROIs) [8].
C) **Phase-locking value** PLV (time-frequency map showing stability of phase difference) [5].
D) Mean PLV values within the frequency band 0.07-0.13 Hz belonging to a subset of 14 ROIs related to motion were extracted and stored as **14x14 connectivity matrices**
E) **GraphVar toolbox** [9] - analysis and visualization of brain connectivity matrices.

Results

- Top row figures show the inter-regional connections for which the mean **phase-locking value was significantly (p<0.05) different between two tasks**, namely rest and self-paced motion.
- Bottom row shows the inter-regional connections for which the **time length of significant phase-locking segments was significantly (p<0.05) different between two tasks**, namely rest and self-paced motion.
- Line thickness is proportional to the significance of the **inter-task effect**.
- Several **regions known to be involved in movement planning and execution** show significant inter-task differences. These regions are mostly located in the **left hemisphere**.
- The **second rest period shows a higher number of significant connections** (when compared with self-paced motion) than the first rest period.

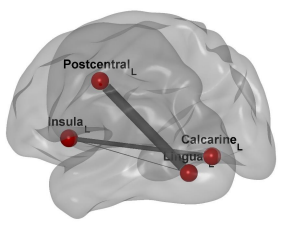

Group comparison, Mean Phase Locking, Rest1 > Self

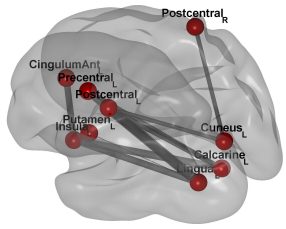

Group comparison, Mean Phase Locking, Rest2 > Self

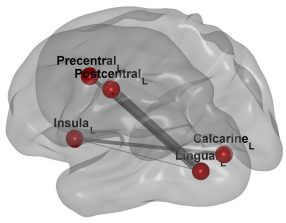

Group comparison, length of significant segments, Rest1 > Self

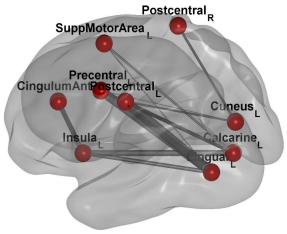

Group comparison, length of significant segments, Rest2 > Self

Conclusions

• This approach allowed to identify several **motor-related ROIs** that show **differences in phase-locking between the Rest and Self-Paced Motion states**.

• These differences are mostly in the **left hemisphere**, which was expected given that right-hand motion is involved.

• The involvement of the **insula** is in line with previous studies suggesting the importance of this region in this context.

• The fact that **similar results were obtained for mean phase-locking value and time-length of significant phase-locking period** is encouraging for future studies, because the former method does not require statistical validation (e.g. surrogate-based) and is therefore computationally much faster.

• **Differences between the first and second rest periods** (which were separated by the two motion tasks) are intriguing and may suggest habituation or practice effects.

•This methodological approach allowed to make a contribution towards the characterization of the functional connectivity and chronometry of brain circuits related to voluntary motor behavior. Although these results are preliminary, they suggest the potential of this approach.

References

[1] Sun et al (2015) NeuroImage 28:227-237 [2] Roebroeck et al (2005) NeuroImage 25:230-242 [3] Vanhatalo et al (2004) PNAS 101:5053-5057 [4] Pfurtscheller et al (2012) Neurosci Lett 508:89-94 [5] Lachaux et al (1999) Human Brain Mapping 8:194-208 [6] Chao-Gan et al (2010) Front Syst Neurosci 4:1-7 [7] Tzourio-Mazoyer et al (2002) NeuroImage 15:273-289 [8] Grinsted et al (2004) Nonlin Processes Geophys 11:561-566 [9] Kruschwitz JD et al (2015) Journal of Neuroscience Methods 245: 107-115.

Acknowledgements

We thank Thomas Zussner for fMRI data acquisition and storage within the BioMedTech project at the University of Technology in Graz, Austria and Professors Andreas Schwerdtfeger and Rudolf Stollberger for valuable support. This research was supported by Fundação para a Ciência e Tecnologia (FCT) and Ministério da Ciência e Educação (MCE) Portugal (PIDDAC) under grant UID/BIO/00645/2013.

APPENDIX B

ABSTRACT

This appendix contains the abstract submitted and accepted for a poster presentation in the 22^{nd} Annual Meeting of the Organization for Human Brain Mapping to be held in June 26-30, 2016 in Geneva, Switzerland.

Brain circuits involved in self-paced motion: the influence of 0.1 Hz waves

João Gens[1,2], Joana Brito[2], Alexandre Andrade[2], Hugo Ferreira[2], Karl Koschutnig[3,4],David Fink[3,4], Gert Pfurtscheller[4,5]

1 – Faculdade de Ciências e Tecnologia da Universidade Nova de Lisboa, Portugal
2-Instituto de Biofísica e Engenharia Biomédica, Faculdade de Ciências da Universidade de Lisboa, Portugal
3-Department of Psychology, University of Graz, Austria
4-BioTechMed-Graz, Austria
5-Institute for Knowledge Discovery (BCI-Lab), Graz University of Technology, Austria

Introduction: The neural mechanisms behind human voluntary motion are not fully characterized yet, in spite of numerous research studies. Slow (~0.1 Hz) oscillations that may partially overlap with the well-known Mayer waves of autonomic origin are known to have a powerful modulatory effect on several cognitive and physiological phenomena, including free movement (Pfurtscheller et al, 2014).

Methods: This study is based on fMRI data acquired from 25 right-handed, young and healthy subjects. All the subjects were submitted to a protocol consisting of two rest sessions, a self-paced motion (button-press) task and a visually-cued (0.1 Hz stimulus) motion (button-press) task. No training was performed and no instruction was given about the timing of the movements. Functional images were acquired on a 3.0-T scanner (Magnetom Skyra, Siemens). A multiband echo planar Imaging (EPI) sequence with a multiband factor of 6 was applied with the following features: voxel size of $2x2x2mm^3$, TR/TE= 871/34 ms, flip angle=52°, matrix 90x104, 66 contiguous axial slices, FOV= $180x208\ mm^2$. 400 volumes and 650 volumes were acquired for rest and motion sessions, respectively. Functional data were pre-processed using DPARSFA toolbox where time courses of 90 regions based on the AAL atlas were extracted. Functional connectivity was computed between brain regions using wavelet phase coherence and a surrogate based statistical test was carried out in order to identify significant connectivity values. The final outputs were mean phase-locking (PL) matrices reflecting inter-regional phase coherence around 0.1 Hz, matrices reflecting the length of significant PL segments and phase-derived temporal delays. These matrices formed the basis for subsequent analyses.

Results: Using the GraphVar toolbox, pairs of regions for which mean PL differs significantly and pairs of regions for which the time length of significant PL segments were significant between rest and self-paced movement were identified. Postcentral gyrus, Lingual gyrus, Calcarine and the Insula, all located in the left hemisphere, were involved. The second rest period shows a higher number of significant connections (when compared with self-paced motion) than the first rest period. An inter-group comparison between subjects with low and high standard deviation of inter-movement intervals highlighted a higher mean PL between left insula and left anterior cingulum for the former. Regarding time delays, the most striking observation is the very reproducible delay between the

Insula and the supplementary motor area, confirming the role of this pair of regions in the maintenance of slow oscillations relevant for the modulation of motor behavior.

Conclusions: Differences between rest and self-paced motion involved several areas known to be involved in the spontaneous initiation of movement and in the putative influence of 0.1 Hz waves associated with the baroreflex loop, notably the Insula. Higher phase-locking between Insula and Anterior cingulum for subjects with more regular self-paced button-pressing patterns lends credence to the importance of these regions in this context (Pfurtscheller et al, 2014). This methodological approach allowed to make a contribution towards the characterization of the functional connectivity and chronometry of brain circuits related to voluntary motor behavior. We expect that, with the advent of faster fMRI sequences, phase-based approached such as this have the potential to make a significant impact in connectivity and chronometry analyses.